RUNX2-GENETICALLY ENGINEERED SKELETAL MYOBLASTS FOR BONE TISSUE ENGINEERING

A Dissertation
Presented to
The Academic Faculty

by

Charles Alan Gersbach

In Partial Fulfillment
of the Requirements for the Degree
Doctor of Philosophy in Biomedical Engineering

Georgia Institute of Technology
August 2006

RUNX2-GENETICALLY ENGINEERED SKELETAL MYOBLASTS FOR BONE TISSUE ENGINEERING

Approved by:

Dr. Andres J. Garcia, Advisor
School of Mechanical Engineering
Georgia Institute of Technology

Dr. Barbara D. Boyan
Department of Biomedical Engineering
Georgia Institute of Technology

Dr. Joseph M. Le Doux
Department of Biomedical Engineering
Georgia Institute of Technology

Dr. Anthanassios Sambanis
School of Chemical Engineering
Georgia Institute of Technology

Dr. Robert E. Guldberg
School of Mechanical Engineering
Georgia Institute of Technology

Dr. Grace K. Pavlath
Department of Pharmacology
Emory University

Date Approved: May 4, 2006

For Grampie, who started me down this path, and
Cathy, who supports me throughout it

ACKNOWLEDGEMENTS

First and foremost I want to thank my thesis advisor, Dr. Andrés García, for the mentorship he has provided throughout my undergraduate and graduate education. Andrés introduced this "gringo" (yours truly) to biomedical research through an undergraduate research project the summer following my sophomore year. Mystified by attempts to create biomaterials with a 3-hole punch and transparency paper, he convinced me that my knack for creative, but ultimately unsuccessful, problem-solving strategies was best suited for graduate school. He would later eat his words when I opted to complete my thesis in his laboratory. Nonetheless, he has been infinitely supportive throughout my time here, continually going above and beyond his duties as thesis advisor to ensure that I have every opportunity for success and that my graduate school experience is as enjoyable as possible. Above all, he has been a friend and source of advice on topics ranging far beyond academics and research. It is certain that any of my present and future successes are wholly attributable to his support and guidance.

I am also greatly thankful for the advisement of my thesis committee members. Dr. Bob Guldberg has been a considerable resource for orthopedic- and tissue engineering-related expertise and equipment. Dr. Joe Le Doux, who advised me through my first rotation project, was essential to developing the inducible expression system and generously donated his time and expertise to troubleshooting gene therapy protocols and strategies. Dr. Barbara Boyan, in addition to providing insights in bone biology, has persistently reinforced the significance of data interpretation and representation – a valuable lesson for my research career, and I will never speak the b-word again without thinking twice. Dr. Grace Pavlath and Dr. Anthanassios Sambanis have also been critical

in providing knowledge and reagents related to muscle cell biology and inducible gene expression systems, respectively. Finally, all of my committee members have also served as excellent examples of successful and fulfilling careers in biomedical research.

This thesis would not have been possible without the assistance and guidance of the administration and staff of the Department of Biomedical Engineering, the Georgia Tech/Emory Center for the Engineering of Living Tissues, and the Petit Institute for Bioengineering and Biosciences. In particular, I want to personally thank Dr. Robert Nerem for his relentless pursuit of the creation of extraordinary opportunities for Georgia Tech students. I am also grateful to Dr. Ajit Yoganathan and Dr. Steve DeWeerth for their persistent development of the Biomedical Engineering Ph.D. curriculum. Tracey Couse and Angela Lin provided essential technical assistance for procedures involving histological analysis, micro-computed tomography, and mechanical testing. Additionally, Dr. TJ Murphy and the Kensey Nash Corporation generously donated retroviral vectors and collagen scaffolds, respectively.

The most rewarding part of graduate school has been the friendships that developed along the way. Particular thanks go to Ben Byers, who served as an excellent mentor when I entered the lab and started me down the path to Runx2 glory. Thanks to Ben Keselowsky for teaching me exactly what I could get away with in the lab; to Nate Gallant and Jeff Capadona for extracurricular activities, especially those involving fermented beverages and playing cards; to the "lab mom", Kristin Michael, for planning lab social events, ensuring birthdays were always recognized, and keeping the lab tidy via threatening emails; to Jenn Phillips, my partner in Runx2 crime, for keeping me on my toes through "rigorous scientific discussion"; to Mr. Fantastic, aka Tim Petrie, for

keeping me 1) company during late evenings in the lab and 2) keenly aware of my caloric intake; to our lab managers, Kellie Burns and Linzy Bryant, for keeping the lab operations smooth and atmosphere light. Thanks to Chris Gemmiti for introducing me to fantasy baseball, earlybirds at Bobby Jones, and keeping ABC in existence for the duration of my time in Atlanta; to Craig Duvall for his relentless pursuit of good times and his efforts to include me in them; to Jeff Gross for being a first-rate non-roommate and teaching me molecular biology during trips between the Emory and Georgia Tech campuses; to Blaise Porter for taking years off of my life during the Days of Blaise; to Srin Nagaraja for post-Silver Lake Loop cocktails; and to Geela Lin for taking it easy on me during drinking and billiards.

My family has been an incredible support throughout the completion of this thesis and all others endeavors. I am particularly thankful to my parents for encouragement through all of my pursuits; to Matt and Amy for their always entertaining visits to Atlanta, to my grandparents for their guidance – in particular Grampie, who initiated my interest in science and engineering; to Mark and Joan for providing a place to escape from school; and to the Reyes' for accepting me into their family. Last, but certainly not least, my eternal gratitude belongs to Cathy, who has truly added new meaning to everything I do, for her infinite patience in providing invaluable support and love.

Finally, this research was funded by the National Institute of Health, National Science Foundation, and Georgia Tech/Emory Center for the Engineering of Living Tissues.

TABLE OF CONTENTS

LIST OF TABLES

LIST OF FIGURES

LIST OF SYMBOLS AND ABBREVIATIONS

ALP	alkaline phosphatase
ANOVA	analysis of variance
aTc	anhydrotetracycline
bFGF	basic fibroblast growth factor
BMP	bone morphogenetic protein
BSP	bone sialoprotein
Cbfa	core binding factor-alpha
COL	collagen
eGFP	enhanced green fluorescent protein
ELISA	enzyme-linked immunosorbent assay
FBS	fetal bovine serum
FT-IR	Fourier transform infrared
GAPDH	glyceraldehyde-3-phosphate dehydrogenase
H&E	hematoxylin and eosin
Id	inhibitor of differentiation
IRES	internal ribosomal entry site
LMP	LIM-mineralization protein
LTR	long terminal repeat
MAPK	mitogen-activated protein kinase
Mbs	primary skeletal myoblasts
Micro-CT	micro-computed tomography
MRF	myogenic regulatory factor

Neo(r)	neomycin resistance
OCN	osteocalcin
OSX	osterix
PBS	phosphate-buffered saline
PCR	polymerase chain reaction
RT	reverse transcription
Runx	runt-related gene
SEM	standard error of the mean
Tet	tetracycline
tetO	tet operon
TGF-β	transforming growth factor-beta
3D	three-dimensional
TpnT	troponin T
tTA	tetracycline-controlled transactivator
VEGF	vascular endothelial growth factor
Zeo(r)	zeocin resistance

SUMMARY

Bone substitutes are required for the healing of large bone defects, including orthopedic, craniofacial, and dental reconstructions. Bone tissue engineering has emerged as a promising strategy to address the limitations of currently used bone substitutes. The central paradigm of these approaches is the incorporation of cells, a scaffold, and bioactive factors into an implantable construct. However, the efficacy of these strategies has been limited by the availability of a readily accessible, controlled, and sustained mineralizing cell source. This work aims to meet this need by inducing osteoblastic differentiation of primary skeletal muscle cells by genetic engineering with the Runx2 osteoblastic transcription factor. The *overall objective* of this research was to engineer an inducible cell source for bone tissue engineering that addresses the limitations of current cell-based approaches to orthopedic regeneration. Our *central hypothesis* was that inducible Runx2 overexpression in skeletal myoblasts would stimulate differentiation into a regulated osteoblastic phenotype for bone tissue engineering applications.

We first tested the central hypothesis by retrovirally overexpressing a constitutive Runx2 transgene in primary skeletal muscle cells in monolayer culture. Runx2 inhibited myogenic differentiation in these cells, as evident by downregulated muscle-specific gene expression and suppressed myotube formation. Runx2 stimulated osteoblastic differentiation, as demonstrated by upregulation of osteoblastic gene expression and alkaline phosphatase biochemical activity. Furthermore, Runx2-engineered myoblasts showed significant deposition of a hydroxyapatite mineral. Interestingly, Runx2

overexpression had a more potent effect on osteoinduction relative to treatment with soluble BMP-2 protein, which may have been the result of bypassing BMP-2-stimulated autoregulatory factors. Collectively, these results demonstrate that Runx2 stimulates transdifferentiation of primary skeletal muscle cells into an osteoblastic phenotype.

These cells were further examined in the environment of a three-dimensional tissue-engineered construct. Runx2-engineered myoblasts or control cells were seeded onto fibrous collagen scaffolds and cultured up to 8 weeks in static conditions *in vitro*. Cells were viable on these scaffolds for prolonged culture times. Runx2-engineered cells upregulated osteogenic and downregulated myogenic gene expression on the scaffolds, similar to cells in monolayer culture. Finally, the Runx2-overexpressing myoblasts produced a hydroxyapatite mineral coating on these scaffolds. Although mineral deposition was confined to the construct periphery, colocalizing with cell viability, the mineral coating was sufficient to improve the mechanical properties of the constructs 30-fold. These results established Runx2-engineered skeletal myoblasts as a promising cell source for bone tissue engineering.

Further characterization of these cells involved an *in vitro* and *in vivo* comparison with myoblasts retrovirally engineered to overexpress BMP-2, a well-characterized osteogenic factor used in bone tissue engineering strategies. Retroviral delivery of BMP-2 or Runx2 stimulated differentiation into an osteoblastic phenotype, as demonstrated by the induction of osteogenic gene expression, alkaline phosphatase activity, and matrix mineralization in monolayer culture and on collagen scaffolds both *in vitro* and in an intramuscular site *in vivo*. In general, BMP-2 stimulated osteoblastic markers faster and to a greater extent than Runx2, although experimental conditions were identified under

which these two factors produced similar effects. Additionally, Runx2-engineered cells did not utilize paracrine signaling via secreted osteogenic factors, in contrast to cells overexpressing BMP-2, as demonstrated by conditioned media studies and activation of Smad signaling. These results emphasize the complexity of gene therapy-based orthopedic therapeutics as an integrated relationship of differentiation state, proliferative capacity, construct maturation, and paracrine signaling of osteogenic cells. This study was significant in evaluating proposed therapeutic systems and defining a successful strategy for integrating gene medicine and orthopedic regeneration.

Although e*x vivo* gene therapy is a promising approach to orthopedic regenerative medicine, the unregulated production of osteoinductive molecules has also resulted in abnormal bone formation and tumorigenesis. To address these limitations, we developed a retroviral system to deliver the Runx2 osteoblastic transcription factor under control of the tetracycline-inducible (tet-off) promoter in primary skeletal myoblasts. Runx2 expression was tightly regulated by anhydrotetracyline (aTc) concentration in cell culture media. Osteoblastic gene expression, alkaline phosphatase activity, and matrix mineralization were also controlled by aTc in a dose-dependent manner. Additionally, osteoblastic differentiation was temporally regulated by adding and removing aTc from the culture media. Engineered cells were seeded onto collagen scaffolds and implanted intramuscularly in the hind limbs of syngeneic mice. *In vivo* mineralization by these constructs was regulated by supplementing the drinking water with aTc, as demonstrated by micro-computed tomography and histological analyses. Collectively, these results present a novel system for regulating osteoblastic differentiation of a clinically relevant autologous cell source. This system is significant in developing controlled and effective

orthopedic gene therapy strategies and studying the regulation of osteoblastic differentiation.

In summary, this work has established Runx2-engineered primary skeletal myoblasts as a promising cell source for bone tissue engineering. These cells have been characterized in monolayer culture and in tissue engineered constructs *in vitro* and *in vivo*. The degree of Runx2-stimulated osteoblastic differentiation compares favorably with that of BMP-2-based strategies, the current standard in orthopedic gene therapy. Finally, we have engineered a system to exogenously regulate Runx2-stimulated osteoblastic differentiation. This work has successfully identified strategies to address cell sourcing limitations of bone tissue engineering and alternate methods for orthopedic gene therapy, as well as enhance our understanding of the molecular biology of osteoblastic differentiation.

CHAPTER 1

SPECIFIC AIMS

Bone tissue engineering has emerged as a promising alternative to currently used bone substitutes. The central paradigm of these approaches is the incorporation of cells, a scaffold, and bioactive factors into an implantable construct. However, the efficacy of these strategies has been limited by the availability of a sustained, mineralizing cell source. In response to this need, *ex vivo* gene therapy with osteogenic factors has been used to enhance osteoblastic phenotype and *in vivo* bone healing. The majority of these strategies utilize the constitutive overexpression of soluble signaling proteins, resulting in unregulated secretion of potent osteoinductive molecules which primarily act on native cells surrounding the implant site. Although this method is successful in stimulating osteoblastic differentiation, this effect is unregulated with respect to magnitude and kinetics of cell activity. In contrast to these approaches, our group has previously demonstrated that genetic engineering of an osteogenic cell source with the osteoblastic transcription factor Runx2, an intracellular effector, dramatically enhances the phenotype and *in vivo* mineralization by these cells. However, an autologous osteogenic cell source is painful and difficult to obtain in large numbers and has passage-dependent and age-related decreases in mineralization. This research focuses on using this strategy to induce osteogenesis in skeletal myoblasts, a source of mesenchymal progenitor cells available in large numbers and compatible with *in vitro* expansion and gene therapy protocols. Additionally, this project establishes methods to control the magnitude and kinetics of Runx2-induced osteogenesis as strategies to regulate the *in vitro* engineering of tissues

and circumvent the aberrant effects of unregulated overexpression of an osteogenic factor.

Our *central hypothesis* was that inducible Runx2 overexpression in skeletal myoblasts stimulates differentiation into a regulated osteoblastic phenotype for bone tissue engineering applications. The *overall objective* of this research was to engineer an inducible cell source for bone tissue engineering that addresses the limitations of current cell-based approaches to orthopedic regeneration.

Aim 1: Analyze the effects of Runx2 overexpression in skeletal myoblasts.

The effects of Runx2 expression in skeletal myoblasts were assessed in monolayer culture *in vitro* utilizing a constitutive retroviral delivery system. The *working hypothesis* was that overexpression of the osteoblastic transcription factor Runx2 stimulates differentiation of skeletal myoblasts into an osteoblastic phenotype. Osteoblastic differentiation was assessed by gene expression, alkaline phosphatase biochemical activity, and matrix mineralization. Myogenic differentiation was assessed by gene expression and myotube formation.

Aim 2: Evaluate Runx2-overexpressing skeletal myoblasts as a mineralizing cell source for bone tissue engineering.

The *working hypothesis* was that Runx2-genetically engineered skeletal myoblasts produce a mineralized matrix in tissue-engineered constructs for bone tissue engineering applications. Cell-seeded tissue-engineered constructs were cultured *in vitro* and analyzed for osteoblastic behavior and mineral deposition. Engineered cells were also

implanted intra-muscularly in mice to assess the mineralization potential of these cells *in vivo*. Mineralization was investigated by micro-CT, histological analysis, and FTIR spectroscopy. Runx2-engineered cells were also compared to cells overexpressing BMP-2, the standard soluble osteogenic factor used for gene therapy-based orthopedic regeneration.

Aim 3: Engineer a system to regulate the magnitude and kinetics of Runx2-stimulated osteoblastic differentiation.

The *working hypothesis* was that the effects of Runx2 overexpression can be exogenously regulated by a retroviral tetracycline-inducible expression system. Skeletal myoblasts were engineered with a tetracycline-inducible expression system incorporating the Runx2 gene. Cells were then analyzed for osteoblastic differentiation in response to varying concentrations of tetracycline, including gene expression, alkaline phosphatase activity, and matrix mineralization. Cells engineered with the inducible Runx2 expression system were implanted intramuscularly into syngeneic mice receiving tetracycline though the drinking water. Exogenous regulation of *in vivo* mineralization by these cells was monitored by micro-CT and histological analyses.

This work is *significant* because it provides insights into the biological role of the Runx2 transcription factor in determining cell lineage, addresses cell sourcing limitations of bone tissue engineering, and establishes a controlled and effective approach for orthopedic gene therapy. This research is *innovative* because it utilizes overexpression of an osteoblastic transcription factor to redirect the differentiation of non-osteoblastic cells

for therapeutic applications and develops a unique strategy for the regulation of transgene expression in ex vivo gene therapy approaches to bone repair.

CHAPTER 2

LITERATURE REVIEW

Bone Structure and Function

Bone tissue serves several important functions in the human body[1]. First, the skeleton provides structural support for the body and its associated tissues and organs. Bones such as the ribs, skull, and vertebrae also provide protection to vital organs including the heart, lungs, brain, and spinal cord. The marrow cavities of bones serve as housing for bone marrow, cells of the immune system, and hematopoetic and mesenchymal stem cells. Bone also acts as a reservoir and regulator of calcium and phosphate ions in the body, and provides attachment points for muscle, tendons, and ligaments to apply force and generate motion.

Bone consists of a cell-secreted protein matrix, predominantly consisting of type I collagen (>95%), as well as other noncollagenous calcium binding and signaling proteins, including osteocalcin, osteopontin, bone sialoprotein, and osteonectin[2]. The mineral component of bone, representing 60-75% of the total weight, consists of hydroxyapatite, a poorly crystalline lattice structure of calcium and phosphate ($Ca_{10}(PO_4)_6(OH)_2$). Biological hydroxyapatite contains several ionic substitutions, most notably carbonate, and is embedded in an oriented fashion in the fibrillar collagenous matrix. The human skeleton consists of trabecular and cortical bone. Cortical bone constitutes the long bones, small bones, and flat bones, and is comprised of a hierarchy of geometric units to maximize the mechanical properties of the material. Trabecular, or spongy, bone is present at the ends of long bones and is more porous and less stiff than cortical bone. The presence of both types of bone is essential to fulfilling many functions of bone in the body.

Bone consists of four major cell types, including osteoblasts, osteocytes, osteoclasts, and bone-lining cells[2]. Osteoblasts are responsible for generating bone tissue at the bone surface, including matrix secretion and remodeling and mineral deposition[3]. Osteocytes are terminally differentiated osteoblasts which have become embedded within the bone matrix. These cells are involved in sensing mechanical forces within the bone tissue and participate in the remodeling process. Osteoclasts are large multi-nucleated cells of hematopoetic origin that resorb bone through mineral dissolution and enzymatic digestion of the organic matrix. Bone-lining cells cover resting bone surfaces and can also regulate bone maintenance directly, or through the recruitment of osteoblasts or osteoclasts.

Bone Formation and Healing

Bone formation, or ossification, occurs through two distinct mechanisms: intramembranous ossification and endochondral ossification[2]. Endochondral ossification is responsible for the formation of bones of the extremities and weight bearing bones, such as vertebrae, and occurs via a preexisting cartilage template. Hypertrophic chondrocytes at the bone-cartilage interface initiate calcification of the cartilage. Subsequently, these cells become apoptotic, leading to the invasion of vascular supply and osteoblasts that secrete the appropriate bone matrix. This tissue subsequently fuses into an unstructured woven bone and is remodeled into lamellar bone of aligned collagen fibrils. Intramembranous ossification occurs without a cartilage intermediate during the development of the flat bones of the skull and face. Ossification begins with the infiltration of mesenchymal progenitor cells into a fibrous matrix and their subsequent osteoblastic differentiation. These cells initiate the assembly of osteoid, the uncalcified bone matrix. Trabecular bone and vascular structures then begin to form within this tissue. As the trabecular bone fragments thicken they begin to fuse into continuous

plates, and the irregular woven bone is replaced via remodeling with structured lamellar bone.

Following bone damage, a hematoma and fibrin clot develop in the site of fracture. Cells of the immune system, including macrophages and leukocytes, clean and remove the damaged tissue. Osteoblasts and osteoprogenitors infiltrate the tissue from the blood stream and neighboring periosteal and marrow tissues and begin to secrete organic matrix which is subsequently mineralized[1]. Importantly, this process may be hindered by infection, lack of blood supply, fracture instability, or lack of sufficient material. In such cases, or when the fracture is too large to repair itself, bone grafting procedures may be necessary to repair the defect[4].

Osteoblastic Differentiation and the Runx2 Transcription Factor

Osteoblastic differentiation has been described as a developmental sequence consisting of proliferation, matrix synthesis and maturation, and matrix mineralization[5]. Throughout the proliferative phase, osteoblast activity is primarily restricted to type I collagen secretion. As proliferation decreases, differentiation is marked by a transient increase in alkaline phosphatase activity. The mature osteoblastic phenotype is characterized by osteocalcin expression, which is upregulated before the initiation of matrix mineralization. Terminal osteoblastic differentiation is associated with hydroxyapatite deposition in the secreted organic matrix.

Osteoblastic differentiation has primarily been studied through experiments with soluble osteoinductive factors discovered in demineralized bone matrix, most notably bone morphogenetic proteins (BMPs)[6]. Osteogenic induction by BMPs has been extensively studied in myogenic and pluripotent cell lines and primary cells. BMPs, a subdivision of the transforming growth factor beta (TGF-β) superfamily, comprise a

highly conserved and expanding family of 15 genes critical to embryogenesis and bone formation[7,8]. The exceedingly complex molecular mechanisms of BMP signaling are under continuous investigation, but several important aspects of select pathways have been determined. BMP-2 acts as a dimer by binding to a heterotetramer of type I and type II transmembrane serine/threonine kinase receptor proteins, inducing autophosphorylation of the intracellular domains. Upon activation by BMP-2, these receptors phosphorylate the intracellular signaling molecule Smad1/5. Activated Smad1/5 then associates with Smad4 and translocates to the nucleus, where it interacts with the osteoblast-specific transcription factor Runx2/Cbfa1/Osf2/AML3 and upregulates osteoblastic gene expression[9,10]. BMP-2 induces osteoblastic markers in the myogenic C2C12 and pluripotent C3H10T1/2 cell lines, including increased alkaline phosphatase activity and osteocalcin mRNA expression and promoter activity[11-14]. BMP-2 also suppresses myogenesis in these cell lines, which is typically demonstrated by inhibited myotube formation and reduced activity of myogenic regulatory factors (MRFs), such as MyoD and myogenin[15,16]. MyoD determines myoblastic cell fate, and myogenin acts downstream of MyoD by regulating commitment to myogenic differentiation[17]. Upregulation of Id-1 (inhibitor of differentiation/DNA binding-1) by BMP-2 is responsible for reduction of MRF activity by competitively binding E proteins that are necessary for MRF function[18,19].

Runx2, a member of the runt homology domain family of transcription factors, is required for osteoblastic differentiation and endochondral and intramembranous bone formation[20,21]. Heterozygous mutation of the Runx2 gene is implicated in the human skeletal disorder cleidocranial dysplasia[22,23], and the homozygous mutation in mice

results in a complete lack of mineralization and immediate postnatal death[21]. Our laboratory has previously demonstrated that sustained expression of Runx2 in osteogenic and pluripotent cell lines upregulates osteoblast-specific gene expression and induces *in vitro* mineralization in a cell type-dependent manner[24]. These results established the requirement for other cofactors in addition to Runx2 to induce cell-mediated mineralization. These results also demonstrate that increased osteocalcin expression and alkaline phosphatase activity are insufficient markers to define terminal and functional osteoblastic differentiation (e.g. matrix mineralization).

BMP-2-induced osteogenesis has several known points of regulation upstream of Runx2 transcriptional activation. The protein noggin blocks the extracellular interaction of BMPs with their receptors by competitive dimerization[25,26]. The inhibitory smad, Smad6, blocks BMP signaling by physically preventing the interaction between BMP receptors and Smad1/5, and inhibiting subsequent activation[7]. Smad5 signaling can also be blocked by Smurf1, which targets Smad5 for degradation and thereby facilitates myogenic differentiation and antagonizes BMP-2 induced osteogenesis[27,28]. Finally, Runx2 activity can be directly regulated by other transcription factors such as HES-1, Msx2, Dlx5, and TLE proteins. The basic helix loop helix protein HES-1 promotes Runx2 transcriptional activity in ROS17/2.8 cells through a direct physical interaction[29]. The homeobox protein Msx2 is expressed in proliferating immature osteoblasts and inhibits terminal osteoblastic differentiation, possibly by repressing Runx2 activity[30,31]. Dlx5, another homeobox protein which is expressed in differentiating osteoblasts, is required for BMP-2 induced osteogenesis and modulates Runx2 activity by inhibiting Msx2-mediated suppression[31-33]. TLE1 and TLE2 colocalize with Runx2 in the nucleus

and repress its activity via interactions with the Runx2 C-terminal transactivation domain[34]. The numerous levels of regulation in this cascade indicate that signaling via BMP-2 stimulation does not necessarily result in robust and exclusive Runx2 transcriptional activity and other accessory signaling pathways modulate signal transduction.

Bone Grafting

Orthopaedic reconstructions have a significant socioeconomic impact worldwide, as evidenced by the 2.2 million operations requiring bone substitutes each year[4]. Existing bone substitutes include autografts, allografts, and synthetic materials[35,36]. Autografting involves the harvest of autogenous bone, typically from the iliac crest, for implantation into an osseous defect. Although successful in many cases, this procedure is limited by the availability of healthy tissue, donor site morbidity, and pain associated with the harvest[4,36]. Allografts, typically cadaver bone from bone banks, suffer from reduced biological and mechanical properties after processing and possible disease transmission[4]. Synthetic materials, including titanium, ceramics, and synthetic hydroxyapatite, generally incite host inflammation and fail to adequately integrate and remodel with the surrounding native tissue[37]. Bone tissue engineering has emerged as a promising alternative to these strategies. The general paradigm of these approaches focuses on incorporating cells, a scaffold, and bioactive factors into an implantable construct[38,39].

Cell Sources for Bone Tissue Engineering

Current applications of bone tissue engineering have been hindered by availability of a sustained, mineralizing cell source that can generate mechanically robust constructs

for large defects. Terminally differentiated osteoblasts, the cells responsible for bone formation, are difficult to obtain in large numbers and fail to proliferate and substantially populate typical tissue-engineered constructs. Immortalized osteogenic cell lines have the potential to form tumors *in vivo*. Osteogenic precursors, such as bone marrow stromal cells, are capable of osteoblastic differentiation and mineralization[40], and have been used in many cases to successfully heal bone defects[41-46]. However, these cells are also difficult and painful to obtain in suitable quantities[38], typically de-differentiate and lose phenotype following *in vitro* culture and expansion[47-49], and demonstrate an age-related decrease in osteogenic capacity[50]. A promising alternative to these cell sources is the induction of sustained osteogenesis in non-osteoblastic cells using genetic engineering approaches.

BMPs have been used extensively to induce osteogenesis in non-osteoblastic cell types, including bone marrow stromal cells[51-54], dermal and gingival fibroblasts[55,56], and skeletal myoblasts[13,57]. In fact, skeletal myoblasts have been used extensively in combination with BMPs to generate bone tissue in both ectopic and osseous environments[58-60]. Skeletal myoblasts represent a clinically relevant autologous source of mesenchymal progenitor cells that are readily accessible in large quantities from muscle biopsies. They are easily purified and expanded under the appropriate culture conditions and contain a subpopulation of muscle-derived stem cells[61]. Furthermore, the use of autologous cells in a clinical setting avoids immunological complications involved in allogeneic and xenogeneic cell-based strategies. Myoblasts are also compatible with gene transfer technologies and achieve high levels of transduction by viral gene therapy[62].

Orthopedic Gene Therapy

Gene Delivery Systems

Orthopedic gene therapy consists of *in vivo* approaches, when the gene delivery vehicle is directly implanted or injected into the body, and *ex vivo* strategies, when cells are genetically manipulated *in vitro* and subsequently implanted into the bone defect[63]. Both approaches have been widely used for bone regeneration. Although *in vivo* gene therapy benefits from the simplicity of a cell-free approach, *ex vivo* gene therapy allows for greater efficiency and target specificity and avoids the safety risks involved with direct exposure to gene carriers.

Gene delivery vehicles for orthopedic regeneration have included plasmid DNA[64] and viral gene carriers, including retrovirus[43,65-67], lentivirus[68], adenovirus[69,70], and adeno-associated virus[71-73]. Although plasmid DNA is easy to produce, has low immunogenicity, and avoids many safety issues associated with viral gene delivery, this method is still hindered by limitations of toxicity, specificity, and efficiency. However, systems incorporating plasmid DNA into complexes with cationic lipids or polymers are currently under development to address these concerns[74].

Viruses have been selected through evolution for the ability to enter cells and deliver their genetic material into the nucleus of target cells and are therefore much more efficient than methods involving plasmid DNA. Adenoviruses contain a DNA genome and enter the cell by binding to virus receptors and inducing internalization through interactions with integrins. Once inside the cell, the virion disassembles and the DNA is released into the nucleus, where it remains as an episome for days/weeks before degradation. Adenoviruses display high transduction efficiencies of most cell types, have a large cloning capacity (36 kb), and can be prepared at high titers. However, the

significant inflammatory response incited by adenoviral capsid proteins and pre-existing antibodies to these particles limit their efficacy *in vivo*. Adeno-associated viruses have recently emerged as a particularly promising delivery vehicle considering the broad cell tropism and lack of an inflammatory response. These vectors generally remain as a transient episome within the nucleus, although a fraction of particles do integrate into the chromosomal DNA. The major limitation of this vector is the small cloning capacity (<5 kb), thus prohibiting the delivery of large or multiple genes with a single vector. Retroviral and lentiviral vectors contain an RNA genome with moderate cloning capacity (8 kb) that can integrate into chromosomal DNA, thus making these vectors attractive for gene therapy strategies that require prolonged expression. However, retroviral transgene expression may still be limited by gene methylation or promoter silencing. Integration into chromosomal DNA can also cause insertional mutagenesis, in which pathological states are caused by deregulation of endogenous gene expression by the integrated vector. While retroviruses can only transduce dividing cells, since they require breakdown of the nuclear membrane to gain access to host DNA, lentiviruses can transduce both dividing and nondividing cells. The optimal gene delivery vehicle for a specific application is typically selected based on the desired expression kinetics, cloning capacity, biocompatibility, and susceptibility of the target cell type.

Osteogenic Transgenes

The vast majority of orthopedic gene therapy strategies focus on the overexpression of BMPs. In particular, BMP-2[52,68,75], BMP-4[64,66], and BMP-7[43,55] have all been used to stimulate osteoblastic differentiation and bone formation. BMP-engineered cells are particularly potent inducers of bone formation *in vivo*, as secreted BMP protein can stimulate the differentiation of native osteoprogenitors[76]. The considerable success of BMP-based strategies led to the targeting of downstream regulators of BMP signaling, particularly the Runx2 transcription factor. Runx2-based

gene therapy has been successful in stimulating osteoblastic differentiation of bone marrow stromal cells and enhancing bone formation and repair.[56,67,77-79] Additionally, coexpression of osteogenic and angiogenic factors, such as VEGF, has led to a synergistic enhancement in bone healing[64,72,80]. Promising results have also been achieved with strategies focusing on RANK-L,[72] constitutively active BMP receptors,[73] LIM-mineralization protein,[81] and synergistic approaches incorporating multiple transgenes[70,78] and transgenes supplemented with glucocorticoids[82,83] or immunosuppressive agents.[84,85]

Inducible Expression Systems

Constitutive overexpression of osteogenic transgenes has been successful in stimulating osteoblastic differentiation and bone regeneration. However, the unregulated overexpression of these proteins also risks aberrant effects of uncontrolled cell signaling, including tumorigenesis[86,87] and bone overproduction,[88,89] when bone growth exceeds the defect site. Inducible expression systems have been utilized to address these concerns and control the activity of genetically engineered cells.[74] These systems typically drive transgene expression from inducible promoters regulated by engineered and/or non-mammalian transcription factors. The activity of these transcription factors is controlled by exogenous chemical agents which permit ("on" state) or repress ("off" state) transgene expression. In principle, an *ex vivo* inducible gene therapy strategy involves implanting engineered cells into a bone defect site and maintaining an optimized level of transgene expression in the "on" condition. When adequate healing has occurred, cells are moved to the "off" condition to prevent any adverse effects of prolonged transgene overexpression. Additionally, incorporating regulation into these systems allows analysis of unique patterns of transgene expression, including varying the duration and magnitude

of expression, cycling expression over time, and coordinating the sequential presence of multiple exogenously expressed genes.

The most widely characterized of these systems is the tetracycline inducible expression system, first described by Gossen and Bujard.[90] The original system utilizes the tetracycline-controlled transactivator (tTA). In the absence of tetracycline, tTA binds the tet operon and activates transcription of a downstream gene of interest. However, in the presence of subtoxic levels of tetracycline, the antibiotic binds to tTA, blocking binding of the tet operon and subsequent transactivation in a dose-dependent manner. This system is compatible *in vitro* by adding tetracycline to the cell culture media and *in vivo* by delivering aTc via the drinking water. This "tet-off" version was later modified to a "tet-on" system, in which transactivation increases with tetracycline concentration.[91] Despite the greater clinical relevance of the tet-on derivative, the tet-off system is widely reported as having a greater degree of inducibility, including lower expression levels in the "off" state and higher expression levels in the "on" state.[92] However, recent modifications of the "tet-on" system have shown improved induction levels and lower basal activity in the "off" state.[93,94] Many other promising inducible expression systems have been designed based on promoters that are responsive to a variety of environmental and physiological stimuli.[74,95] The clinical success of these systems will be dependent on the efficient delivery of multiple vectors, biocompatibility of the inducing agent, immunologic tolerance of the engineered or non-mammalian protein components, limited promoter interference, efficient repression in the "off" state, and appropriate expression levels in the "on" state.

Inducible expression systems have been incorporated into genetic engineering strategies for regulated osteoblastic differentiation and bone regeneration. Gazit and colleagues initially utilized the "tet-off" system to regulate *in vitro* osteoblastic differentiation, ectopic bone formation, and regeneration of a long bone segmental defect by a BMP-2-engineered mesenchymal stem cell line.[88] This system was subsequently used to direct spinal fusion[96] and study the kinetics of BMP-2-induced osteochondral differentiation.[97] Building on these promising results, the BMP-2 transgene was incorporated into an AAV-2-based "tet-on" expression system for *in vivo* gene delivery by direct viral injection.[71] This approach was successful in effectively controlling ectopic bone formation and repairing critically-sized cranial defects. Peng et al. have also exploited a retroviral tetracycline-regulated gene expression system to control bone formation by BMP-4-engineered muscle-derived stem cells.[65] Additionally, this study identified optimal self-inactivating deletions within the retroviral long terminal repeat to enhance expression from the inducible promoter, which may be limited in certain applications due to promoter interference.[98] This system was also used in combination with overexpression of autoregulatory factors, providing an additional level of control that may stimulate bone formation that better resembles the native tissue.[89]

CHAPTER 3

RUNX2-STIMULATED TRANSDIFFERENTIATION OF PRIMARY SKELETAL MYOBLASTS INTO AN OSTEOBLASTIC PHENOTYPE*

Introduction

Osteogenic induction by bone morphogenetic proteins (BMPs) has been extensively studied in myogenic and pluripotent cell lines and primary cells. BMPs, a subdivision of the transforming growth factor beta (TGF-β) superfamily, comprise a highly conserved and expanding family of 15 genes critical to embryogenesis and bone formation[7,8]. The exceedingly complex molecular mechanisms of BMP signaling are under continuous investigation, but several important aspects of select pathways have been determined. BMP-2 acts as a dimer by binding to a heterotetramer of type I and type II transmembrane serine/threonine kinase receptor proteins, inducing autophosphorylation of the intracellular domains. Upon activation by BMP-2, these receptors phosphorylate the intracellular signaling molecule Smad1/5. Activated Smad1/5 then associates with Smad4 and translocates to the nucleus, where it interacts with the osteoblast-specific transcription factor Runx2/Cbfa1/Osf2/AML3 and upregulates osteoblastic gene expression[9,10]. BMP-2 induces osteoblastic markers in the myogenic C2C12 and pluripotent C3H10T1/2 cell lines, including increased alkaline phosphatase activity and osteocalcin mRNA expression and promoter activity[11-14]. BMP-2 also suppresses myogenesis in these cell lines, which is typically demonstrated by

* Modified from
C.A. Gersbach, B.A. Byers, G.K. Pavlath, and A.J. Garcia, *Runx2/Cbfa1 stimulates transdifferentiation of primary skeletal myoblasts in a mineralizing osteoblastic phenotype.* Experimental Cell Research, 2004. 300:406-417.

inhibited myotube formation and reduced activity of myogenic regulatory factors (MRFs), such as MyoD and myogenin[15,16]. MyoD determines myoblastic cell fate, and myogenin acts downstream of MyoD by regulating commitment to myogenic differentiation[17]. Upregulation of Id-1 (inhibitor of differentiation/DNA binding-1) by BMP-2 is responsible for reduction of MRF activity by competitively binding E proteins that are necessary for MRF function[18,19].

Runx2, a member of the runt homology domain family of transcription factors, is required for osteoblastic differentiation and endochondral and intramembranous bone formation[20,21]. Heterozygous mutation of the Runx2 gene is implicated in the human skeletal disorder cleidocranial dysplasia[22,23], and the homozygous mutation in mice results in a complete lack of mineralization and immediate postnatal death[21]. We have previously demonstrated that sustained expression of Runx2 in osteogenic and pluripotent cell lines upregulates osteoblast-specific gene expression and induces *in vitro* mineralization in a cell type-dependent manner[24]. These results established the requirement for other cofactors in addition to Runx2 to induce cell-mediated mineralization. These results also demonstrate that increased osteocalcin expression and alkaline phosphatase activity are insufficient markers to define terminal and functional osteoblastic differentiation (e.g. matrix mineralization).

BMP-2-induced osteogenesis has several known points of regulation upstream of Runx2 transcriptional activation. The protein noggin blocks the extracellular interaction of BMPs with their receptors by competitive dimerization[25,26]. The inhibitory smad, Smad6, blocks BMP signaling by physically preventing the interaction between BMP receptors and Smad1/5, and inhibiting subsequent activation[7]. Smad5 signaling can also

be blocked by Smurf1, which targets Smad5 for degradation and thereby facilitates myogenic differentiation and antagonizes BMP-2 induced osteogenesis[27,28]. Finally, Runx2 activity can be directly regulated by other transcription factors such as HES-1, Msx2, Dlx5, and TLE proteins. The basic helix loop helix protein HES-1 promotes Runx2 transcriptional activity in ROS17/2.8 cells through a direct physical interaction[29]. The homeobox protein Msx2 is expressed in proliferating immature osteoblasts and inhibits terminal osteoblastic differentiation, possibly by repressing Runx2 activity[30,31]. Dlx5, another homeobox protein which is expressed in differentiating osteoblasts, is required for BMP-2 induced osteogenesis and modulates Runx2 activity by inhibiting Msx2-mediated suppression[31-33]. TLE1 and TLE2 colocalize with Runx2 in the nucleus and repress its activity via interactions with the Runx2 C-terminal transactivation domain[34]. The numerous levels of regulation in this cascade indicate that signaling via BMP-2 stimulation does not necessarily result in robust and exclusive Runx2 transcriptional activity and other accessory signaling pathways modulate signal transduction. Therefore, it is difficult to derive conclusions about the specific function of Runx2 using BMP-2 induction, whereas direct exogenous expression provides a more accurate depiction of the activity of Runx2 in the absence of extraneous BMP-2 signals.

While numerous studies have assessed the effects of BMPs on myogenic cells, this work evaluates the effect of the downstream transcription factor Runx2 on the differentiation of primary skeletal myoblasts. Transient upregulation of Runx2 in response to TGF-β is not sufficient for osteoblastic differentiation, and it has been suggested that sustained Runx2 expression may be necessary for commitment to the

osteoblastic phenotype[14,99]. Additionally, several groups have observed minimal mineralization capacity of cells transiently expressing Runx2 by adenoviral delivery[56,78]. Therefore, we used retroviral delivery of Runx2 to assess the effects of sustained and significant exogenous expression levels. We have included samples treated with BMP-2 at 300 ng/ml as a reference to the extensive literature involving BMP-2 and myogenic cells. Interestingly, not only did forced expression of this single transcription factor redirect the fate of these cells, but the effect was greater than that of treatment with the BMP-2 growth factor. These results demonstrate that sustained Runx2 expression induces transdifferentiation of primary skeletal myoblasts into an osteoblastic phenotype, including osteogenic gene expression, enzyme activity, and biological mineral deposition.

Materials and Methods

Cell Culture

Primary myoblasts were isolated from the tibialis anterior muscles of adult male Balb/c mice and cultured in selective growth media (Ham's F10, 20% fetal bovine serum, 5 ng/ml bFGF (Promega, Madison, WI), 100 U/ml penicillin G sodium, 100 μg/ml streptomycin sulfate), yielding cultures that were greater than 99% myogenic by desmin staining[100]. Cells were cultured on tissue culture plastic dishes coated with 0.01% type I collagen (Vitrogen, Palo Alto, CA) in a humidified 5% CO_2 atmosphere at 37 ºC. Cell culture media and antibiotics were obtained from Invitrogen (Carlsbad, CA), fetal bovine serum was purchased from Hyclone (Logan, UT), and all other cell culture supplements and reagents were acquired from Sigma (St. Louis, MO).

Retroviral Transduction

The Runx2 retroviral vector[24] uses the promoter activity of the 5' long terminal repeat (LTR) to express a single bicistronic mRNA encoding the murine cDNA for the type II MASNSLF Runx2 isoform[101,102], followed by an internal ribosomal entry site (IRES) and a zeocin resistance-enhanced green fluorescent protein fusion protein (Zeo:eGFP), allowing for noninvasive analysis of transduction efficiency (Fig. 3.1A). Plasmid DNA was purified from transformed E. coli using Megaprep kits from Qiagen (Valencia, CA). Retroviral stocks were produced by transient transfection of helper-virus free ΦNX amphotropic producer cells with plasmid DNA as previously described[24]. ΦNX cells were cultured in growth media (DMEM, 10% fetal bovine serum, 100 U/ml penicillin G sodium, 100 μg/ml streptomycin sulfate) in a humidified 5% CO_2 atmosphere at 37 °C and plated 9 x 10^4 cells/cm^2 24 h prior to transfection. Cells were transfected with 0.5 μg/cm^2 of plasmid DNA, either Runx2 or empty vector (no Runx2 insert), using calcium phosphate coprecipitation and 25 μM chloroquine for 8-12 h prior to refeeding with fresh growth media. Twenty-four hours after the start of the transfection, media was replaced with fresh growth media and dishes were transferred to a humidified 5% CO_2 atmosphere at 32 °C for enhanced stability of retroviral particles. Retroviral supernatants were collected at 48, 60, and 72 h post-transfection, filtered through a 0.45 μm cellulose acetate filter, aliquoted, snap frozen, and stored at -80 °C until use.

Primary myoblasts were cultured up to 12 passages and plated on 0.01% collagen-coated tissue culture polystyrene at 2 x 10^4 cells/cm^2 24 h prior to retroviral transduction[62]. Cells were transduced with 0.2 ml/cm^2 of retroviral supernatant

supplemented with 4 μg/ml hexadimethrine bromide (Polybrene), 5 ng/ml bFGF, and 10% fetal bovine serum, and centrifuged at 2500 rpm (1200 g) for 30 min in a Beckman model GS-6R centrifuge with a swinging bucket rotor. After infection, growth media was reapplied, and the cells were returned to 37°C and transduced again 12-16 h later to increase transduction efficiency. After the final transduction, retroviral supernatants were replaced with differentiation media (αMEM, 10% fetal bovine serum, 100 U/ml penicillin G sodium, 100 μg/ml streptomycin sulfate, 50 μg/ml L-ascorbic acid and 2.1 mM sodium β-glycerophosphate), supplemented with or without 300 ng/ml recombinant BMP-2 (Kamiya Biomedical, Seattle, WA). Cell culture media and BMP-2 were replaced every 3 days until terminal assay. No differences were observed between empty vector retrovirus (negative control) and unmodified cells in all experiments.

Real Time RT-PCR

Total RNA was isolated at 1, 3, and 7 days post transduction using the RNeasy RNA isolation kit (Qiagen). cDNA synthesis was performed on DNaseI-treated (27 Kunitz units/sample) total RNA (1 μg) by oligo(dT) priming using the Superscript™ First Strand Synthesis System for RT-PCR (Invitrogen). Real-time PCR using SYBR Green intercalating dye was performed with the ABI Prism 7700 Sequence Detection System (Applied Biosystems, Foster City, CA, 40 cycles, melting: 15 sec at 95ºC, annealing and extension: 60 sec at 60ºC)[24]. Real-time PCR oligonucleotide primers (Table 3.1) were designed using ABI Primer Express software and purchased from IDTDNA (Coralville, IA). Primer specificity was confirmed by agarose gel electrophoresis and ABI Prism 7700 Dissociation Curve Software. Standards for each gene were amplified from cDNA

using real-time oligonucleotides (Table 3.1), purified using a Qiagen PCR Purification kit, and diluted over a functional range of concentrations. Transcript concentration in template cDNA solutions was quantified from a linear standard curve, normalized to 1 μg of total RNA, and expressed as femtomoles of transcripts per μg of total RNA. Detection limits for each gene were determined by reactions without cDNA and were at least an order of magnitude below the most dilute sample.

Western Blotting

Cells were washed with PBS and lysed in cold radioimmunoprecipitation assay (RIPA) buffer (1% Triton X-100, 1% sodium deoxycholate, 0.1% SDS, 150 mM NaCl, 150 mM Tris-HCl pH 7.2, 350 μg/ml phenylmethylsulfonyl fluoride, 10 μg/ml leupeptin, 10 μg/ml aprotinin, and 1 mM sodium orthovanadate) for 20 min. Lysates were pipetted up and down ~25 times to shear the DNA and then clarified by centrifugation at 10,000g for 10 min. Protein concentration was then determined using a Micro BCA protein assay kit (Pierce, Rockford, IL). Equal amounts of protein (25 μg) were boiled in Laemmli sample buffer (2% SDS, 10% glycerol, 100 mM DTT, 60 mM Tris-HCl pH 6.8, and 0.001% bromophenol blue) for 10 min and separated by SDS-PAGE. Proteins were transferred by electrophoresis onto nitrocellulose membranes and blocked with Blotto (5% non-fat dry milk, 0.02% sodium azide, 0.2% Tween 20 in PBS w/o Ca^{2+}/Mg^{2+}) overnight at 4ºC. Membranes were then incubated with 1 μg/ml anti-AML3 (Oncogene, San Diego, CA) or 9 μg/ml anti-GAPDH (Chemicon, Temecula, CA) in Blotto for 1 h at room temperature under gentle rocking. Membranes were washed in TBS-Tween (20 mM Tris HCl pH 7.6, 137 mM NaCl, 0.1% Tween 20) for 30 min and incubated in

Table 3.1. Oligonucleotides for Real Time PCR

Target cDNA (Accession #)	Sense Primer	Antisense Primer
Runx2 (AF010284)	5'-AGCCTCTTCAGCGCAGTGAC-3'	5'-CTGGTGCTCGGATCCCAA-3'
MyoD (XM_124916)	5'-CGGCTACCCAAGGTGGAGAT-3'	5'-ACCTTCGATGTAGCGGATGG-3'
Myogenin (NM_031189)	5'-CTGACCCTACAGACGCCCAC-3'	5'-TGTCCACGATGGACGTAAGG-3'
Id-1 (XM_130599)	5'-ACGACATGAACGGCTGCTACT-3'	5'-GCTCACTTTGCGGTTCTGG-3'
Osteocalcin (X04142)	5'-CGGCCCTGAGTCTGACAAA-3'	5'-GCCGGAGTCTGTTCACTACCTT-3'
Alkaline Phosphatase (NM_007431)	5'-GGGACTGGTACTCGGATAACGA-3'	5'-CTGATATGCGATGTCCTTGCA-3'
Bone Sialoprotein (L20232)	5'-TCCTCCTCTGAAACGGTTTCC-3'	5'-GGAACTATCGCCGTCTCCATT-3'
Osterix (AF184902)	5'-CCCCTGCTCCTTCTAGGCC-3'	5'-CCGTCAACGACGTTATGCTCT-3'
Dlx5 (NM_010056)	5'-TCAGTACCTCGCCCTGCC-3'	5'-TGTGTTTGCGTCAGTCCTAGAGA-3'
Noggin (NM_008711)	5'-AGCGAGATCAAAGGGCTGG-3'	5'-CTCAGGCGCTGTTTCTTGC-3'
Smad6 (AF010133)	5'-AAGATCGGTTTTGGCATACTGC-3'	5'-CCCCGGTTGTAGGCCC-3'
Msx2 (NM_013601)	5'-CCGCCGCCCAGACATAT-3'	5'-TTCCGGTTGGTCTTGTGTTTC-3'
HES-1 (NM_008235)	5'-GGAGAGGCTGCCAAGGTTTT-3'	5'-GCAAATTGGCCGTCAGGA-3'

secondary antibody (biotin-conjugated anti-rabbit/mouse IgG, 1:20,000 dilution in Blotto, Jackson ImmunoResearch, West Grove, PA) for 1 h at room temperature. Membranes were washed again in TBS-Tween for 30 min and incubated in tertiary antibody (alkaline phosphatase-conjugated anti-biotin IgG, 1:10,000 dilution in Blotto, Sigma) for 1 h at room temperature. After antibody incubation, membranes were washed in TBS-Tween for 30 min and immunoreactivity was detected using ECF fluorescent substrate (Amersham Bioscience, Piscataway, NJ) and a Fuji Image Analyzer.

Immunofluorescence Staining

At 7 days post-transduction, cells were fixed in 70% ethanol:37% formaldehyde:glacial acetic acid (20:2:1) for 10 min and blocked in 5% horse serum for 1 h. Cells were stained for myosin and DNA with mouse anti-sarcomeric myosin antibody MF20 (3.2 μg/ml, Developmental Studies Hybridoma Bank, Iowa City, IA) for 1 h, followed by biotin-SP-conjugated donkey anti-mouse IgG (3.75 μg/ml, Jackson ImmunoResearch) for 1 h, followed by anti-biotin FITC conjugate (10 μg/ml, Sigma) and

ethidium homodimer-2 (200 nM, Molecular Probes, Eugene, OR) for 1 h. Cells were washed twice with PBS and incubated for 10 min in 5% horse serum after each antibody incubation. Images of stained cells were captured using a Nikon Eclipse E400 fluorescence microscope with a 20X objective, SPOT RT camera, and ImagePro Plus image acquisition software (Media Cybernetics, Silver Springs, MD).

Alkaline Phosphatase Biochemical Activity

As a marker of osteoblastic enzyme activity, alkaline phosphatase (ALP) activity was quantified at 7 days post-transduction as previously described[24]. Cells were rinsed and scraped into ice-cold 50 mM Tris·HCl, pH 7.4. Following sonication and centrifugation, total soluble protein concentration was quantified using the MicroBCA Protein Assay Kit. Equal amounts of protein (2.5 μg) were added to 60 μg/mL 4-methyl-umbelliferyl-phosphate fluorescent substrate in diethanolamine buffer (pH 9.5). Following incubation for 60 min at room temperature, the fluorescence was read at 360 nm excitation/465 nm emission on an HTS 7000 Plus BioAssay Reader (Perkin Elmer, Norwalk, CT). Enzymatic activity was standardized using purified calf intestinal alkaline phosphatase (Sigma) and normalized to total protein concentration.

von Kossa Histochemical Analysis

Cultures were fixed in 70% ethanol at 14 and 21 days and examined histochemically for mineralized matrix by von Kossa staining for phosphate deposits. Plates were stained with 5% $AgNO_3$ under uniform light exposure for 30 min, fixed in 5% Na_2SO_3 for 2 min, and air-dried. Mineralized surface area was quantified by

automated capturing and averaging of twenty-four representative 2X images using Image Pro analysis software.

FTIR Spectroscopy

Cell culture samples at 21 days post-transduction were fixed in 100% ethanol, scraped from the culture dish, and dried at 50ºC overnight. Bone samples were scraped from a lyophilized rat cranium. Bulk samples were mixed with KBr (Sigma) and pressed into pellets. Samples were analyzed with a Nicolet Nexus 470 FTIR spectrometer (ThermoNicolet, Madison, WI) equipped with a DTGS detector. 64 scans were acquired at 4 cm^{-1} resolution under N_2 purge.

Data Analysis

All analyses were performed on assays conducted at least three times, each with unique Runx2 retroviral supernatant preparations, and two independent isolates of primary skeletal myoblasts. No differences were observed between unmodified and empty vector transduced cells in all assays. Data are reported as mean ± standard error of the mean (SEM), and statistical comparisons using SYSTAT 8.0 were based on an analysis of variance (ANOVA) and Tukey's test for pairwise comparisons within timepoints, with a p-value < 0.05 considered significant. In order to make the variance independent of the mean, statistical analysis of real-time PCR data was performed following logarithmic transformation of the raw data[24].

Results

Retrovirally transduced cells were analyzed for eGFP expression by fluorescence microscopy and flow cytometry, using a Becton-Dickinson FACS Vantage SE Cell Sorter (Fig. 3.1A). High levels of eGFP were detected in approximately 50% of the cells at 72 h post-transduction. Transgene expression was still detectable at 21 days post-transduction (data not shown), demonstrating sustained and integrated expression of the target gene by the retroviral vector. Runx2 mRNA expression was assessed by real time RT-PCR in transduced cells and samples treated with 300 ng/ml of BMP-2 as a reference to the extensive literature involving BMP-2 and myogenic cells (Fig. 3.1B). Runx2 mRNA expression was upregulated by BMP-2 at 3 and 7 days relative to control cells, and was elevated approximately three orders of magnitude over both BMP-2-treated and control cells in Runx2-transduced cells at all time points. Substantial amounts of Runx2 protein were detected by Western blotting at approximately 60 kDa in transduced samples at 3 and 7 days post-transduction (Fig. 3.1C). Runx2 protein was not detectable in BMP-2 treated cells, likely due to lower levels of the transcription factor present in these samples.

Forced Expression of Runx2 Inhibits Myogenesis

Myogenesis is a complex process, regulated by MRFs, in which mononucleated myoblasts terminally differentiate and fuse into large multinucleated myotubes capable of contraction. Myogenesis was induced in skeletal myoblasts by culture in differentiation media, and gene expression was assessed at 1, 3, and 7 days post-retroviral transduction (Fig. 3.2A).

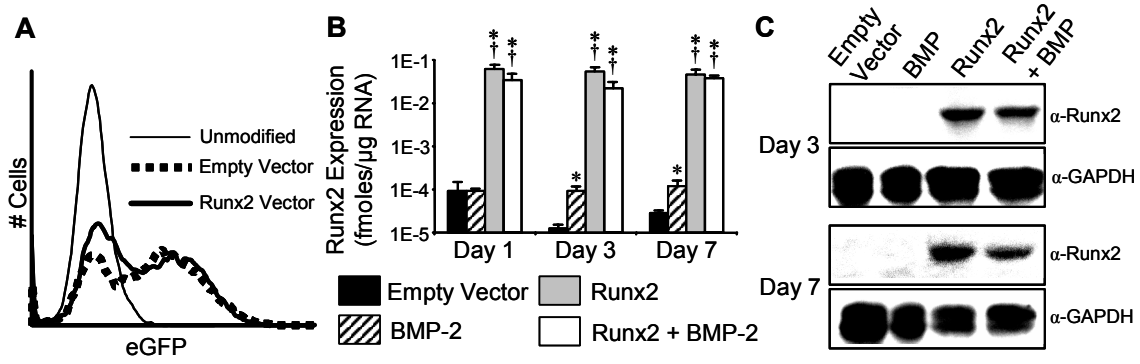

Figure 3.1. Retroviral expression of Runx2 in primary skeletal myoblasts. (A) Detection of transduction efficiency by eGFP expression by flow cytometry at 3 days post-transduction. Unmodified cells were used to detect autofluorescence. Empty vector and Runx2 vector transduced approximately 50% of primary myoblasts. (B) Runx2 mRNA expression determined by real time RT-PCR at 1, 3, and 7 days post-transduction (Mean + SEM, n=6). Runx2 expression was upregulated by BMP-2 at 3 and 7 days and by approximately three orders of magnitude in transduced cultures. * different from Empty Vector, † different from BMP-2, ($p<7E-6$). (C) Runx2 protein levels analyzed by Western blotting at 3 and 7 days. Significant amounts of Runx2 (~60 kDa) were present in transduced cultures, but Runx2 protein was undetectable in BMP-2-treated or empty vector cultures. Blots for GAPDH (~36 kDa) are included as internal loading controls.

MyoD and myogenin mRNA levels were highest in control cells, and were repressed in Runx2-treated samples at day 7, suggesting that Runx2 inhibits myogenesis in these cells. In contrast to the effects of Runx2, BMP-2 treatment did not alter the expression of these MRFs ($p>0.83$). However, mRNA expression of troponin T, a tropomyosin binding molecule and common marker of myogenic differentiation downstream of MRFs, was downregulated by an order of magnitude by both Runx2 and BMP-2 treatments (data not shown).

Expression of Id-1, a known inhibitor of myogenesis, was high at day 1 and decreased in Runx2 transduced cells and controls as differentiation progressed. However, Id-1 mRNA levels remained elevated in BMP-2 treated samples at days 3 and 7, suggesting that Runx2 overexpression and BMP-2 treatment inhibit myogenesis by distinct mechanisms. While Runx2 inhibits expression of MRFs, BMP-2 upregulates expression of an inhibitor of MRF activity (Id-1). This finding could be explained by parallel BMP-2-activated signaling pathways distinct from Runx2 transactivation. Alternatively, saturating levels of Runx2 may upregulate a repressor of Id-1. However, in cultures treated with both Runx2 and BMP-2, Id-1 levels remained high, showing that Runx2 does not repress Id-1 expression, and confirming that Runx2 is only one of several downstream targets of BMP-2 signaling.

Visual inspection by phase contrast microscopy and immunofluorescence staining for sarcomeric myosin confirmed the functional significance of these shifts in mRNA expression (Fig. 3.2B-C). Elongated myotubes were clearly visible in empty vector control cultures at 7 days post-transduction. The formation of myotubes was reduced in BMP-2 treated cultures, and several rounded, mononucleated cells were detectable.

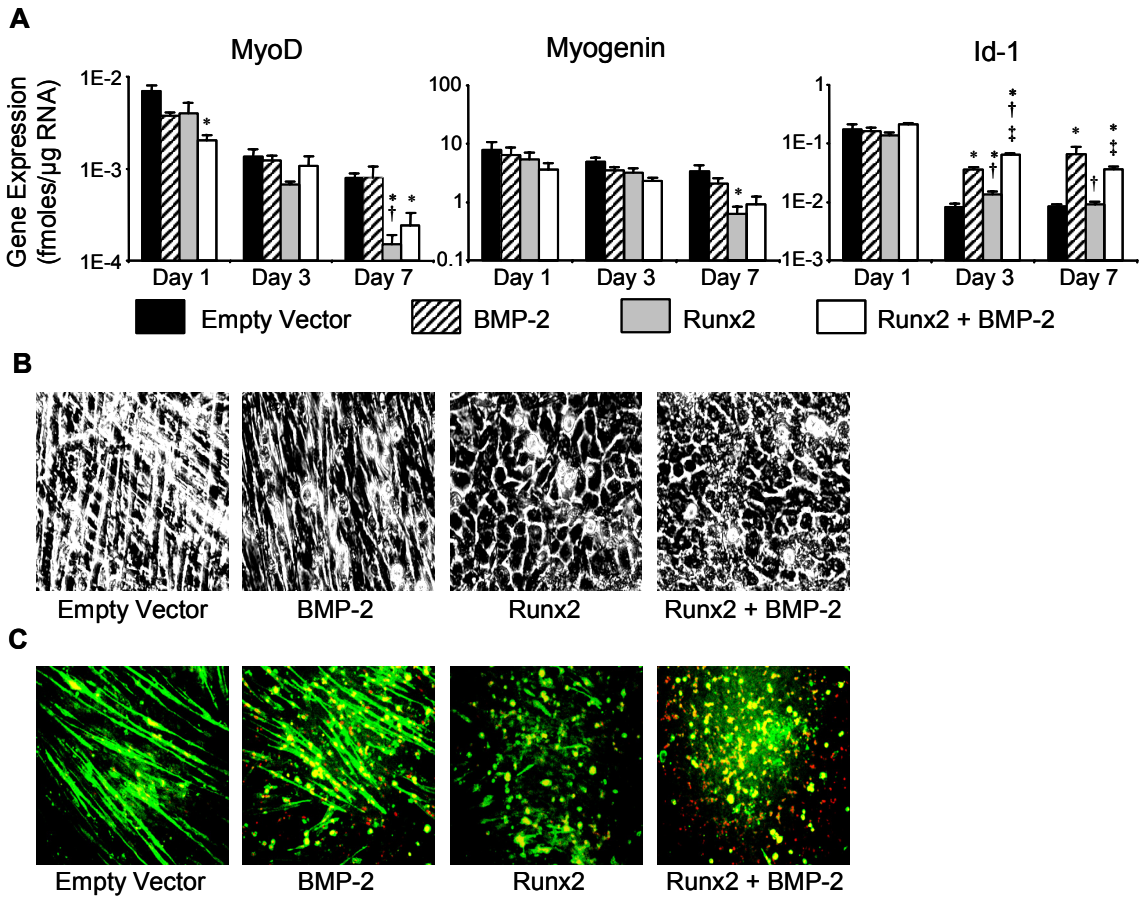

Figure 3.2. Runx2 inhibits myogenesis. (A) Myogenic gene expression was analyzed at 1, 3, and 7 days post-transduction by real time RT-PCR (Mean + SEM, n=6). MyoD mRNA levels were repressed in Runx2 cultures at day 7 and co-treated cultures at days 1 and 7 relative to empty vector controls. MyoD levels in Runx2 cultures were lower than BMP-2 treated cells at day 7. Myogenin expression was repressed in Runx2 cells relative to control cultures at day 7. Id-1 expression was high at day 1 and decreased with time, but remained elevated in BMP-2 treated cells and days 3 and 7. * different from Empty Vector, † different from BMP-2, ‡ different from Runx2 ($p<0.05$). (B) Phase contrast micrographs at 21 days post-transduction. Empty vector cells formed large multinucleated myotubes, while BMP-2 and Runx2 treated cells developed a cuboidal morphology typical of osteoblast cultures. (C) Immunofluorescence staining for sarcomeric myosin at 7 days post-transduction. Elongated multinucleated myotubes were present in control cells. Myotube formation was reduced in BMP-2 treated cultures and no multinucleated structures were visible in Runx2 or dual treated samples.

Runx2 and Runx2/BMP-2 co-treated cultures displayed no multinucleated structures. A fraction of cells remained positive for myosin in Runx2 cultures but were rounded and mononucleated, potentially representing non-transduced cells. Cells treated with either Runx2 or BMP-2 for 21 days developed into a cuboidal cobblestone morphology, typical of osteoblast cultures[103].

Runx2 Upregulates Osteoblastic Gene Expression

Osteogenic gene expression was assessed at 1, 3, and 7 days post-retroviral transduction. The markers of osteoblastic differentiation osteocalcin (OCN), alkaline phosphatase (ALP), bone sialoprotein (BSP), osterix (OSX), and Dlx5 were analyzed to assess the effects of sustained Runx2 expression on osteogenesis in primary skeletal myoblasts (Fig. 3.3). OCN is an extracellular matrix protein and a marker of mature osteoblasts, ALP is an osteoblastic metabolic enzyme involved in mineral deposition, and BSP is an osteoblastic matrix molecule that is responsible for mineralized nodule nucleation[104]. OSX is a zinc-finger transcription factor required for bone mineralization[105] and Dlx5 is an osteoblastic transcription factor shown to accelerate osteoblastic differentiation[106]. Forced Runx2 expression and BMP-2 treatment resulted in upregulated mRNA expression of all five osteogenic genes that generally increased with time (note logarithmic scale). At 7 days, Runx2 overexpression induced greater levels of OCN, BSP, OSX, and Dlx5 mRNA compared to BMP-2 treatment. Co-treatment of Runx2 and BMP-2 resulted in enhanced effects compared to either treatment alone on OCN, BSP, OSX, and Dlx5 expression at early time points. By 7 days the enhanced effect of simultaneous Runx2 and BMP-2 treatment was absent for all genes

except Dlx5, suggesting a time dependent increase in the osteogenic activity of both treatments that was eventually saturated by high levels of Runx2 in transduced cultures. Interestingly, a synergistic effect of co-treatments on Dlx5 expression was present at all time points, suggesting Runx2 acts cooperatively with other BMP-2-induced factors or the existence of Runx2-dependent and Runx2-independent mechanisms for Dlx5 upregulation. Fibronectin and osteopontin, two extracellular matrix proteins produced by osteoblasts, were also upregulated by BMP-2 and Runx2 at 7 days post-transduction (data not shown).

BMP-2 is also known to stimulate mesenchymal progenitor cells into chondrogenic and adipogenic lineages[107,108] and Runx2 has been recently implicated in chondrogenesis[109]. Therefore we assessed alcian blue staining and Sox9 expression for chondrogenesis, and adipsin and PPARγ expression for adipogenesis. No differences were observed for any of these markers amongst treatment groups (data not shown), including empty vector controls and unmodified cells, suggesting that the response to BMP-2 and Runx2 is specific to osteogenesis in these cells.

Sustained Runx2 Induces Functional Osteogenesis

ALP biochemical activity and matrix mineralization were analyzed to assess the functional effects of BMP-2 and Runx2-stimulated osteogenic gene expression. ALP enzymatic activity at 7 days was induced by both Runx2 and BMP-2 (Fig. 3.4). Similar to the trends in expression profiles for several osteogenic genes at 7 days, activity in Runx2-transduced samples was greater than in BMP-2 treated cells, and the combined treatment had no effects over Runx2 alone. von Kossa staining for phosphate deposits

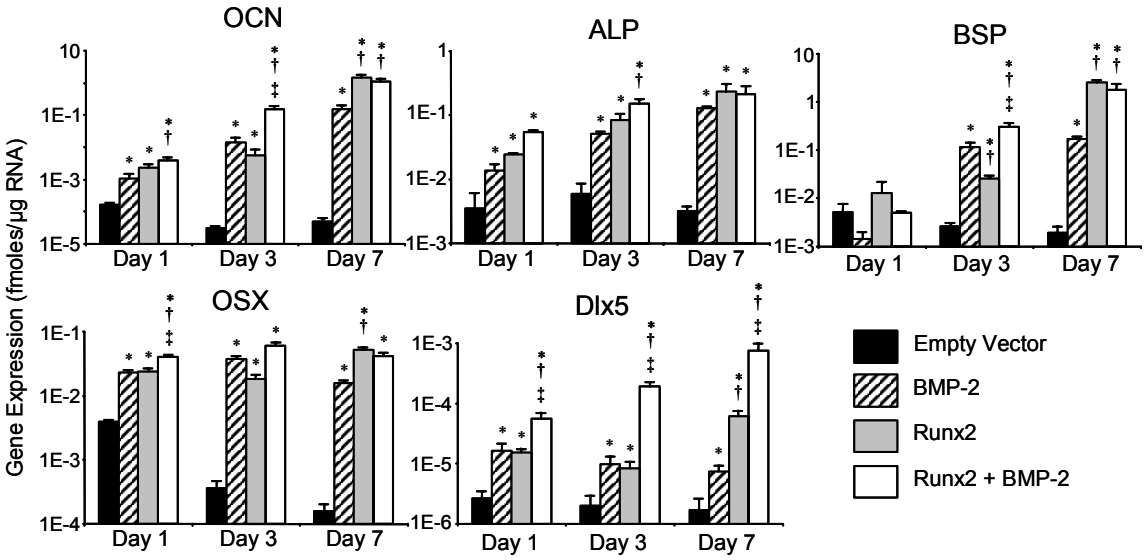

Figure 3.3. Runx2 upregulates osteogenic gene expression. Osteogenic gene expression was evaluated at 1, 3, and 7 days post-transduction by real time RT-PCR (Mean + SEM, n=6). Osteocalcin (OCN), alkaline phosphatase (ALP), bone sialoprotein (BSP), osterix (OSX), and Dlx5 were upregulated by BMP-2 treatment and exogenous expression of Runx2. Retroviral Runx2 expression saturated induction at 7 days for all genes but Dlx5, which showed a synergistic increase in expression with Runx2 and BMP-2 co-treatment. * different from Empty Vector, † different from BMP-2, ‡ different from Runx2 ($p<0.05$).

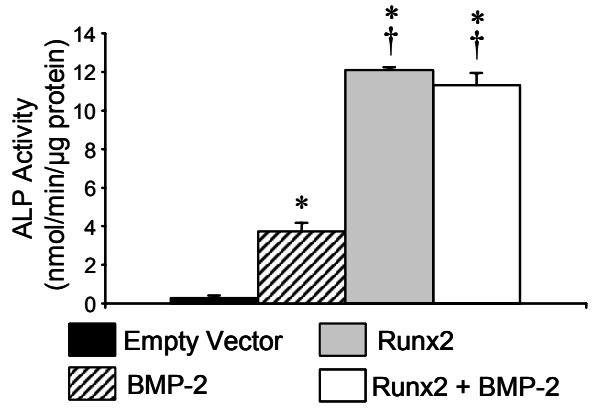

Figure 3.4. Runx2 stimulates alkaline phosphatase biochemical activity. ALP activity was assessed at 7 days post-transduction (Mean + SEM, n=3). ALP activity was undetectable above background in control cells but was upregulated in response to BMP-2. Forced Runx2 expression induced ALP activity levels above controls and BMP-2 samples, and co-treatment with Runx2 and BMP-2 was equivalent to Runx2 alone. * different from Empty Vector, † different from BMP-2 ($p<0.001$).

was used as a marker of matrix mineralization at 14 and 21 days post transduction (Fig. 3.5A). Empty vector control cultures exhibited no mineral deposition, and Runx2-treated samples displayed strong positive stains for phosphate deposits similar to that of MC3T3-E1 premature osteoblasts used as positive controls (data not shown). BMP-2 treated samples developed a light hazy stain, and sparse mineralized nodules were detectable at higher magnifications (Fig. 3.5B). FTIR spectroscopy was used to analyze the chemical composition of the mineral phase in cultures at 21 days post-transduction as well as explanted bone from rat cranium (Fig. 3.5C). Absorption bands representing organic components in the extracellular matrix and lipid content were present in all samples at 1655 cm^{-1} (Amide I, C=O), 1550 cm^{-1} (Amide II, N-H and C-N), 1460 cm^{-1} (CH_2), 1380 cm^{-1} (CH_3), and 1240 cm^{-1} (C-N and N-H)[110]. Bands at 710 and 760 cm^{-1} coincide with aromatic hydrocarbon peaks of a polystyrene standard, representing residual tissue culture plastic in the sample from the harvest procedure. Runx2 and cranial bone samples displayed an enhanced peak at 1100 cm^{-1} (P-O), as well as additional peaks at 870 cm^{-1} (C-O) and a split peak at 600 cm^{-1} (P-O), representing the characteristic bands of a carbonate-containing, poorly crystalline hydroxyapatite[110]. These additional bands were absent in empty vector cultures and barely detectable in BMP-2 treated samples, likely due to minimal mineral deposition as visualized by the von Kossa staining. Samples treated with both Runx2 and BMP-2 produced spectrograms similar to that of Runx2 alone.

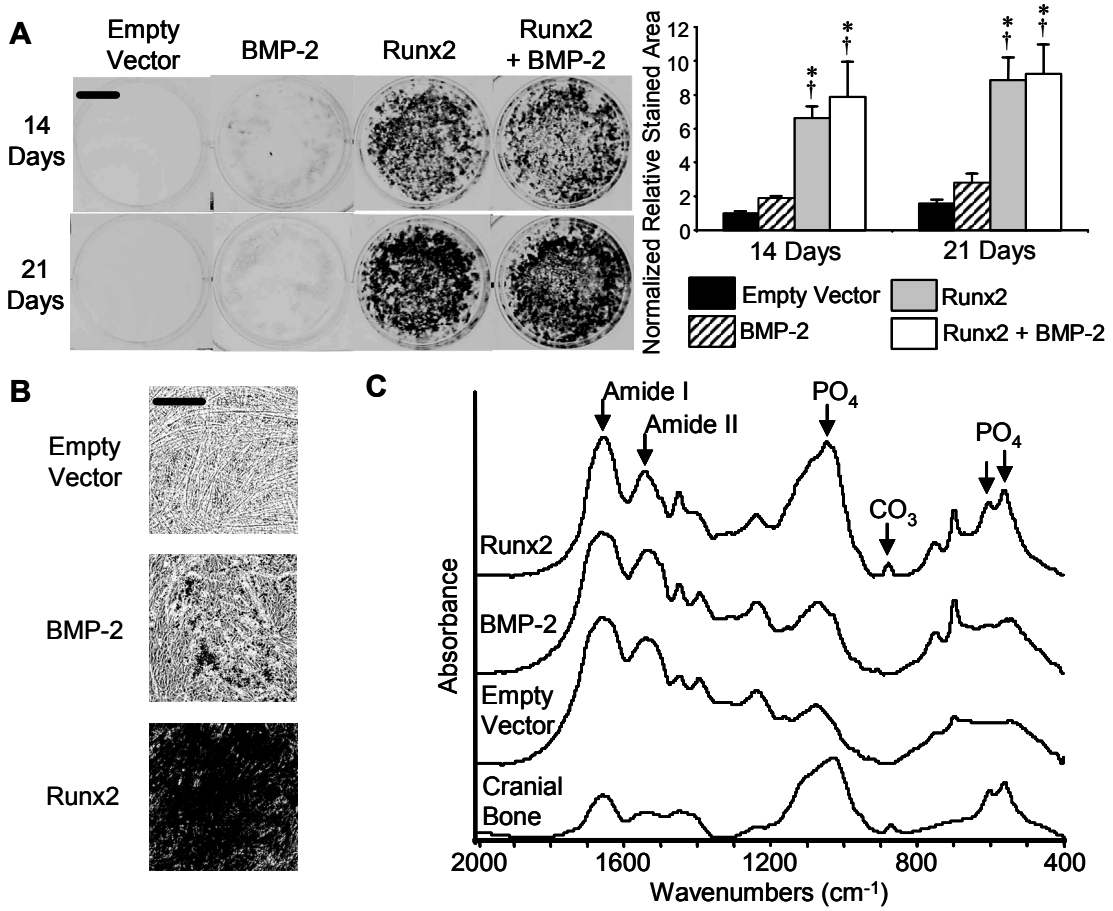

Figure 3.5. Runx2 induces mineral deposition. (A) Matrix mineralization was assessed by von Kossa staining for phosphate deposits at 14 and 21 days post-transduction (Mean + SEM, n=6). Controls contained no stained regions and BMP-2 treatment produced a light hazy stain. Runx2 and co-treated samples developed densely mineralized regions and heavy stains. Stains were quantified by automated capturing and averaging of twenty-four representative 2X images. * different from Empty Vector, † different from BMP-2 ($p<0.05$). Scale bar indicates 10 mm. (B) Sparse nodules were detectable by higher magnification in BMP-2 treated samples. Scale bar indicates 300 μm. (C) Chemical composition of the mineral phase was analyzed by FTIR spectroscopy. Adsorption bands at 1655 cm^{-1} (Amide I, C=O), 1550 cm^{-1} (Amide II, N-H and C-N), 1460 cm^{-1} (CH_2), 1380 cm^{-1} (CH_3), and 1240 cm^{-1} (C-N and N-H) represent bonds in the extracellular matrix and lipid content. Runx2 and cranial bone samples displayed an enhanced peak at 1100 cm^{-1} (P-O), as well as additional peaks at 870 cm^{-1} (C-O) and a split peak at 600 cm^{-1} (P-O), representing the characteristic bands of a carbonate-containing, poorly crystalline hydroxyapatite. These additional bands were absent in empty vector cultures, and were barely visible in BMP-2 treated samples, likely due to minimal mineral deposition as detected by von Kossa staining. Samples treated with both Runx2 and BMP-2 produced spectrograms similar to that of Runx2 alone.

BMP-2 Induces Negative Regulators of Osteogenesis

These results show that Runx2 induces osteoblastic gene expression, enzyme activity, and biological mineralization to higher levels than treatment with the osteogenic growth factor BMP-2. Based on these results, we hypothesized that direct forced expression of Runx2 bypasses several upstream stages of BMP-2 induced control of the osteogenic response. To test this hypothesis, we examined the expression profiles of several osteogenic activators and repressors upstream of Runx2-dependent transcription (Fig. 3.6). Noggin, an inhibitor of BMP-2 activity, was unaffected by Runx2, but was upregulated by BMP-2 at 7 days. Noggin was also upregulated in cultures treated simultaneously with BMP-2 and Runx2. Smad6, an inhibitor of BMP-2 signaling through its activated receptor, and Msx2, a direct inhibitor of Runx2 activity, were upregulated by Runx2 relative to empty vector controls, but expression increased to greater levels with BMP-2 treatment. HES-1, which increases Runx2 activity, was unaffected by Runx2 but was downregulated by BMP-2, and Runx2 rescued the BMP-2 induced suppression in co-treated samples. These results suggest that direct forced expression of Runx2 bypasses parallel signaling pathways stimulated by BMP-2 that mediate the subsequent osteogenic response to this growth factor.

Discussion

Transdifferentiation has been defined as "the conversion of a cell of one tissue lineage into a cell of an entirely distinct lineage, with concomitant loss of the tissue-specific markers and function of the original cell type, and acquisition of markers and function of the transdifferentiated cell type"[111]. The cells used in this study were >99%

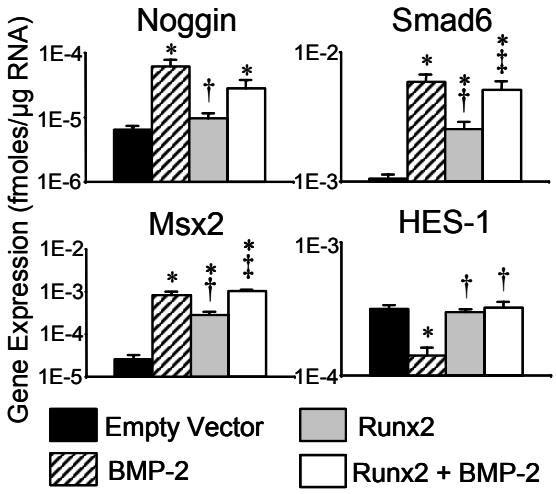

Figure 3.6. Forced expression of Runx2 bypasses BMP-2 stimulated regulatory control of osteogenesis. Regulatory gene expression was evaluated at 7 days post-transduction by real time RT-PCR (Mean + SEM, n=6). Noggin expression was induced by BMP-2 but was unaffected by Runx2. Smad6 and Msx2 were induced by Runx2 relative to controls, but to even greater levels by BMP-2. Co-treatment with Runx2 and BMP-2 did not alter the levels of noggin, Smad6, or Msx2 expression relative to BMP-2 alone. HES-1 was downregulated by BMP-2 but not Runx2, and Runx2 rescued the BMP-2 induced suppression in co-treated cells. * different from Empty Vector, † different from BMP-2, ‡ different from Runx2 ($p<0.03$).

desmin positive, a common marker of myoblastic cell fate, and <5% positive for CD34 or Sca-1 (data not shown), markers of stem cell populations present in muscle tissue[61]. Additionally, these cells have previously been shown to be >99% myogenic[100]. Runx2 overexpression in skeletal myoblasts resulted in the loss of myoblastic markers MyoD and myogenin as well as myotube formation. These cells also gained several osteogenic markers, and more importantly the osteoblastic function of matrix mineralization, demonstrating Runx2-stimulated transdifferentiation. Furthermore, we have observed similar myogenic inhibition and osteoinduction, including mineralization, in Runx2-overexpression experiments with the clonal C2C12 myogenic cell line (unpublished results), providing additional evidence for transdifferentiation.

The osteoinductive effects of BMP-2 on non-osteoblastic cell types are well documented. However, the BMP signaling cascade is remarkably elaborate, involving the coordinated function of numerous ubiquitous signaling molecules including extracellular matrix proteins[112], Smads[7], protein kinase D[113], protein kinase C[114], and mitogen-activated protein kinases (MAPKs)[115-120]. Therefore it is particularly noteworthy that the exogenous expression of a single transcription factor downstream of the many regulators of BMP signaling is capable of reprogramming a committed myogenic cell type into an osteoblastic differentiation cascade. Additionally, forced expression of Runx2 had a more potent osteogenic effect than BMP-2 treatment, which may be explained by several hypotheses. First, we have shown that BMP-2 concomitantly positively and negatively regulates osteogenesis, resulting in a less potent signal, whereas Runx2 overexpression may serve as a more specific osteogenic stimulus. Therefore, the greater osteogenic effect of Runx2 may, in part, be the result of bypassing upstream

regulatory mechanisms by targeting a transcriptional activator downstream of the growth factor signaling pathway. Also, Huard and colleagues have identified a subpopulation of BMP-2 sensitive muscle derived stem cells in myoblast isolates[58,61]. The cells used in the present study may contain a similar subpopulation, resulting in osteogenic induction in only a fraction of the cells. This would result in a reduced amount of osteogenic gene expression and alkaline phosphatase activity, and sparse mineralization, as observed here. In addition, this study uses recombinant BMP-2 expressed in E. coli. BMP-2 is a highly glycosylated protein and proper mammalian post-translational modifications may result in a more potent effect. Additionally, we used 300 ng/ml of BMP-2 as a reference to the vast amount of literature evaluating BMP-2 function at this concentration, but this dosage does not necessarily saturate BMP-2 signaling.

The differential expression of Id-1, noggin, Smad6, Msx2, and HES-1 in response to BMP-2, Runx2, and Runx2 and BMP-2 co-treatments, demonstrate that there are several other factors involved in the regulation of this complex process and that BMP-2 is serving functions in addition to Runx2-dependent osteogenesis in this system. In addition to the negative regulation of osteogenesis mentioned above, Runx2 has been reported to autoregulate its own expression[121]. Therefore, BMP-2-induced Runx2 is capable of self-regulation, whereas the retroviral system drives expression from a viral promoter which acts independently of endogenous osteogenic repression and activation mechanisms. This results in the greater levels of Runx2 mRNA in transduced cultures relative to BMP-2 treatment and represents another control of BMP-2 induced osteogenesis. It is also important to note that these shifts in mRNA levels do not necessarily reflect the magnitude of protein expression and activity, as many genes,

including Runx2, are subject to translational regulation and post-translational protein modification and regulation[122]. Runx2 expression and activity can also respond to other pathways, such as signaling by extracellular matrix proteins, MAPKs, fibroblast growth factor-2, mechanical loading, parathyroid hormone, and tumor necrosis factor-α[112,123-127].

Previous work demonstrated that transient expression of Runx2, via transfection[11], adenoviral transduction[56,78], or TGF-β signaling[14], is not sufficient for conversion of non-osteogenic cells into an osteoblastic phenotype. In the present study, using retroviral transduction, a constitutive Runx2 gene was integrated and expressed at high levels for 21 days *in vitro*. This sustained expression was sufficient for conversion into an osteoblastic phenotype. Previous reports demonstrate that although both BMP-2 and TGF-β induce Runx2 expression in the C2C12 myogenic cell line, only BMP-2 upregulates cofactors necessary for osteoblastic conversion, namely Dlx5[33]. Lee et al. have also shown that Dlx5 antisense can block BMP-2-induced Runx2 expression and osteoblastic conversion, but not TGF-β-induced Runx2 expression. Dlx5 expression was still induced by BMP-2 in Runx2 knockout murine fetal calvarial cells, suggesting that Runx2 does not play a role in Dlx5 expression[128]. In addition, Lee et al. have shown that Dlx5 can upregulate OSX expression independent of Runx2 by transfecting Dlx5 into Runx2 knockout cells. These observations have led to a proposed model of a linear signaling cascade initiated with Smad1/5 activation, followed by Dlx5 expression, resulting in independent upregulation of Runx2 and OSX[128]. However, this model is not consistent with the present results. We demonstrate that Runx2 upregulates both Dlx5 and OSX, and co-treatment with BMP-2 and Runx2 results in a synergistic effect on Dlx5 expression. Taken together with these previous results, the current findings establish

Runx2-dependent and -independent pathways for Dlx5 and OSX expression. This suggests that the observed osteogenesis induced by these transcription factors is not simply defined by a linear signaling cascade, but rather a complex model composed of multiple feedback loops. This model is further strengthened by evidence that exogenous expression of one of the constituents of this cycle results in upregulation of other cycle members.

Osteoblastic differentiation represents a complex process involving numerous signaling cascades which synergize to direct the high order functions of matrix mineralization and bone formation. We have replicated several osteoblastic markers and functions in skeletal myoblasts using forced expression of Runx2. However, not all elements of osteoblasts are represented in these cells, as demonstrated in this study by the absence of regulatory factors such as noggin. Previous studies have identified distinct differences in the chemical and biological makeup of mineralized matrix produced *in vitro* by osteoblasts from different sources[129,130]. This result is not suprising given the wide range of practices involved in cell line development, primary cell isolation and purification, and culturing conditions. Using FTIR spectroscopy, we have identified the mineralized matrix produced by Runx2 overexpressing primary myoblasts as a carbonate containing, poorly crystalline apatite, similar to that produced by primary osteoblast cultures[130].

In conclusion, we have demonstrated Runx2-induced mineralization and functional osteogenesis in primary skeletal myoblasts. This work suggests that sustained Runx2 expression is necessary for conversion into an osteoblastic phenotype and that Runx2 regulates other transcriptional activators critical to osteoinduction, including Dlx5

and OSX. These results assist in elucidating the function of Runx2 in osteogenesis and its role in BMP-2 signaling. This work also provides insights into the plasticity of committed mesenchymal cells and supports the potential of Runx2-induced osteogenesis for therapeutic treatment of osseous defects.

CHAPTER 4

RUNX2-GENETICALLY ENGINEERED SKELETAL MYOBLASTS MINERALIZE COLLAGEN SCAFFOLDS *IN VITRO**

Introduction

Orthopaedic reconstructions have a significant socioeconomic impact worldwide, as evidenced by the 2.2 million operations requiring bone substitutes each year[4]. Existing bone substitutes include autografts, allografts, and synthetic materials[35,36]. Autografting involves the harvest of autogenous bone, typically from the iliac crest, for implantation into an osseous defect. Although successful in many cases, this procedure is limited by the availability of healthy tissue, donor site morbidity, and pain associated with the harvest[4,36]. Allografts, typically cadaver bone from bone banks, suffer from reduced biological and mechanical properties after processing and possible disease transmission[4]. Synthetic materials, including titanium, ceramics, and synthetic hydroxyapatite, generally incite host inflammation and fail to adequately integrate and remodel with the surrounding native tissue[37]. Bone tissue engineering has emerged as a promising alternative to these strategies. The general paradigm of these approaches focuses on incorporating cells, a scaffold, and bioactive factors into an implantable construct[38,39].

Current applications of bone tissue engineering have been hindered by availability of a sustained, mineralizing cell source that can generate mechanically robust constructs for large defects. Terminally differentiated osteoblasts, the cells responsible for bone

* Modified from
C.A. Gersbach, B.A. Byers, G.K. Pavlath, R.E. Guldberg, and A.J. Garcia, *Runx2/Cbfa1-Genetically Engineered Skeletal Myoblasts Mineralize Collagen Scaffolds In vitro.* Biotechnology and Bioengineering, 2004. 88(3):369-378.

formation, are difficult to obtain in large numbers and fail to proliferate and substantially populate typical tissue-engineered constructs. Immortalized osteogenic cell lines have the potential to form tumors *in vivo*. Osteogenic precursors, such as bone marrow stromal cells, are capable of osteoblastic differentiation and mineralization[40], and have been used in many cases to successfully heal bone defects[41-46]. However, these cells are also difficult and painful to obtain in suitable quantities[38], typically de-differentiate and lose phenotype following *in vitro* culture and expansion[47-49], and demonstrate an age-related decrease in osteogenic capacity[50]. A promising alternative to these cell sources is the induction of sustained osteogenesis in non-osteoblastic cells using genetic engineering approaches.

Bone morphogenetic proteins (BMPs) have been used extensively to induce osteogenesis in non-osteoblastic cell types, including bone marrow stromal cells[51-54], dermal and gingival fibroblasts[55,56], and skeletal myoblasts[13,57]. BMP growth factors act extracellularly by binding to transmembrane receptors, inducing an intracellular signaling cascade[7,8]. BMP signaling upregulates the osteoblastic transcriptional activator Runx2/Cbfa1, which acts as a scaffold for several other transcriptional regulators and accessory factors, including Smads[9-11], Cbfβ[131], TLE/Groucho[34], HES-1[29], and AP-1 factors[132]. This composite transcriptional apparatus regulates osteoblastic gene expression and functional osteogenesis[20,24,133]. Runx2 is required for osteoblastic differentiation as well as endochondral and intramembranous bone formation[20,21]. Heterozygous mutation of the Runx2 gene is implicated in the human skeletal disorder cleidocranial dysplasia[22,23], and the homozygous mutation in mice causes immediate postnatal death[21].

Skeletal myoblasts have been used extensively in combination with BMPs to generate bone tissue in both ectopic and osseous environments.[58-60] The positive results of these BMP-based gene therapy strategies with skeletal myoblasts led to our hypothesis that sustained forced expression of Runx2, a downstream regulator of BMP signaling, will stimulate transdifferentiation of primary skeletal myoblasts into a mineralizing osteoblastic phenotype. Primary skeletal myoblasts represent a clinically relevant autologous source of mesenchymal progenitor cells that are readily accessible in large quantities from muscle biopsies. They are easily purified and expanded under the appropriate culture conditions and contain a subpopulation of muscle-derived stem cells[61]. Furthermore, the use of autologous cells in a clinical setting avoids immunological complications involved in allogeneic and xenogeneic cell-based strategies. Myoblasts are also compatible with gene transfer technologies and achieve high levels of transduction by viral gene therapy[62].

In the present study, we demonstrate that Runx2-genetically engineered skeletal myoblasts are a promising cell source for osteoblastic matrix production and *in vitro* mineral deposition on collagen scaffolds. These results are significant in overcoming several limitations of cell-based therapeutic and tissue engineering strategies for the treatment of large osseous defects.

Materials and Methods

Cell Culture

Primary myoblasts were isolated from the tibialis anterior muscles of adult male Balb/c mice and cultured in selective growth media (Ham's F10, 20% fetal bovine serum,

5 ng/ml bFGF (Promega, Madison, WI), 100 U/ml penicillin G sodium, 100 μg/ml streptomycin sulfate), yielding cultures that are greater than 99% desmin positive[100]. Cells were cultured on tissue culture plastic dishes coated with 0.01% type I collagen (Cohesion, Palo Alto, CA) in a humidified 5% CO_2 atmosphere at 37 ºC. Cell culture media and antibiotics were obtained from Invitrogen (Carlsbad, CA), fetal bovine serum was purchased from Hyclone (Logan, UT), and all other reagents were acquired from Sigma (St. Louis, MO).

Retroviral Transduction

The Runx2 retroviral vector[24] uses the promoter activity of the 5' long terminal repeat (LTR) to express a single bicistronic mRNA encoding the murine cDNA for the type II MASNSLF Runx2 isoform[101,102,134], followed by an internal ribosomal entry site (IRES) and a zeocin resistance-enhanced green fluorescent protein fusion protein (Zeo:eGFP), allowing for noninvasive detection of transduction efficiency. Plasmid DNA was purified from transformed E. coli using plasmid megaprep kits from Qiagen (Valencia, CA). Retroviral stocks were produced by transient transfection of helper-virus free ΦNX amphotropic producer cells with plasmid DNA as previously described[24]. Briefly, ΦNX cells were cultured in growth media (DMEM, 10% fetal bovine serum, and 100 U/ml penicillin G sodium, 100 μg/ml streptomycin sulfate) in a humidified 5% CO_2 atmosphere at 37 °C and plated at 9 x 10^4 cells/cm^2 24 hours prior to transfection. Cells were transfected with 0.5 μg/cm^2 of plasmid DNA, either Runx2 or control vector (no Runx2 insert), using calcium phosphate coprecipitation and 25 μM chloroquine for 8-12 hours prior to refeeding with fresh growth media. Twenty-four hours after the start of the

transfection, media was replaced with fresh growth media and cultures were transferred to a humidified 5% CO_2 atmosphere at 32 °C for enhanced stability of retroviral particles. Retroviral supernatants were collected at 48, 60, and 72 hours post-transfection, filtered through a 0.45 μm cellulose acetate filter, aliquoted, snap frozen, and stored at -80 °C until use.

Primary myoblasts were cultured up to 12 passages and plated on 0.01% collagen-coated tissue culture polystyrene at 2 x 10^4 cells/cm^2 24 hours prior to retroviral transduction[62]. Cells were transduced with 0.2 ml/cm^2 of retroviral supernatant supplemented with 4 μg/ml hexadimethrine bromide (Polybrene), 5 ng/ml bFGF, and 10% fetal bovine serum, and centrifuged at 2500 rpm (1200 g) for 30 minutes in a Beckman model GS-6R centrifuge with a swinging bucket rotor. After transduction, growth media was reapplied, and cultures were returned to 37°C and transduced again 12-16 hours later in order to increase transduction efficiency. Control vector (no Runx2 insert) retrovirus served as a negative control for all experiments. After the final transduction, retroviral supernatants were replaced with growth media. Retrovirally transduced cells were analyzed for eGFP expression by fluorescence microscopy and flow cytometry, using a Becton-Dickinson FACS Vantage SE Cell Sorter. Unmodified cells were used to monitor autofluorescence. High levels of eGFP were detected in 51 ± 2% of Runx2-engineered cells and 60 ± 1% of control cells by flow cytometry at 72 hours post-transduction, and no selection protocols were performed to isolate transduced cells.

Scaffold Seeding

Fibrous collagen disks (8 mm x 1.5 mm, Kensey Nash, Exton, PA) were incubated overnight in 10% FBS in phosphate buffered saline (PBS). The average pore size of these scaffolds was 61.7 μm with a 93.7% pore volume, as measured by mercury porosimetry. Forty-eight hours after the second transduction, 500,000 cells in 25 μl of growth media were seeded onto each side of the disk in a non-tissue culture treated 24 well plate. Four hours later, scaffolds were immersed in 2 ml of growth media. After twenty-four hours, scaffolds were transferred to non-tissue culture-treated 12 well plates in 4 ml of differentiation media (αMEM, 10% fetal bovine serum, 100 U/ml penicillin G sodium, 100 μg/ml streptomycin sulfate, 50 μg/ml L-ascorbic acid and 3 mM sodium β-glycerophosphate). Media was replaced every three days until terminal assay.

Cell Viability

Scaffolds were rinsed in PBS and incubated in 4 μM calcein AM and 4 μM ethidium homodimer-1 (Molecular Probes, Eugene, OR) in PBS for 30 minutes under gentle agitation. After incubation, scaffolds were rinsed (3 x 10 min) in PBS and analyzed with a Zeiss LSM 510 Confocal Microscope using Ar and HeNe lasers and a 5X objective lens. The eGFP signal from cells not loaded with calcein was undetectable by confocal microscopy at this low magnification. Images acquired from scaffolds seeded with unmodified cells were similar to those of genetically modified cells, confirming that green fluorescence observed by confocal microscopy was due to the presence of calcein, and not eGFP.

DNA Content

Constructs were rinsed with PBS and frozen at -80°C at 1, 21, and 42 days post scaffold seeding. Scaffolds and serially diluted cell standards were thawed, lyophilized, and digested at 60°C in 500 μl of 0.25 mg/ml proteinase K (Fisher Scientific) in 100 mM ammonium acetate (pH 7.0) for 24 hours. Digested samples were assessed for DNA content with the PicoGreen dsDNA Quantitation Kit (Molecular Probes). Raw data were converted to cell number using a linear standard curve. DNA content of scaffolds seeded with genetically modified cells was similar to that of scaffolds seeded with unmodified cells, confirming that proteinase K digestion of eGFP ablated any residual endogenous fluorescence.

Real Time RT-PCR

Total RNA was isolated at 7 and 21 days post scaffold seeding using the RNeasy isolation kit with RNAlater stabilization reagent (Qiagen). cDNA synthesis was performed on DNaseI-treated (27 Kunitz units/sample) total RNA (0.5 μg) by oligo(dT) priming using the Superscript™ First Strand Synthesis System for RT-PCR (Invitrogen, Carlsbad, CA). Real-time PCR using SYBR Green intercalating dye was performed with the ABI Prism 7700 Sequence Detection System (Applied Biosystems, Foster City, CA) (40 cycles, melting: 15 sec at 95ºC, annealing and extension: 60 sec at 60ºC)[24]. Real-time PCR oligonucleotide primers were designed using ABI Primer Express software and purchased from IDTDNA (Coralville, IA). Primer specificity was confirmed by agarose gel electrophoresis and ABI Prism 7700 Dissociation Curve Software. Runx2 (Accession # NM_009820) primer sequences were 5'- GGCCTTCAAGGTTGTAGCCC -3'

(forward) and 5'- CCCGGCCATGACGGTA -3' (reverse); myoD (Accession # XM_124916) primers were 5'-CGGCTACCCAAGGTGGAGAT-3' (forward) and 5'-ACCTTCGATGTAGCGGATGG-3' (reverse); myogenin (Accession # NM_031189) primers were 5'-CTGACCCTACAGACGCCCAC-3' (forward) and 5'-TGTCCACGATGGACGTAAGG-3' (reverse); troponin T (Accession # AJ131711) primer sequences were 5'-TCAATGTGCTCTACAACCGCA-3' (forward) and 5'-ACCCTTCCCAGCCCCC-3' (reverse). All other primer sequences have been described previously[24]. Standards for each gene were amplified from cDNA using real-time oligonucleotides, purified using a Qiagen PCR Purification kit, and diluted over a functional range of concentrations. Transcript concentration in template cDNA solutions was quantified from a linear standard curve and normalized to 1 μg of total RNA. Detection limits for each gene were determined by reactions without cDNA and are represented by dotted lines where applicable.

Micro-computed Tomography

In vitro mineralization of 3-D scaffolds was quantified by high resolution X-ray micro-computed tomography (micro-CT) using a Scanco Medical μCT 40 imaging system (Bassersdorf, Switzerland). Specimens were scanned in formalin at 16 μm voxel resolution and evaluated at a threshold corresponding to a linear attenuation of 0.88 cm^{-1}, filter width of 1.2, and filter support of 2.0. The reconstructed and thresholded 3-D images were evaluated using direct distance transformation methods to calculate mineralized matrix volume within each construct[135].

Histological Analysis

Formalin-fixed constructs were paraffin embedded, and 5 μm sections were stained with hematoxylin-eosin to observe cellular distribution or von Kossa-nuclear fast red to detect phosphate deposits in the 3-D collagen scaffolds.

FTIR Spectroscopy

Scaffolds at 42 days post-transduction were fixed in 100% ethanol and dried at 50ºC overnight. Bone samples were scraped from a lyophilized rat cranium and used as a positive control. Bulk samples were mixed with KBr (Sigma) and pressed into pellets. Samples were analyzed with a Nicolet Nexus 470 Fourier transform infrared (FTIR) spectrometer (ThermoNicolet, Madison, WI) equipped with a DTGS detector. Sixty-four scans were acquired at 4 cm^{-1} resolution under N_2 purge.

Mechanical Testing

Scaffolds were rinsed in PBS, measured for height and diameter, submerged in PBS, and analyzed by unconfined compression with solid platens at 0.15 mm per minute after preloading with 0.02 N, with a DDL Info 650R uniaxial electromechanical testing system (TestResources, Shakopee, MN). Stress-strain data were determined from load and displacement measurements after normalization by area and height, respectively. Stress-strain curves were characterized by a toe-in region, followed by a linear elastic segment, before a distinct failing region. Compressive modulus was determined by the slope of the linear elastic region of the stress-strain curve from immediately after the toe-in region to before yielding.

Data Analysis

All analyses were performed in triplicate in independent experiments conducted at least two times, each with unique Runx2 retroviral supernatant preparations and two independent isolates of primary skeletal myoblasts. No differences were observed between unmodified and control vector transduced cells for all assays. Data are reported as mean ± standard error of the mean (SEM), and statistical comparisons using SYSTAT 8.0 were based on an analysis of variance (ANOVA) and Tukey's test for pairwise comparisons with a p-value less than 0.05 considered significant. In order to evaluate the variance independent of the mean, statistical analysis of real-time RT-PCR data was performed following logarithmic transformation of the raw data[24].

Results

Cellular Viability

DNA content was assessed at 1, 21, and 42 days post-seeding to determine seeding efficiency and cell numbers throughout the culture period (Fig. 4.1A). No differences between Runx2-engineered and control cultures were observed at any time point. Approximately 450,000 cells were present on scaffolds at 1 day, corresponding to a cell seeding efficiency of 44.8 ± 1.5%. DNA content decreased with time for both treatments, possibly due to the removal of nonadherent cells still present in the scaffolds at earlier time points or cell death resulting from mass transfer limitations after matrix and mineral deposition at the surface of the mature construct. Nevertheless, significant amounts of cells were present on the scaffolds after six weeks of *in vitro* culture.

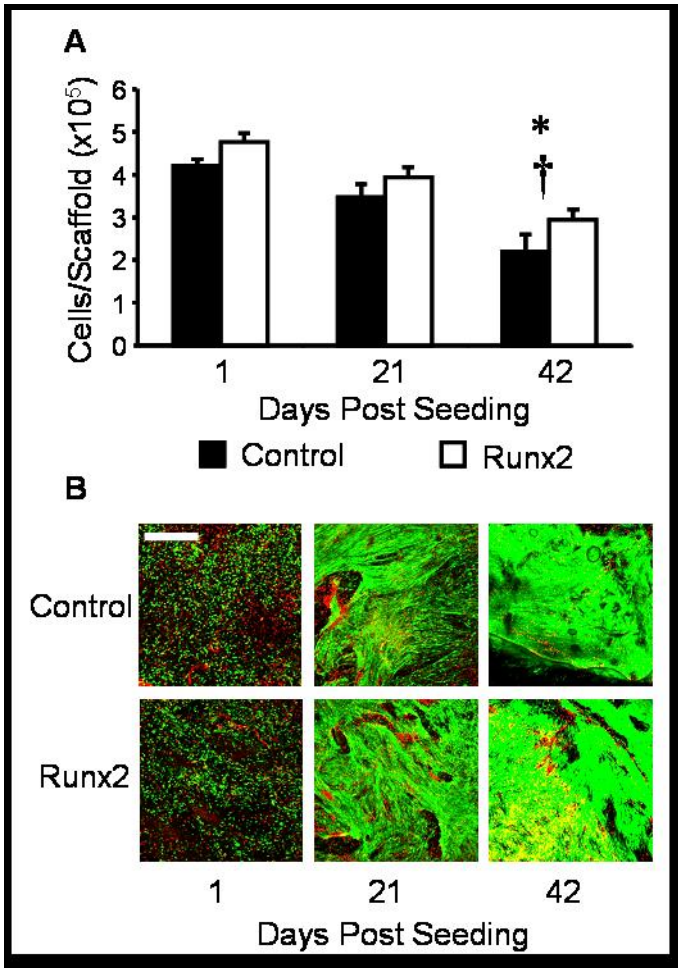

Figure 4.1. Cell number and viability on collagen scaffolds. (A) DNA content was used to evaluate cell number over culture time (mean + SEM, n=6). Approximately 450,000 cells were present on scaffolds 1 day post-seeding, representing a seeding efficiency of 44.8 ± 1.5%. DNA content decreased with time, although large numbers of cells were still present after six weeks of *in vitro* culture. * different from 1 Day ($p<2E-5$). † different from 21 Days ($p<0.004$). (B) Live/dead staining confirmed cell viability at the construct periphery at all time points. Cells were rounded at 1 day and were spread and confluent on the construct surface at later time points. Scale bar = 1 mm.

Cell viability was assessed by Live/Dead fluorescence staining throughout six weeks of culture and no differences were evident between treatments (Fig. 4.1B). Dense cell populations were present at the construct surface at all time points. At one day post-seeding cells were rounded, but at later time points they were spread and confluent. Minimal cell death (<10%) was observed throughout the constructs, as determined by ethidium incorporation, although few isolated small necrotic regions were present.

Osteogenic and Myogenic Gene Expression

Osteogenic and myogenic gene expression was analyzed via real-time RT-PCR at 7 and 21 days post seeding (Fig. 4.2). Runx2 expression was upregulated 10- and 100-fold in transduced cultures at 7 and 21 days, respectively. Alkaline phosphatase (ALP) is an enzyme responsible for phosphate precipitation and mineral incorporation[104]. Osteocalcin (OCN), bone sialoprotein (BSP), and collagen α1 (I) (COLα1(I)) are osteoblastic extracellular matrix molecules present in bone and markers of osteoblastic differentiation[104]. Runx2 overexpression significantly upregulated all four of these osteoblastic markers by as much as 10,000-fold relative to controls. MyoD and myogenin are transcriptional activators that belong to the family of myogenic regulatory factors (MRFs). MyoD determines myoblastic cell fate, and myogenin acts downstream of MyoD by regulating commitment to myogenic differentiation[17]. Expression of both of these MRFs was downregulated by Runx2 overexpression. Troponin T, a tropomyosin binding molecule and common marker of myogenic differentiation downstream of MRFs, was also repressed by Runx2. Shifts in mRNA expression were detectable as early as one day post-transduction in these cells (data not shown) and other cell types with the same

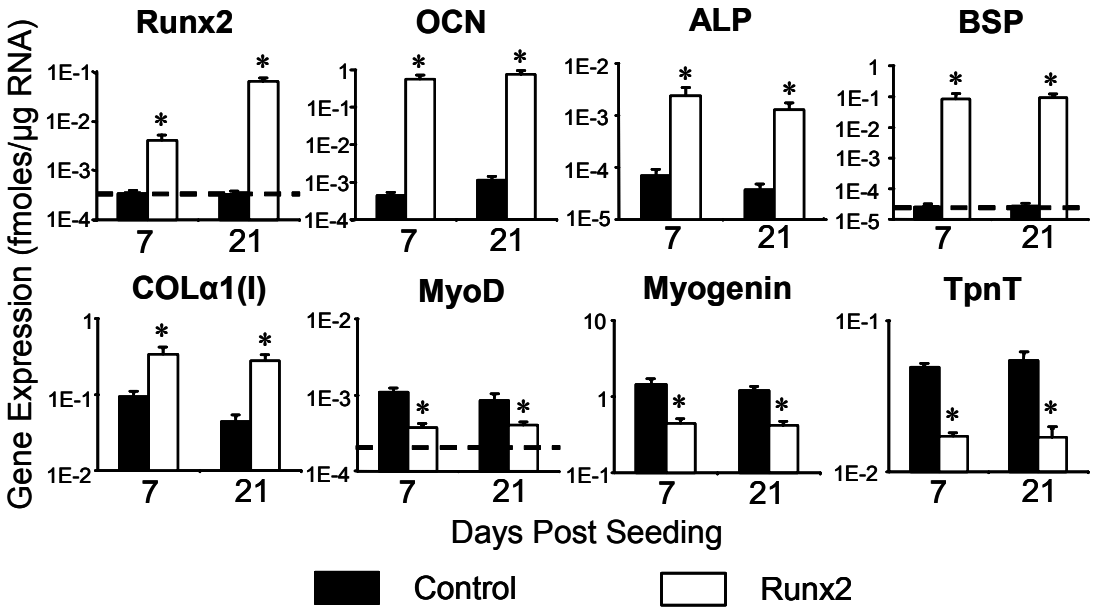

Figure 4.2. Runx2 induces osteogenic and represses myogenic gene expression in skeletal myoblasts cultured in 3-D collagen scaffolds. Gene expression was analyzed at 7 and 21 days post-transduction by real time RT-PCR (mean + SEM, n=6). Runx2 upregulated the expression of osteoblastic genes osteocalcin (OCN), alkaline phosphatase (ALP), bone sialoprotein (BSP), and collagen α1 (I) (COLα1(I)). Runx2 downregulated myogenic gene expression, including MyoD, myogenin, and troponin T. * different from control ($p<0.05$). Dotted line represents assay detection limit.

retroviral vector[24]. These results demonstrate that forced expression of Runx2 in skeletal myoblasts induces osteoblastic gene expression and represses the myogenic phenotype in three-dimensional culture.

Runx2 has also been implicated in chondrogenesis[109], and muscle derived cells are capable of both chondrogenic[107] and adipogenic[136] pathways. Therefore we assessed alcian blue staining and Sox9 expression for chondrogenesis, and adipsin and PPARγ expression for adipogenesis in monolayer culture (data not shown). No differences were observed for any of these markers amongst treatment groups, including empty vector controls and unmodified cells, suggesting that the response to Runx2 is specific to osteogenesis in these cells.

Mineral Deposition and Cellular Distribution

Mineral deposition on collagen scaffolds was quantified by microCT at 21 and 42 days post-seeding (Fig. 4.3). Mineralized regions were detected primarily on the sides of the scaffold at 21 days, and mineralization spread to the face of the constructs by 42 days. Mineralization was confined to the periphery of the scaffolds (Fig. 4.4B), which is typical of constructs cultured under static conditions due to limitations in mass transport of nutrients and waste products. No mineralization was detectable in constructs seeded with control myoblasts.

Histological analyses were used to evaluate cellular distribution and matrix mineralization throughout the scaffold. Staining by von Kossa revealed mineralized regions on the sides of the construct containing Runx2-modified cells at 21 days, and across the face of the scaffold at 42 days, corroborating microCT results (Fig. 4.4A).

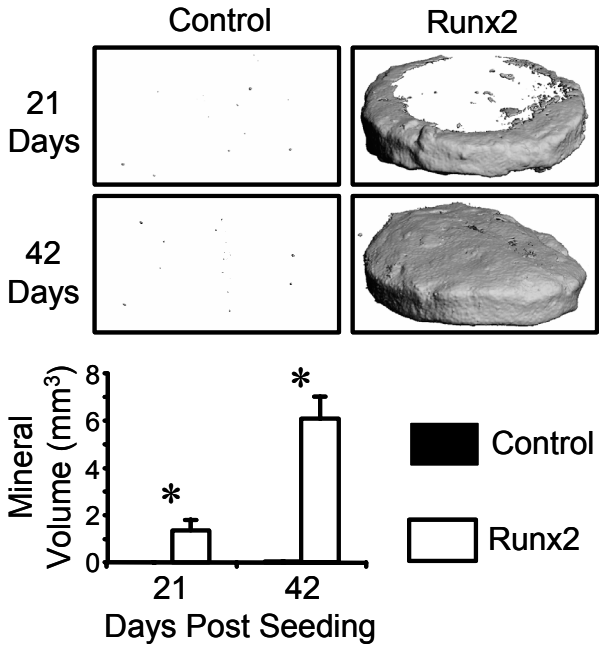

Figure 4.3. Runx2-expressing skeletal myoblasts deposit mineralized matrix on collagen scaffolds. Mineralized regions on tissue-engineered constructs were detected by microCT (mean + SEM, n=6). Control myoblasts demonstrated no mineral deposition. Mineralization initiated on the sides of the collagen disk, as seen at 21 days, and spread to the face of the disk at later time points (42 days). * different from control ($p<0.03$).

Regions positive for von Kossa staining were confined to the outer 100-200 μm of the scaffold. No von Kossa staining was evident on scaffolds seeded with control cells. Hematoxylin-eosin staining at 42 days showed dense cell populations only at the periphery of constructs seeded with both Runx2-modified and control cells, indicating that cells were unable to penetrate or survive in the construct interior (Fig. 4.4C).

FTIR spectroscopy was used to analyze the chemical composition of the mineral phase in scaffolds at 42 days post-transduction (Fig. 4.5). Explanted bone from rat cranium was used as a control. Absorption bands representing peptide bonds in the collagen scaffold and deposited extracellular matrix were present in all samples at 1655 cm^{-1} (Amide I, C=O) and 1550 cm^{-1} (Amide II, N-H and C-N)[110]. Runx2 and cranial bone samples displayed an enhanced peak at 1100 cm^{-1} (P-O), as well as an additional peak at 870 cm^{-1} (C-O) and a doublet at 600 cm^{-1} (P-O), representing the characteristic bands of a carbonate-containing, poorly crystalline hydroxyapatite, the mineral phase of bone[110]. These additional bands were absent in control cultures.

Mechanical compression testing at 42 days post-seeding was used to determine the contribution of the mineral phase to the mechanical integrity of the constructs (Fig. 4.6). Scaffolds seeded with Runx2-treated cells exhibited an elastic modulus of 78.0 ± 12.8 kPa, a 30-fold increase over control scaffolds.

Discussion

This work demonstrates the ability of Runx2-overexpressing primary skeletal myoblasts to form three-dimensional mineralized tissue-engineered constructs *in vitro*. Skeletal myoblasts, genetically engineered to overexpress Runx2, were viable on fibrous

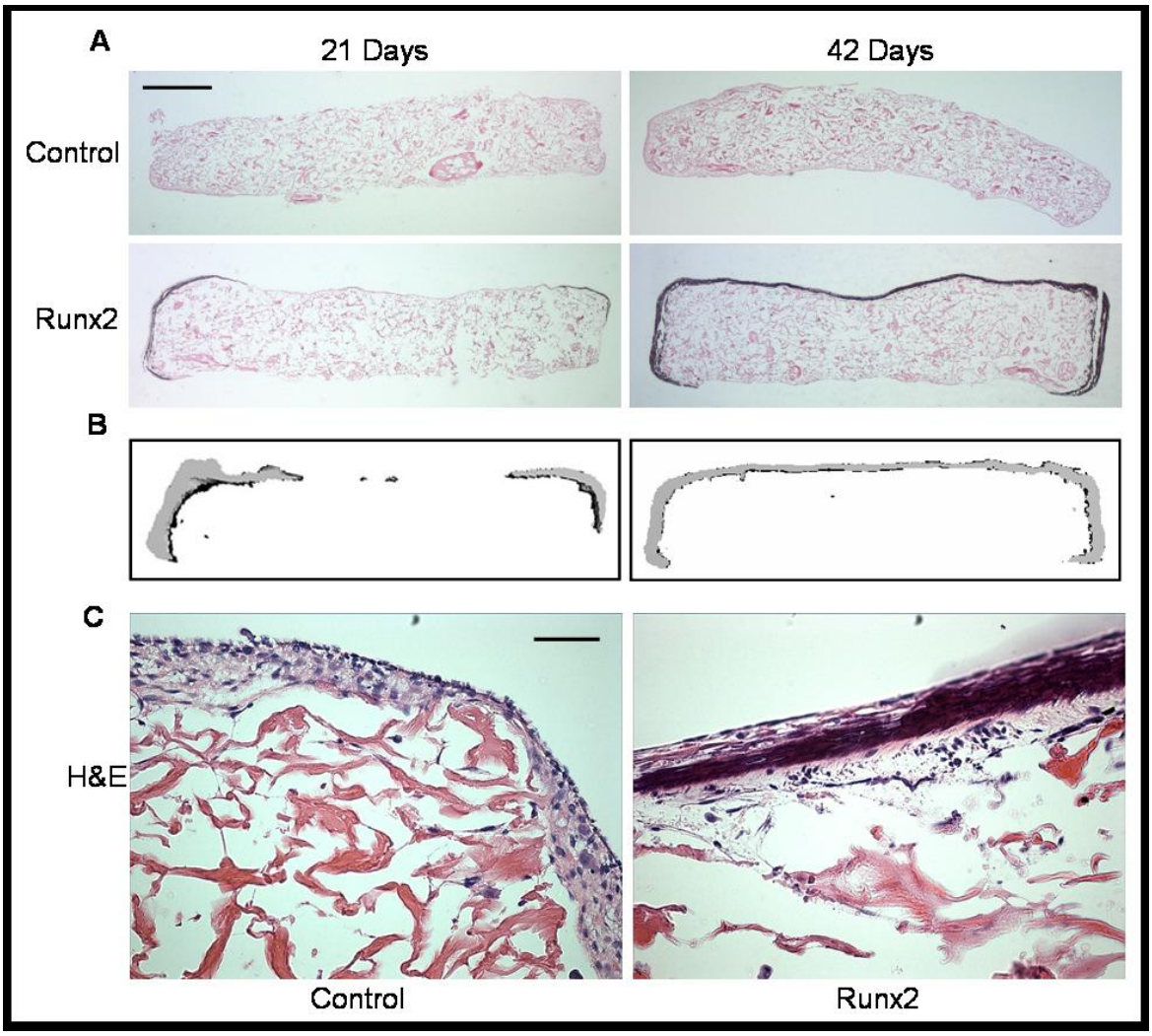

Figure 4.4. Histological analysis of cell-seeded collagen scaffolds. (A) Phosphate deposits in the mineralized matrix were visualized by von Kossa-nuclear fast red staining. von Kossa positive regions were isolated to the periphery of the scaffold. Scale bar = 1 mm. (B) Cross sections of reconstructed microCT images of Runx2-engineered constructs at 21 and 42 days post-seeding, demonstrating mineralization confined to the borders of the scaffold and corroborating von Kossa staining. (C) Hematoxylin-eosin (H&E) staining at 42 days assessed cellular distribution in the construct. Cells (purple) were present at the edge of the scaffold, and did not penetrate into the interior of the collagen scaffold (pink). Scale bar = 250 μm.

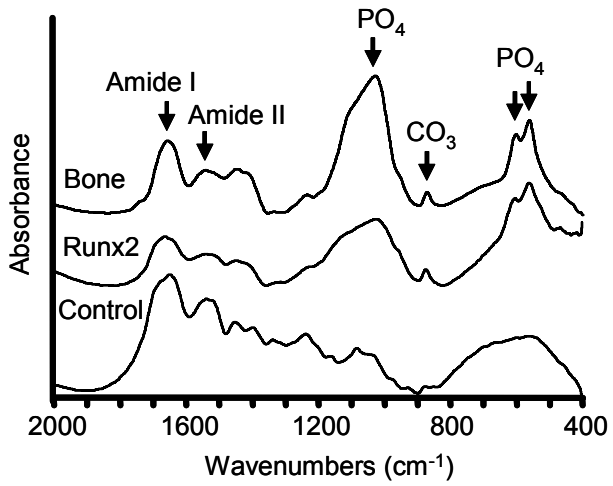

Figure 4.5. Chemical composition of the mineral phase was analyzed by FTIR spectroscopy. Adsorption bands at 1655 cm^{-1} (Amide I, C=O) and 1550 cm^{-1} (Amide II, N-H and C-N) represent bonds in the extracellular matrix and lipid content. Runx2 and cranial bone samples displayed an enhanced peak at 1100 cm^{-1} (P-O), as well as additional peaks at 870 cm^{-1} (C-O) and a split peak at 600 cm^{-1} (P-O), representing the characteristic bands of a carbonate-containing, poorly crystalline hydroxyapatite. These additional bands were absent in control cultures.

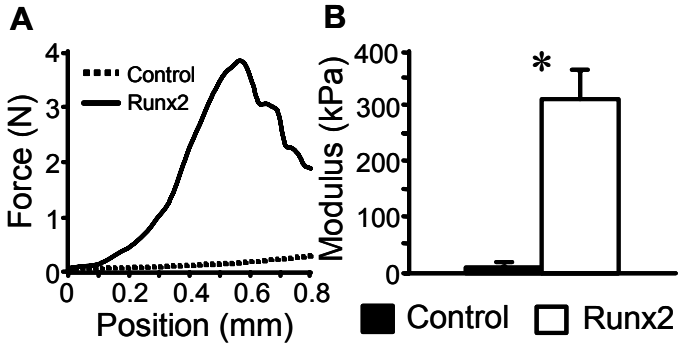

Figure 4.6. Mechanical compression testing of cell-seeded scaffolds. Constructs were compressed in PBS using a DDL Info 650R electromechanical testing system. (A) Representative raw data recorded as load versus position. (B) Raw data was normalized by construct area and height to determine elastic modulus (mean + SEM, n=9). Runx2 scaffolds exhibited a modulus of approximately 78.0 ± 12.8 kPa, a 30-fold increase over controls. * different from control ($p<4E-5$).

collagen scaffolds, upregulated osteogenic gene expression, downregulated myogenic gene expression, and deposited mineralized regions of hydroxyapatite at the periphery of the constructs, as detected by microCT, histological analysis, and FTIR spectroscopy. Cell distribution was confined to the construct periphery (~100-200 μm), a common phenomena associated with transport limitations of static *in vitro* culture[137-139]. Mineral deposition typically occurred on only one face of the collagen scaffold at 42 days post-seeding, potentially due to scaffold processing artifacts or cell localization as a result of the static cell seeding protocol. Although the mineral deposition was localized to the periphery, it was still sufficient to improve the mechanical integrity of the constructs 30-fold. While the elastic modulus of these mineralized constructs was several orders of magnitude below that of native trabecular bone (~80 MPa), optimization of this system, including dynamic culture conditions, may improve both the distribution of mineralized matrix and mechanical properties of the constructs.

Osteoblastic differentiation represents a complex process involving numerous signaling cascades which synergize to direct the high order functions of matrix mineralization and bone formation. We have replicated several osteoblastic markers and functions in skeletal myoblasts using forced expression of Runx2. However, not all required elements for physiological bone formation are present in these *in vitro* cultures. This is evident by the absence of osteoid and the morphological features of native lamellar bone tissue in the histological analysis in Figure 4.4 and other studies assessing the *in vitro* maturation of tissue engineered constructs seeded with a mineralizing cell source[140,141]. Previous studies have also identified distinct differences in the chemical and biological makeup of von Kossa-positive material and mineralized matrix produced

in vitro by osteoblasts from different sources[129,130]. This result is not surprising given the wide range of practices involved in cell line development, primary cell isolation and purification, and culturing conditions. Using FTIR spectroscopy, we have identified the mineralized matrix produced by Runx2 overexpressing primary myoblasts as a carbonate containing, poorly crystalline apatite, similar to that produced by primary osteoblast cultures[130]. Therefore, although the tissue-engineered constructs produced by the genetically engineered myoblasts are not necessarily identical in physical structure to native bone, they do replicate the physiological composition of bone tissue, and thus are a promising prospect for the healing of osseous defects.

Several groups have shown that dynamic perfusion culture of cell-seeded scaffolds improves cellular viability, proliferation, and matrix mineralization throughout the scaffold[137-139,141]. Additionally, architectural, mechanical, and biological properties of the scaffold play an equally important role as cell behavior in developing a successful tissue-engineered construct[142,143]. We selected collagen-based scaffolds because this biological material has been used and characterized extensively for numerous medical applications including tissue engineering[144,145]. Collagen scaffolds are biocompatible, biodegradable, and generally exhibit weak antigenicity *in vivo*. In contrast to many polymeric scaffolds, collagen matrices are both osteoconductive and osteoinductive by playing a functional role in osteoblastic signaling and differentiation[112,146-148].

Previous studies have demonstrated minimal mineralization by cells expressing Runx2 via a transient adenoviral vector[56,78]. In contrast, the present results show significant levels of mineralization using sustained Runx2 expression from an integrated retroviral vector. This suggests that sustained and/or threshold levels of Runx2

expression may be necessary for induction of matrix mineralization and conversion of non-osteogenic cells into a mineralizing osteoblastic phenotype. It is not surprising that prolonged expression of an exogenous osteogenic factor is necessary to effect long-term functions such as matrix mineralization. Furthermore, we have previously established cell-type dependence of Runx2-induced mineralization[24], demonstrating the importance of cell source selection for bone tissue engineering applications. Ongoing assessment of the osteogenic capacity of the skeletal myoblasts used in this study, including *in vivo* performance and direct comparison of Runx2- and BMP-based gene therapy strategies, is necessary to completely evaluate their utility for bone tissue engineering.

This work is fundamentally different from BMP-based gene therapy strategies, which rely on both autocrine signaling by the genetically engineered cells and paracrine signaling by the secreted growth factor to neighboring endogenous cells, resulting in a hybrid bone tissue consisting of both native and implanted cells[55,76,149]. Although these strategies have been very successful in stimulating bone formation in both ectopic and osseous environments[51,55,57,150], they are still hampered by inadequate control of release kinetics, dosage, and potency. In contrast, this transcription factor-based approach consists solely of an autocrine signal, resulting in an osteogenic response only by the genetically engineered cells. Although this method does not take advantage of osteogenic induction of neighboring cells, it may avoid aberrant effects of unregulated growth factor secretion and provide a more controllable *in vivo* environment after ex vivo genetic modification. Additionally, the ability of genetically engineered cells to mineralize and promote construct maturation *in vitro*, prior to implantation, may play an important role in the ultimate success of healing bone defects via tissue engineering. In

fact, we have previously shown that *in vitro* development of mature mineralized scaffolds synergistically enhances ectopic mineralization *in vivo*[77], suggesting that a cell source capable of *in vitro* mineralization may enhance the *in vivo* performance of these implants. In addition to Runx2- or BMP-based approaches, several groups have identified other mechanisms for osteoinduction. Yang et al. have demonstrated a synergistic effect of combined Runx2 and BMP-2 adenoviral treatments on the C3H10T1/2 pluripotent cell line[78], and exogenous expression of other osteogenic factors, such as LMP-1[151] and Dlx5[106], also enhances osteoblastic differentiation and matrix mineralization.

In summary, this work demonstrates Runx2-genetically engineered primary skeletal myoblasts convert into an osteogenic lineage and mineralize collagen scaffolds *in vitro*. These cells have the potential to overcome many cell sourcing obstacles of bone tissue engineering, including availability and preservation of function. This strategy also establishes the potency of using genetic engineering techniques to target downstream high-order regulatory transcription factors to control cell function for tissue engineering applications.

CHAPTER 5

IN VITRO AND *IN VIVO* OSTEOBLASTIC DIFFERENTIATION OF RUNX2- AND BMP-2-ENGINEERED SKELETAL MYOBLASTS*

Introduction

Orthopedic substitutes are required for 2.2 million surgeries each year[4]. Bone tissue engineering has emerged as a promising approach to address the limitations of autogenous bone grafts, allografts, and synthetic implants[4,35-37]. This strategy incorporates cells, a biodegradable scaffold, and bioactive factors into an implantable construct[38,39]. However, a suitable autologous osteogenic cell source has been difficult to identify due to availability[38], dedifferentiation following *in vitro* expansion[47-49], and an age-related loss of phenotype[50]. Therefore genetic engineering of readily accessible non-osteoblastic cell types and progenitor cells, such as skeletal myoblasts, fibroblasts, and bone marrow-derived cells, has emerged as a promising method to induce osteoblastic differentiation and address these cell sourcing limitations. The vast majority of these approaches utilize osteogenic growth factors, such as bone morphogenetic proteins (BMPs), or osteoblastic transcription factors, including Runx2[63,152]. However, the relative efficacy of these different approaches to induce osteoblastic differentiation remains unclear and is further complicated by varied delivery vehicles, cell types, and evaluation criteria.

* Modified from
C.A. Gersbach, R.E. Guldberg, and A.J. Garcia, *In vitro and In vivo Osteoblastic Differentiation of BMP-2- and Runx2-Engineered Skeletal Myoblasts.* Submitted, 2006.

BMP-2 is the most widely used growth factor to stimulate osteoblastic differentiation[8]. Soluble BMP-2 protein acts in autocrine and paracrine fashions by binding extracellularly to transmembrane receptors and triggering an intracellular signaling cascade mediated by Smad proteins[7]. Activated Smads translocate to the nucleus and upregulate the osteoblastic transcription factor Runx2[9]. Runx2 then coordinates osteoblastic gene expression, including osteocalcin, bone sialoprotein, osteopontin, and alkaline phosphatase[20]. Runx2 expression is required for osteoblastic differentiation[20] and endochondral ossification[21]. BMP-2 signaling also functions via several Smad-independent pathways, including protein kinase C and D and MAPKs[10].

Strategies that engineer cells to express a BMP-2 transgene have been successful in stimulating osteoblastic differentiation and ectopic and orthotopic bone formation *in vivo*[63]. However, concerns regarding release kinetics, dosage, and target cell specificity of this secreted growth factor still remain[152]. Furthermore, unregulated secretion of BMP-2 has been shown to stimulate tumor growth[86,87,153] and bone overproduction[88,89], where bone growth exceeds the defect site. More recently, forced expression of Runx2, an intracellular effector, has been shown to induce osteoblastic differentiation[20], matrix mineralization[24], and *in vivo* bone formation[78]. These results are consistent across pluripotent cell lines[78] and primary cell types including fibroblasts[56,83], skeletal myoblasts[154], and bone marrow stromal cells[77,79,82,155].

These studies have established ex vivo gene therapy with BMP-2 and Runx2 as promising strategies for orthopedic regeneration. However the relative potency and differential effects of these growth factor and transcription factor-based strategies in inducing osteoblastic differentiation are unclear. In particular, the diverse use of transient

and sustained gene delivery vehicles, transformed and primary cell types, and methods for assessing osteoblastic differentiation causes comparisons between studies to be difficult. Therefore, this study focuses on analyzing osteoblastic differentiation of a clinically relevant cell source engineered to express BMP-2 and/or Runx2 from a constitutive retroviral vector to obtain sustained expression of the transgene. Primary skeletal myoblasts were used as a model non-osteoblastic autologous cell source available in large quantities by a muscle biopsy and compatible with *in vitro* expansion[100] and ex vivo gene therapy protocols[62]. Skeletal myoblasts engineered to express BMP-2 and/or Runx2 were assessed for osteoblastic differentiation in both monolayer and tissue-engineered constructs *in vitro*, as well as in an ectopic implantation site in syngeneic mice *in vivo*. Engineered cells were further characterized for their ability to induce osteoblastic differentiation through paracrine signaling.

Materials and Methods

Cell Culture

Primary skeletal myoblasts were isolated from the tibialis anterior muscles of adult male Balb/c mice and cultured in selective growth media (Ham's F10, 20% fetal bovine serum, 5 ng/ml bFGF (Promega, Madison, WI), 100 U/ml penicillin G sodium, 100 μg/ml streptomycin sulfate), yielding cultures that were greater than 99% myogenic by desmin staining[100]. Cells were cultured on tissue culture plastic dishes coated with 0.01% type I collagen (Vitrogen, Palo Alto, CA) in a humidified 5% CO_2 atmosphere at 37 ºC. Cell culture media and antibiotics were obtained from Invitrogen (Carlsbad, CA),

fetal bovine serum was purchased from Hyclone (Logan, UT), and all other cell culture supplements and reagents were acquired from Sigma (St. Louis, MO).

Retroviral Vectors

The pTJ66 retroviral vector[156] and BMP-2 cDNA were generously provided by T.J. Murphy and Scott D. Boden, respectively. The oligonucleotides 5'-AGGCCTAGACTGACAATTGGTATCGATGGCCTACA-3' and 3'-ACATCCGGATCTGACTGTTAACCATAGCTACCGGA-5' were annealed together to create an internal Mfe1 restriction site (underlined) with overhangs compatible with the Sfi1 cloning site of pTJ66. The product was ligated into Sfi1-digested pTJ66 vector. Finally, the human BMP-2 cDNA was digested from the host vector with EcoRI restriction enzyme, ligated into the Mfe1 restriction site of pTJ66, and verified by sequencing the ligation points. The pTJ66-Runx2 vector has been described previously[24].

Retroviral Transduction

Retroviral stocks were produced by transient transfection of helper virus-free ΦNX amphotropic producer cells with plasmid DNA[24]. Primary myoblasts were cultured up to 12 passages and plated on 0.01% collagen-coated tissue culture polystyrene at 2 x 10^4 cells/cm^2 24 h prior to retroviral transduction as described previously[154]. Cells were transduced again 16 hrs later to increase transduction efficiency, and retroviral supernatant was replaced with differentiation media (αMEM, 10% fetal bovine serum, 100 U/ml penicillin G sodium, 100 μg/ml streptomycin sulfate, 50 μg/ml L-ascorbic acid,

3 mM sodium β-glycerophosphate, and 10 nM dexamethasone). Cell culture media was replaced every 3 days until terminal assay, unless noted otherwise.

Osteogenic Differentiation

Quantitative RT-PCR (qRT-PCR), Western blotting, alkaline phosphatase biochemical activity, and von Kossa staining were performed as described previously[154]. Runx2 (Accession # NM_009820) primer sequences were 5'-GGCCTTCAAGGTTGTAGCCC -3' (forward) and 5'- CCCGGCCATGACGGTA -3' (reverse); BMP-2 (Accession # NM_001200) primer sequences were 5'-ATTGTGGCTCCCCCGG -3' (forward) and 5'- TCAGCCAGAGGAAAAGGGC -3' (reverse); VEGF-A (Accession # NM_009505) primers were 5'-CATCTTCAAGCCGTCCTGTGT -3' (forward) and 5'-CAGGGCTTCATCGTTACAGCA -3' (reverse). Other primer sequences have been reported[154]. Secreted BMP-2 protein levels were measured in bulk media samples using an ELISA kit according to the manufacturer's instructions (R&D Systems, Minneapolis, MN). Anti-phospho-Smad1/5/8 and anti-Smad1/5 were purchased from Chemicon (Temecula, CA) and Upstate Biotechnology (Charlottesville, VA), respectively. Calcium content was determined by dissolving mineralized regions with 1 N acetic acid overnight. 25 μl of appropriately diluted sample was added to 300 μl of arsenazo III-containing Calcium Reagent (Diagnostic Services Ltd., Oxford, CT). The absorbance of the resulting samples was read at 650 nm and compared to a linear standard curve of $CaCl_2$ in 1 N acetic acid.

Scaffold Seeding and Analysis

Fibrous collagen disks (5 mm x 1.5 mm, Kensey Nash, Exton, PA) were incubated overnight in 10% FBS in phosphate buffered saline (PBS). At two days post-transduction 250,000 cells in 10 µl of growth media were seeded onto each side of the disk in a non-tissue culture treated 24 well plate, for a total of 500,000 cells/construct. Four hours later, scaffolds were immersed in 2 ml of growth media. After twenty-four hours, growth media was changed to 2 ml of differentiation media. Media was replaced every three days until terminal assay. FT-IR spectroscopy and DNA content were assessed as described previously[157].

Intramuscular Implantation

Scaffolds seeded with engineered or unmodified myoblasts were cultured for 1 or 28 days *in vitro* and implanted into the hind limbs of syngeneic 6 week old immunocompetent male Balb/c mice (Jackson Labs, Bar Harbor, ME) in accordance with an IACUC-approved protocol. A longitudinal 1 cm incision was made in the skin overlying the gastrocnemius muscle, and the muscle was exposed. Scaffolds were inserted into the muscles of both legs through an atraumatic longitudinal split in the direction of the fibers. The muscle was closed over the implants (without suturing) and the skin closed with wound clips. Twenty-eight days after implantation mice were euthanized by CO_2 inhalation and lower legs were harvested, skinned, and fixed in 10% neutral buffered formalin.

Micro-Computed Tomography

Mineralization of cell/scaffold constructs was quantified by high resolution X-ray micro-computed tomography (micro-CT) using a Scanco Medical VivaCT 40 imaging system (Bassersdorf, Switzerland). Specimens were scanned at 21 μm voxel resolution and evaluated at a threshold corresponding to a linear attenuation of 1.92 cm^{-1}, filter width of 1.2, and filter support of 2.0. The reconstructed and thresholded 3-D images were evaluated using direct distance transformation methods to calculate mineralized matrix volume within each construct[135].

Histological Analysis

Formalin-fixed samples were decalcified with 5% formic acid prior to paraffin embedding for hematoxylin-eosin or Masson's trichrome staining. Sections (5 μm) were deparaffinized and stained as indicated.

Data Analysis

Data are reported as mean ± standard error of the mean (SEM), and statistical comparisons using SYSTAT 8.0 were based on an analysis of variance (ANOVA) and Tukey's test for pairwise comparisons, with a p-value < 0.05 considered significant.

Results

Retroviral Overexpression

Primary skeletal myoblasts were cultured up to 12 passages and transduced with empty vector, Runx2, and/or BMP-2 retroviral supernatant. Combined Runx2 and BMP-

2 treatment was performed by mixing equal volumes of retroviral supernatant. The pTJ66 retroviral vector uses the promoter activity of the 5' LTR for transgene expression, followed by an internal ribosomal entry site and a zeocin-resistance-enhanced green fluorescent protein (eGFP) fusion protein, allowing for noninvasive analysis of transduction efficiency[24]. High levels of eGFP transgene expression were confirmed for all treatments by flow cytometry (Fig. 5.1A). Transgene expression was further analyzed by qRT-PCR for Runx2 and BMP-2 mRNA levels (Fig. 5.1B). Runx2 and BMP-2 expression were significantly upregulated by treatment with Runx2 and BMP-2 retrovirus, respectively. Importantly, dilution of retroviral supernatant in the combined treatment did not affect transgene mRNA levels relative to undiluted virus stocks. Protein levels were assessed by Western blot for Runx2 (Fig. 5.1C) and ELISA of the bulk media for BMP-2 (Fig. 5.1D). Neither Runx2 nor BMP-2 protein was detectable in control myoblasts. Retroviral delivery of Runx2 significantly enhanced protein levels at 3 and 7 days. Lower levels of Runx2 protein were also detected in samples treated with BMP-2. Runx2 overexpression alone did not induce BMP-2 expression. However BMP-2 protein in the bulk media was significantly reduced in the combined treatment relative to BMP-2 overexpression alone, despite equivalent BMP-2 mRNA levels. Additionally, secreted amounts of BMP-2 protein decreased over time despite no significant changes in mRNA expression. These observations may be explained by increased internalization or incorporation of soluble BMP-2 into the extracellular matrix assembled by Runx2- or BMP-2-engineered cells, or the upregulation of BMP-2-binding agonists, such as noggin. Nevertheless, these results confirm successful retroviral overexpression of substantial and sustained levels of Runx2 and BMP-2 transgenes in primary skeletal myoblasts.

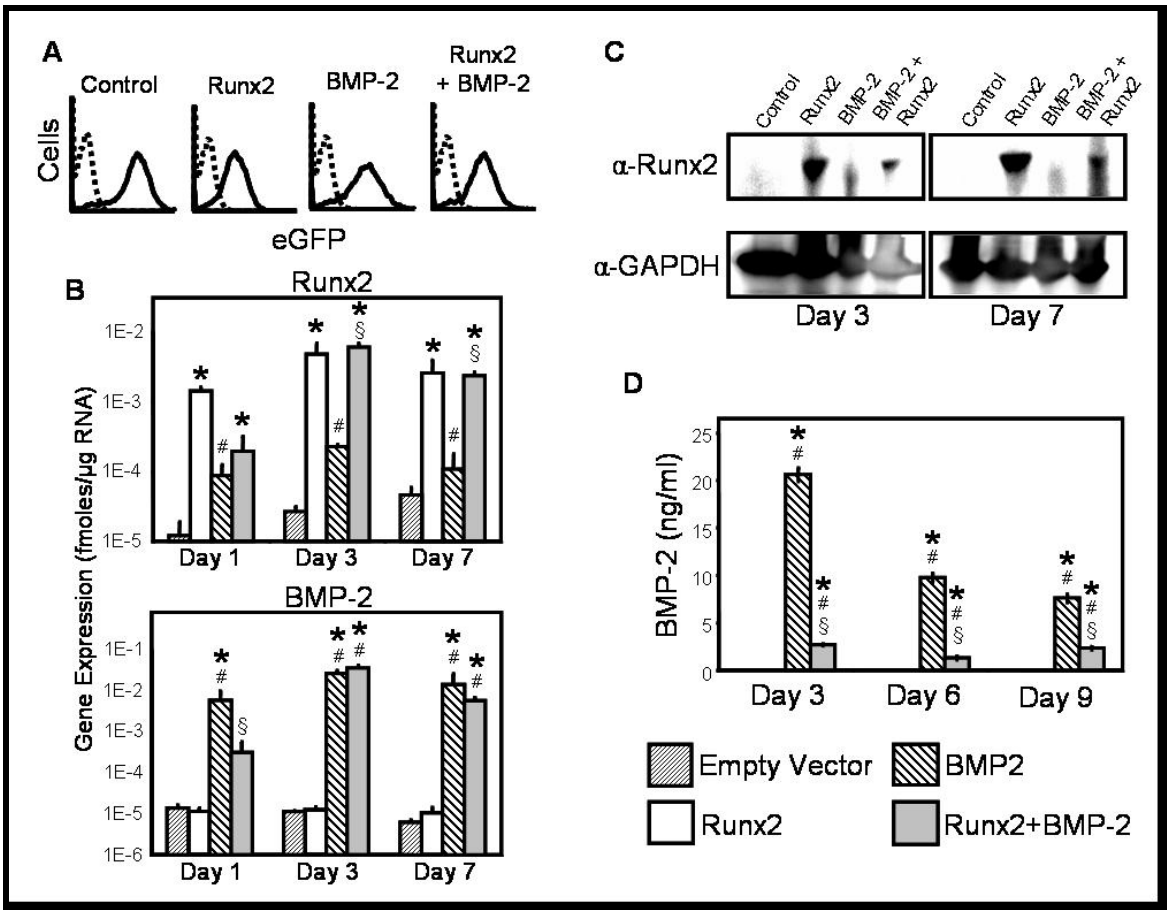

Figure 5.1. Retroviral expression of Runx2 and BMP-2 transgenes. (A) Transduction was confirmed by flow cytometry. (B) Significant levels of Runx2 ($p<1E-8$) and BMP-2 ($p<9E-12$) mRNA were detected by qRT-PCR in samples transduced with the respective virus (mean + SEM, n=3). Elevated protein levels were detected by (C) Western blotting for Runx2 and (D) ELISA of the bulk media for BMP-2 (mean ± SEM, n=3, $p<5E-12$). * vs. empty vector, # vs. Runx2, § vs. BMP-2.

Osteoblastic Differentiation In Vitro

Gene expression was analyzed at 1, 3, and 7 days post-transduction for osteoblastic matrix proteins (osteocalcin and bone sialoprotein), transcription factors (Osterix and Dlx5), mineralization-associated enzymes (alkaline phosphatase), and angiogenic factors (VEGF-A) (Fig. 5.2). Osteocalcin, bone sialoprotein, Osterix, and alkaline phosphatase were all upregulated by Runx2 or BMP-2 at 7 days. Additionally, BMP-2 induced gene expression faster than Runx2 as evident by expression profiles at 1 and 3 days. However, with the exception of bone sialoprotein, all genes showed similar levels in response to Runx2 and BMP-2 treatment after 7 days. Bone sialoprotein was upregulated to a greater extent by BMP-2 relative to Runx2 treatment. Interestingly, the combined treatment of Runx2 and BMP-2 resulted in synergistic effects (note logarithmic scale) on expression of osteocalcin, bone sialoprotein, Dlx5, and VEGF-A at later time points.

Functional osteoblastic differentiation was assessed by alkaline phosphatase biochemical activity and matrix mineralization in monolayer culture. Alkaline phosphatase activity was undetectable in control myoblasts, but significantly induced in Runx2 and BMP-2 overexpressing cells (Fig. 5.3A). At 14 days post-transduction enzyme activity was equivalent in cells with Runx2, BMP-2, and combined treatments. Matrix mineralization was assessed by calcium content (Fig. 5.3B) and von Kossa staining for phosphate deposits (Fig. 5.3C). There were no mineralized regions detected in control samples. Interestingly, Runx2 treated cells showed higher levels of mineralization than BMP-2 treated monolayer cultures for up to 8 weeks, despite similar levels of osteogenic gene expression and alkaline phosphatase activity at late time points.

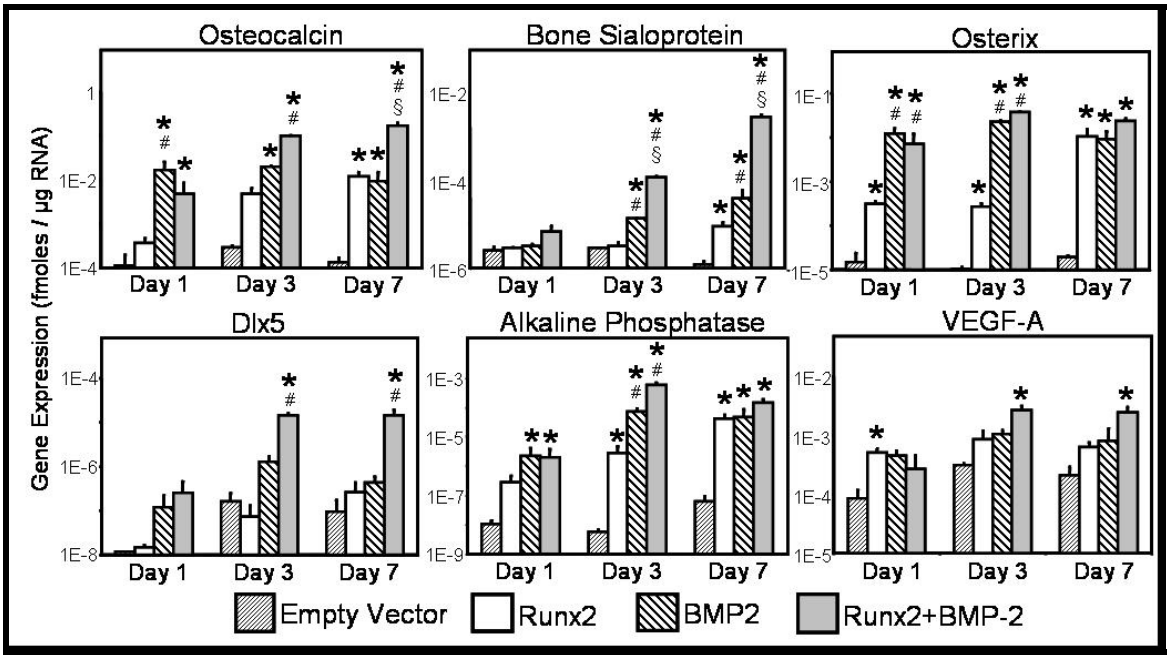

Figure 5.2. Runx2-and BMP-2-induced gene expression was assessed by qRT-PCR analysis of osteoblastic markers including osteocalcin ($p<9E-10$), bone sialoprotein ($p<7E-12$), Osterix ($p<8E-12$), Dlx5 ($p<2E-6$), alkaline phosphatase ($p<9E-12$), and VEGF-A ($p<2E-5$) (mean + SEM, n=3). * vs. empty vector, # vs. Runx2, § vs. BMP-2

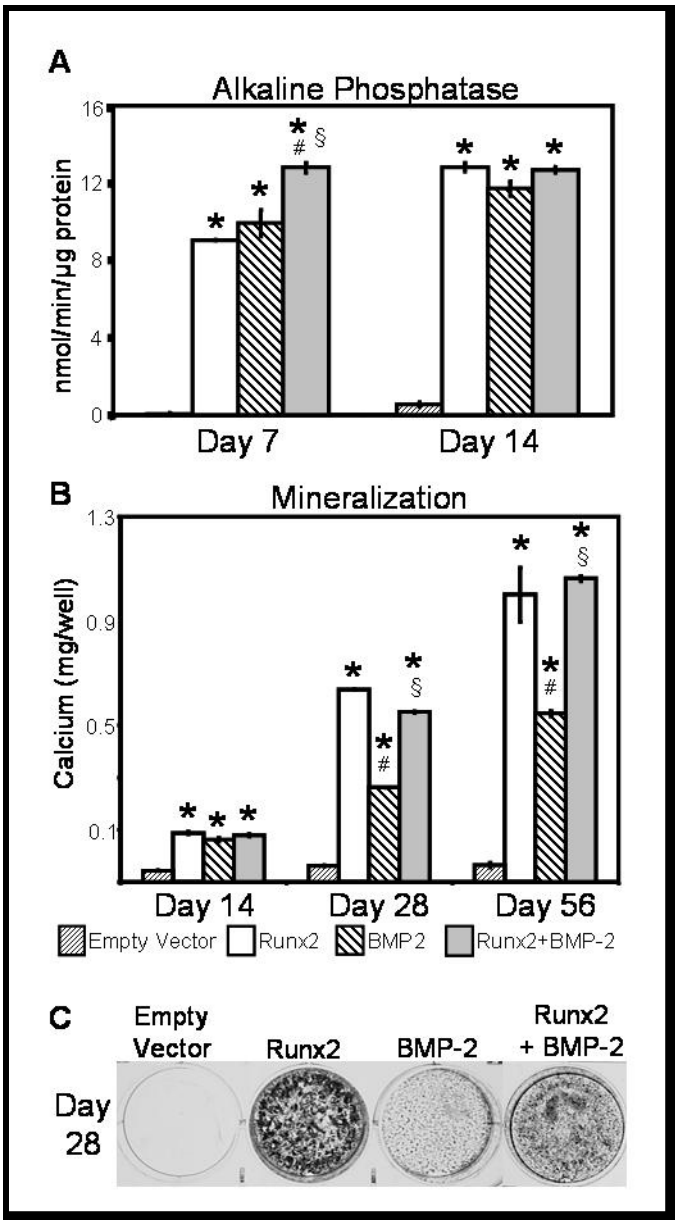

Figure 5.3. Osteoblastic differentiation of Runx2 and BMP-2 engineered myoblasts was analyzed by (A) alkaline phosphatase biochemical activity ($p<7E-12$, mean ± SEM, n=3), (B) calcium content ($p<6E-12$, mean ± SEM, n=3), and (C) von Kossa staining for mineralization. * vs. empty vector, # vs. Runx2, § vs. BMP-2.

Matrix Mineralization In Vivo

Cells were seeded onto fibrous collagen disks to assess osteoblastic differentiation in a three-dimensional, tissue-engineered environment. Mineralization on these scaffolds was assessed by micro-CT (Fig. 5.4A). In contrast to two-dimensional monolayer cultures, BMP-2 expressing cells exhibited significantly higher levels of mineralization compared to Runx2 cells in the cell-scaffold construct. The trends in calcium content of these constructs were similar to the levels of mineralization measured by micro-CT (data not shown). Importantly, the increased amount of mineralization by BMP-2 cells correlated to higher cell numbers in the scaffold (Fig. 5.4B). Constructs containing cells treated with both Runx2 and BMP-2 showed decreased cell numbers compared to BMP-2 engineered cells, similar to cells expressing only Runx2. The *in vitro* mineralization was confirmed to be a carbonate-containing biological hydroxyapatite by FT-IR spectroscopy, similar to that of cranial bone (Fig. 5.4C). Constructs containing control myoblasts exhibited bands corresponding to a mineral-free extracellular matrix.

The cell-seeded collagen scaffolds were implanted intramuscularly into the hind limbs of immunocompetent syngeneic mice to evaluate the mineralization capacity of the genetically engineered cells *in vivo*. Constructs were implanted 24 hrs after cell seeding or after 4 weeks of *in vitro* preculture, since we have previously shown enhanced mineralization *in vivo* after *in vitro* construct development[77]. Mice were euthanized at 4 weeks post-implantation and hind limbs were analyzed for ectopic mineralization by micro-CT and histology (Fig. 5.5). Collagen/cell constructs that were implanted without pre-culture showed moderate levels of mineral deposits for empty vector or Runx2-engineered cells. These mineral levels were not statistically different from mineral levels

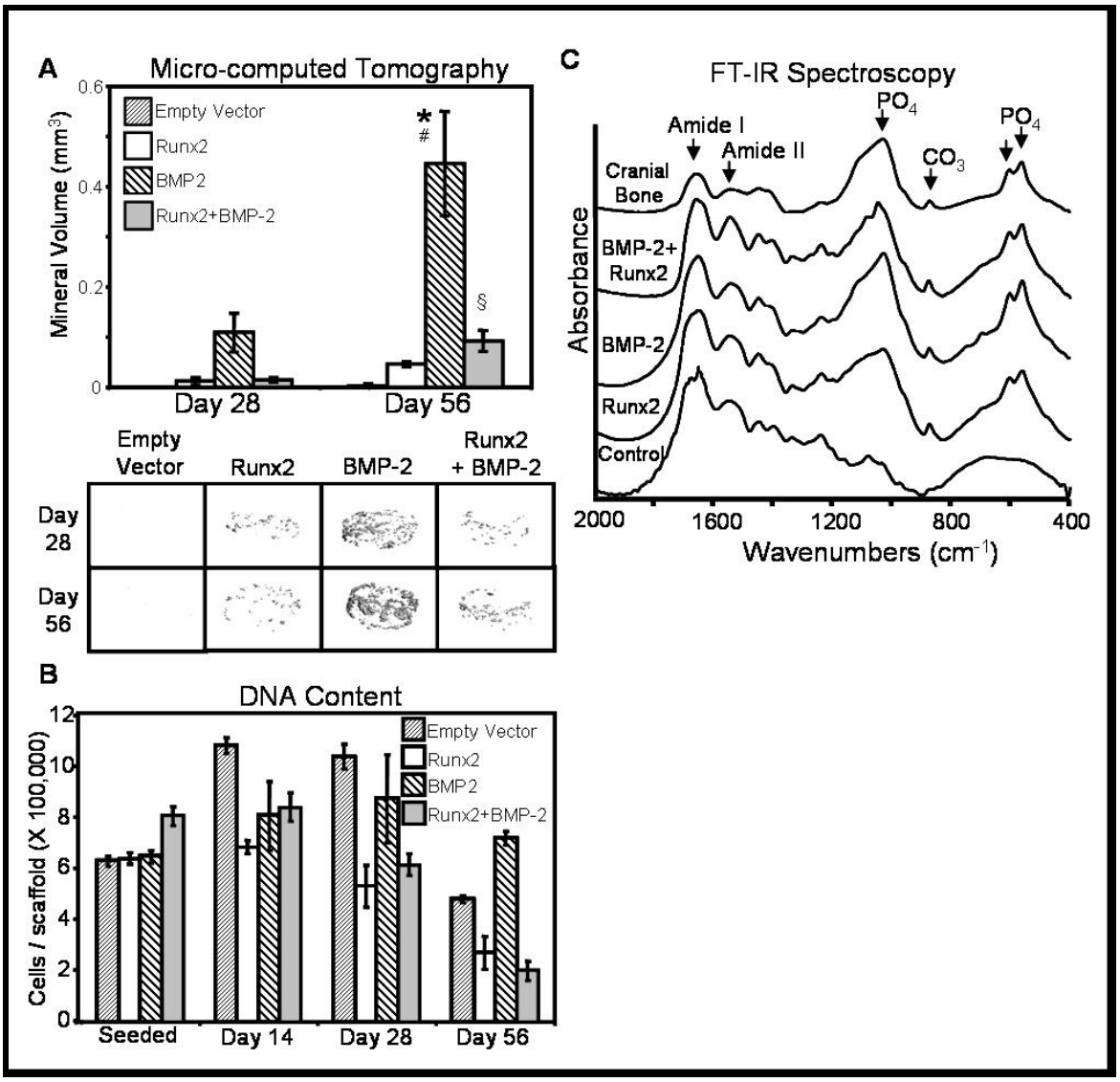

Figure 5.4. Engineered cells were seeded onto fibrous collagen scaffolds and analyzed for mineralization by (A) micro-CT ($p<1E-8$, mean ± SEM, n=6) and (B) DNA content ($p<8E-6$, mean ± SEM, n=3). * vs. empty vector, # vs. Runx2, § vs. BMP-2. (C) *In vitro* mineralization was confirmed to be a biological hydroxyapatite by FT-IR spectroscopy.

for cell-free constructs and scaffolds containing non-engineered myoblasts. Constructs with cells expressing BMP-2 alone or BMP-2 and Runx2 showed significantly greater amounts of ectopic mineralization. In contrast, constructs which matured *in vitro* prior to implantation showed significant and equivalent amounts of mineral for Runx2, BMP-2, and dual treated cells relative to background levels with control cells. Hematoxylin and eosin staining (Fig. 5.5B) showed greater cellularity in pre-cultured mineralized implants relative to empty vector controls, despite greater cell numbers on control scaffolds at implantation. This result is likely due to minimal proliferation of differentiated myocytes in control samples, *in vivo* proliferation of implanted osteogenic cells, and/or recruitment of osteoprogenitors by cells engineered to express osteogenic factors. Masson's trichrome staining (Fig. 5.5C) also showed lower cell numbers in control samples (purple nuclei), as well as acellular residual collagen scaffold (blue and red). Runx2, BMP-2, and dual treated samples showed significant matrix remodeling and/or deposition with collagen staining (blue) aligned and interwoven in highly cellularized regions, resembling early intramembranous bone formation. Histological staining of implants consisting of scaffold only or scaffold with non-engineered cells were similar to empty vector samples for all analyses, suggesting no adverse response to retrovirally transduced cells.

Paracrine Signaling

BMP-2 expressing cells are known to stimulate osteoblastic differentiation of neighboring cells through paracrine signaling by secreted BMP-2 growth factor[55,76]. This effect is attributed to be greatly responsible for the considerable success of BMP-2-based gene therapy strategies[76]. However, unregulated secretion of soluble factors limits the

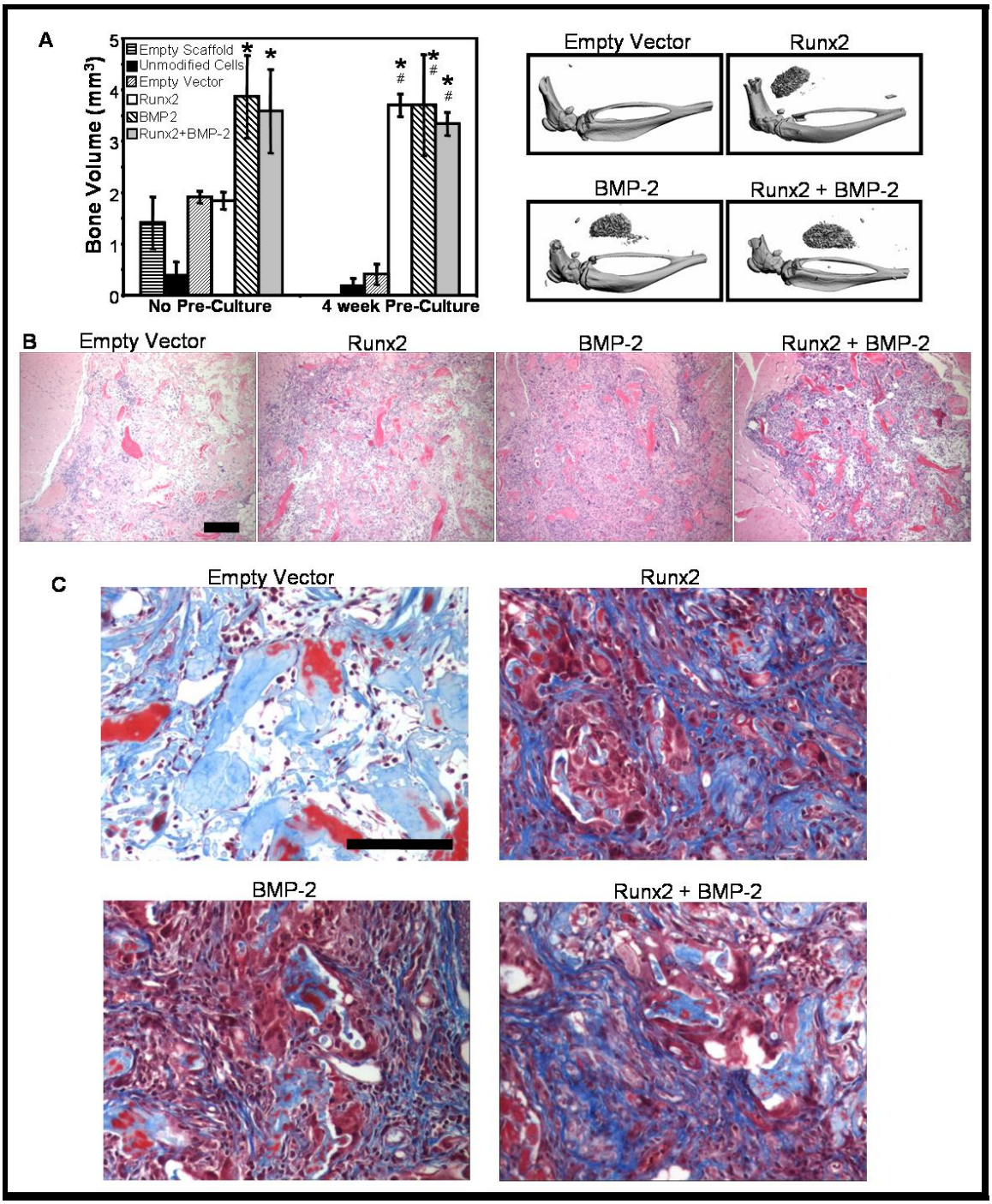

Figure 5.5. Cell-seeded collagen scaffolds were implanted intramuscularly in the hind limbs of immunocompetent syngeneic mice at 1 day post-seeding or after 28 days of *in vitro* pre-culture in differentiation media. (A) Animals were euthanized at 4 weeks post-implantation and formalin-fixed hind limbs were analyzed for ectopic mineralization by micro-CT ($p<8E-7$, mean ± SEM, n=6). * vs. empty vector, # vs. Runx2. Images are representative of pre-cultured implants. Pre-cultured samples were also assessed histologically by (B) hematoxylin and eosin and (C) Masson's trichrome staining. Scale bars indicate 50 μm.

ability to achieve targeted effects and may be responsible for abnormal bone formation[88,89] and tumorigenesis[86,87,153]. It is unclear whether cells overexpressing Runx2, an intracellular effector, also transmit osteogenic signals through secretion of cytokines or growth factors. Therefore we transduced cells with the indicated virus, exchanged media after two days, and harvested conditioned media at 4 days and every other day thereafter. The conditioned media was immediately filtered through a 0.1 μm syringe filter and transferred to non-engineered myoblasts. This process was repeated every 2 days for 8 days, at which point both donor cells and cells receiving conditioned media (recipient cells) were harvested for analysis of osteogenic gene expression by qRT-PCR (Fig. 5.6A). Donor cells, which were treated with the indicated retrovirus, showed similar expression profiles as in Figure 5.2. Interestingly, conditioned media from any group did not effect the expression of osteocalcin, the most frequently characterized target of BMP-2 and Runx2. However conditioned media from BMP-2-engineered cells induced both bone sialoprotein and Osterix expression in recipient cells. Conditioned media from Runx2-engineered cells had no significant effects on any gene investigated. Furthermore, co-treatment with Runx2 and BMP-2 showed a decreased effect on bone sialoprotein and Osterix relative to BMP-2 alone, possibly due to the dilution of BMP-2 protein detected in Figure 5.1D. To further examine the possibility of BMP signaling in Runx2-treated cultures, levels of Smad activation were assessed by Western blot (Fig. 5.6B). Significant levels of Smad phosphorylation were detected in BMP-2-engineered cultures. However, there was no detectable Smad activation in Runx2-overexpressing cells. Collectively, these results suggest that Runx2-overexpressing myoblasts, in contrast

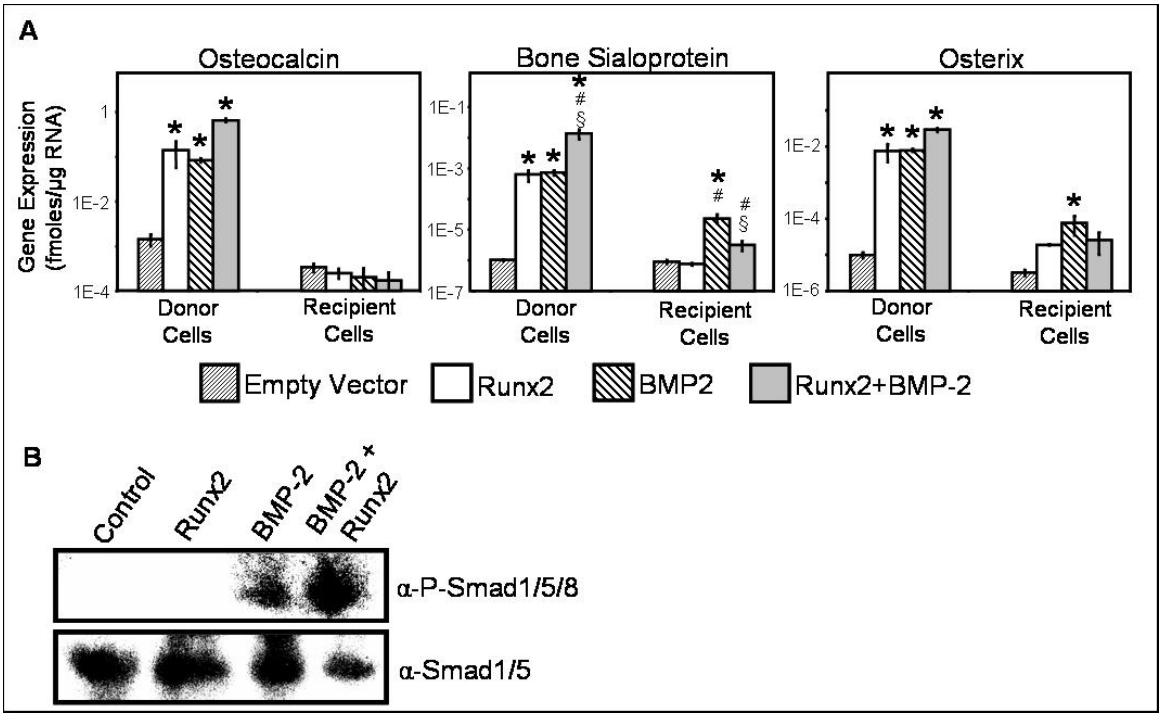

Figure 5.6. Paracrine signaling by genetically engineered cells. (A) Conditioned media studies were performed to analyze the ability of engineered cells to transmit osteogenic signals via soluble growth factors or cytokines. Donor myoblasts were engineered with the indicated retrovirus and differentiation media was exchanged every other day. Starting at 4 days post-transduction, media harvested from donor cells was filtered and added to non-engineered myoblasts (recipient cells) for a total of 8 days. Both donor cells and recipient cells were analyzed by qRT-PCR for osteocalcin ($p<4E-9$), bone sialoprotein ($p<8E-12$), and Osterix ($p<2E-9$) gene expression (mean ± SEM, n=3). * vs. empty vector, # vs. Runx2, § vs. BMP-2. (B) Phosphorylation of Smad signaling molecules was analyzed by Western blot. The presence of phosphorylated Smads in BMP-2-engineered cells confirmed activation of BMP signaling pathways. There was no Smad phosphorylation detected in Runx2-treated samples, demonstrating osteoblastic differentiation in the absence of BMP signaling.

to BMP-2-secreting cells, do not utilize paracrine signaling by soluble factors in stimulating osteoblastic differentiation.

Discussion

Genetic engineering of non-osteoblastic cells with osteogenic factors has emerged as a promising strategy to address cell sourcing limitations associated with bone tissue engineering. However, the relative efficacy of these different approaches to induce osteoblastic differentiation remains unclear and is further complicated by varied delivery vehicles, cell types, and evaluation criteria. The present study provides a direct and quantitative comparison between transcription factor- and growth factor-based strategies to induce osteoblastic differentiation *in vitro* and *in vivo*. We used retroviral delivery to primary skeletal myoblasts inorder to compare sustained expression of Runx2 and BMP-2 transgenes in a clinically relevant autologous cell source[61]. This work supports previous studies which indicate that BMP-2 overexpression may be a more potent osteoinductive strategy[56,78]. However, these results also suggest that Runx2 overexpression can be an equally effective approach under the appropriate conditions or when measured at longer time points.

This study highlights the need for rigorous evaluation of osteoinductive strategies in multiple settings to define an appropriate method to achieve a desired therapeutic outcome. Runx2-overexpressing cells generated greater mineralization in confluent monolayer cultures relative to BMP-2-treated cells. This is consistent with previous results comparing Runx2 overexpression with treatment of recombinant BMP-2 protein[154]. However BMP-2 engineered cells showed significantly greater levels of

mineralization in three-dimensional collagen scaffolds, correlating with greater cell numbers. Runx2 and BMP-2 are both known to mediate proliferation, cell cycle progression, and apoptosis of osteoblastic cells[158,159]. The greater numbers of BMP-2-expressing cells on cultured collagen scaffolds could be explained by Runx2-mediated inhibition of proliferation[158], BMP-2-mediated suppression of apoptosis[159], or differences in osteoblastic activity in two- and three-dimensional culture[160-162]. These results underscore the necessity for measuring several parameters of cell activity in multiple environments when assessing cell sources for gene therapy strategies in orthopedic regeneration.

Yang et al. demonstrated a synergistic effect on osteogenesis with dual treatment of BMP-2 and Runx2 adenoviral vectors in a multipotent mesenchymal cell line[78]. Although we show synergistic effects on osteoblastic gene expression, this effect was not propagated to downstream cellular effects including enzyme activity and mineralization. The inconsistencies between these studies may be the result of differences relating to transient expression in a multipotent cell line versus sustained transgene expression in a lineage-committed primary cell type. We also show diminished detection of secreted BMP-2 in Runx2 co-expressing cultures (Fig. 5.1D) without a loss of osteoblastic activity. This may be the result of enhanced cellular uptake or BMP-2 incorporation in the extracellular matrix. Further investigation is necessary to determine whether these mechanisms contribute to the observed synergy in dually-treated cells. Additionally, we did not observe the development of osteocytes, cartilage, or marrow cavities as reported for Runx2- and BMP-2-engineered cell lines implanted in ectopic sites in immunodeficient mice[78]. Previous studies suggest that this may be the result of using

primary cells and immunocompetent mice in the present work, and longer implantation times may be necessary for the development of more complex tissues[69].

Paracrine signaling by BMP-2-expressing cells plays a central role in stimulating osteogenesis[76,112]. This effect can be advantageous for obtaining an adequate degree of osteoblastic differentiation and mineralization. However, the unregulated secretion of potent signaling molecules limits target cell specificity and risks tumorigenesis[86,87,153] or abnormal bone formation[88,89]. Choi et al. have described a mechanism by which Runx2 induces BMP-2 expression[163], suggesting that Runx2-overexpressing cells may stimulate osteoblastic differentiation via paracrine signaling of secreted factors. Additionally, a recent report suggests that BMP signaling is required for Runx2-stimulated osteoblastic differentiation[164]. However, we did not detect secretion of BMP-2 or BMP-4 into the surrounding media by Runx2-engineered cells. Furthermore, there were no detectable levels of Smad activation in these cells, nor was there any effect of conditioned media from Runx2-engineered cells on osteogenic gene expression. These results suggest that BMP signaling was not involved in Runx2-stimulated osteoblastic differentiation of primary skeletal myoblasts in this system. The discrepancies between these studies may be the result of cell-type dependent effects in stimulating osteoblastic differentiation[24]. In fact, although Runx2 binding sites have been identified in the promoters of the human BMP-2 and BMP-4 genes, deletion of these sites did not alter promoter activity in osteoblastic cells[165].

In addition to BMP-2 and the Runx2 transcription factor, there are several other gene therapy-based strategies under investigation for orthopedic regeneration. Promising results have been achieved by focusing on other members of the BMP family[55,166], VEGF

and RANK-L[72], constitutively active BMP receptors[73], and LIM-mineralization protein[81]. Other studies have demonstrated synergistic effects by incorporating multiple transgenes[70,78] and transgenes supplemented with glucocorticoids[83] or immunosuppressive agents[84,85]. Additionally, the limitations of uncontrolled growth factor secretion and constitutive transgene expression are also being addressed with inducible expression systems[65,71,88] and coexpression of regulatory factors[89].

This study emphasizes the complexity of ex vivo gene therapy as an integrated relationship of cell activity and differentiation state, construct maturation, and paracrine signaling of osteogenic cells. Our results indicate that sustained BMP-2 expression in skeletal myoblasts is a more potent strategy for osteoinduction compared to delivery of the Runx2 transcription factor. However, we also identified conditions in which Runx2 is equally effective as BMP-2 in stimulating osteoblastic differentiation and matrix mineralization. Furthermore, Runx2-based strategies may avoid complications arising from uncontrolled signaling of secreted factors. Collectively, these results underscore the necessity for thorough evaluation of genetically engineered cells to identify the appropriate system for specific clinical needs. This work is significant to evaluating these systems and defining a successful strategy for integrating gene medicine and orthopedic regeneration.

CHAPTER 6

INDUCIBLE REGULATION OF RUNX2-STIMULATED OSTEOGENESIS*

Introduction

Cell-based therapies have emerged as a promising approach for orthopedic regeneration.[38] However, autologous osteoblastic cell sources are limited by availability[38], dedifferentiation following *in vitro* culture[47-49], and an age-related decrease in osteogenic capacity.[50] To address these limitations, genetic engineering has become a central component of many regenerative medicine strategies. Forced expression of differentiation factors is commonly used to enhance cell phenotype or modulate cell function to achieve a therapeutic goal. In particular, cell-based approaches to bone tissue engineering often utilize *ex vivo* gene therapy techniques to induce osteogenesis in non-osteoblastic cell types, including myoblasts[57,157], fibroblasts[55,56], and pluripotent progenitor cells.[51-54] These strategies focus on the constitutive overexpression of osteogenic growth and differentiation factors, such as bone morphogenetic proteins (BMPs)[68,75,166,167] or osteoblastic transcription factors, including Runx2.[67,77,79,155,157] These approaches have been successful in stimulating osteoblastic differentiation and *in vivo* bone formation.[63] However, unregulated overexpression of these proteins risks aberrant effects of uncontrolled cell signaling, including tumorigenesis[86,87] and abnormal bone formation.[88,89]

The use of inducible expression systems is a promising method for controlling the

* Modified from
C.A. Gersbach, J.M. Le Doux, R.E. Guldberg, and A.J. Garcia, *Inducible Regulation of Runx2-Stimulated Osteogenesis.* Gene Therapy, 2006. 13(11):873-882.

behavior of genetically engineered cells.[74] These systems typically drive transgene expression from inducible promoters regulated by non-mammalian transcription factors. The activity of these transcription factors is controlled by exogenous chemical agents which permit ("on" state) or repress ("off" state) transgene expression. In principle, an *ex vivo* inducible gene therapy strategy entails implanting engineered cells into a bone defect site and maintaining transgene expression in the "on" condition. When adequate healing has occurred, cells are moved to the "off" condition to prevent any adverse effects of prolonged transgene overexpression. Additionally, incorporating regulation into these systems allows analysis of unique patterns of transgene expression, including varying duration and magnitude of expression, cycling expression over time, and coordinating the sequential presence of multiple exogenously expressed genes.

The most widely characterized of these systems is the tetracycline inducible expression system, first described by Gossen and Bujard.[90] The original system utilizes the tetracycline-controlled transactivator (tTA), a fusion protein of the E. coli tet repressor and the activating domain of virion protein 16 of the herpes simplex virus. In the absence of tetracycline, tTA binds the tet operon and activates transcription of a downstream gene of interest. However, in the presence of subtoxic levels of tetracycline, the antibiotic binds to tTA, blocking binding of the tet operon and subsequent transactivation in a dose-dependent manner. This "tet-off" version was later modified to a "tet-on" system where transactivation increases with tetracycline concentration.[91] Despite the greater clinical relevance of the tet-on derivative, the tet-off system is widely reported as having a greater degree of inducibility, including lower expression levels in the "off" state and higher expression levels in the "on" state.[92] In addition, this system is

compatible *in vitro* by adding tetracycline to the cell culture media and *in vivo* by delivering aTc via the drinking water.

Both tetracycline-based systems have been used to express BMP transgenes for bone regeneration.[65,71,88] BMP-2, the most widely used BMP for osteoinduction, is a secreted growth factor that acts via autocrine and paracrine mechanisms by binding to the extracellular domain of a transmembrance receptor that activates the intracellular Smad signaling pathway.[7] Activated Smads translocate to the nucleus, upregulating and cooperating with the osteoblast-specific transcription factor Runx2 to induce osteoblastic gene expression.[11] Runx2 is essential for osteoblast differentiation[20] and endochondral ossification.[21]

Although genetic engineering with BMPs has successfully stimulated osteogenesis in many models, concerns over dosage, release kinetics, and target specificity still remain.[152] Forced expression of Runx2, an intracellular effector, enhances the differentiation of an osteogenic cell source[24,82] and stimulates transdifferentiation of primary skeletal myoblasts into an osteoblastic phenotype.[154] Runx2 overexpression has also been recently advocated as a method for maintaining and enhancing an osteoblastic phenotype for bone regeneration[77,79,155,157] and may overcome potential limitations of genetic engineering with secreted growth factors. However, the ability to direct osteoblastic differentiation with an inducible Runx2 expression system has not been demonstrated.

To generate a system for efficient and regulated transgene expression, we utilized a retroviral tet-off expression system[156] to modulate Runx2 expression. Primary skeletal myoblasts were used as a clinically relevant autologous cell source that is responsive to

Runx2 overexpression.[154,157] We demonstrate that the osteogenic effect of Runx2 overexpression in primary skeletal myoblasts can be regulated by a tetracycline-responsive expression system both *in vitro* and *in vivo*. The conversion of Runx2-engineered skeletal myoblasts into an osteoblastic phenotype is inducible, repressible, recoverable after suppression, and dose-dependent with tetracycline concentration. This work is significant in developing controlled, effective gene therapy methods for regenerative medicine and represents a novel strategy for investigating the effects of temporal modulation and magnitude of expression levels on osteoblastic differentiation.

Materials and Methods

Cell Culture

Primary skeletal myoblasts were isolated from the tibialis anterior muscles of adult male Balb/c mice and cultured in selective growth media (Ham's F10, 20% fetal bovine serum, 5 ng/ml bFGF (Promega, Madison, WI), 100 U/ml penicillin G sodium, 100 μg/ml streptomycin sulfate), yielding cultures that were greater than 99% myogenic by desmin staining.[100] Cells were cultured on tissue culture plastic dishes coated with 0.01% type I collagen (Vitrogen, Palo Alto, CA) in a humidified 5% CO_2 atmosphere at 37 ºC. Cell culture media and antibiotics were obtained from Invitrogen (Carlsbad, CA), fetal bovine serum was purchased from Hyclone (Logan, UT), and all other cell culture supplements and reagents were acquired from Sigma (St. Louis, MO).

Retroviral Vectors

Retroviral plasmids pTJ66, pKA23, and pXF40 were generously provided by T.J. Murphy.[156] The tTA gene was digested from the pKA23 plasmid with Sfi1 restriction enzyme and ligated into the Sfi1 cloning site of the constitutive retroviral expression vector pTJ66 (Fig. 6.1A). The pTJ66-tTA retroviral vector uses the promoter activity of the 5' long terminal repeat (LTR) to express a single bicistronic mRNA encoding tTA, followed by an internal ribosomal entry site (IRES) and a zeocin resistance-enhanced green fluorescent protein fusion protein (Zeo(r):eGFP), allowing for noninvasive analysis of transduction efficiency and antibiotic selection for transduced cells (Fig. 6.1B).

Two Sfi1 restriction sites were inserted into the multiple cloning site of pXF40, the retroviral tetracycline-inducible expression vector. The oligonucleotides 5'-CGCGTTGATCAGGCCTTGTAGGCCTAGGGATCCGTAGGCCTACAAGGCCTTC GAAATGCA-3' and 5'-TTTCGAAGGCCAAGTAGGCCTACGGATCCCTAGGCCTA CAAGGCCTGATCAA-3' (Sfi1 sequences underlined) were annealed together, creating Nsi1- and Mlu1-compatible overhangs at each end. This product was then ligated into a linearized pXF40 vector which had been digested with both Nsi1 and Mlu1. Finally, the Runx2 gene was digested from the TJ66 vector with Sfi1 enzyme, and ligated into a Sfi1-digested pXF40 vector. The pXF40-Runx2 vector transcribes the Runx2 gene from the tetracycline-inducible promoter, which consists of seven adjacent copies of the tet operon (tetO). This vector also constitutively expresses the neomycin resistance gene (Neo(r)) by the 5' LTR promoter, allowing for selective purification of transduced cells. All vectors were verified by sequencing the ligation points.

Retroviral Transduction

Retroviral stocks were produced by transient transfection of helper virus-free ΦNX amphotropic producer cells with plasmid DNA as previously described.[24] For production of pXF40-Runx2 retrovirus, cells were maintained in 1 μg/ml anhydrotetracycline (aTc), as inactivating conditions enhance retroviral titer of tetracycline inducible vectors.

Primary myoblasts were cultured up to 12 passages and plated on 0.01% collagen-coated tissue culture polystyrene at 2 x 10^4 cells/cm^2 24 h prior to retroviral transduction.[62] Cells were transduced with 0.2 ml/cm^2 of equal parts pTJ66-tTA and pXF40-Runx2 retroviral supernatant supplemented with 4 μg/ml hexadimethrine bromide (Polybrene), 5 ng/ml bFGF, and 10% fetal bovine serum, and centrifuged at 2500 rpm (1200 g) for 30 min in a Beckman model GS-6R centrifuge with a swinging bucket rotor. Retroviral supernatant was replaced with growth media and 1 μg/ml aTc. Forty-eight hours following transduction, growth media was supplemented with 1 μg/ml aTc, 500 ng/ml G418 sulfate, and 500 ng/ml zeocin. Following two weeks of culture in selective growth media in the "off" condition, cells were plated at 50,000 cells/cm^2 in 0.01% collagen-coated 6-well plates for end-point assays. Twenty-four hours after plating, cells were washed twice with PBS to remove residual aTc, and growth media was replaced with differentiation media (αMEM, 10% fetal bovine serum, 100 U/ml penicillin G sodium, 100 μg/ml streptomycin sulfate, 50 μg/ml L-ascorbic acid, 3 mM sodium β-glycerophosphate, and 10 nM dexamethasone) supplemented with the indicated concentration of aTc. Cell culture media was replaced every 3 days until terminal assay, unless noted otherwise.

Osteogenic Differentiation

Quantitative RT-PCR (qRT-PCR), Western blotting, alkaline phosphatase biochemical activity, and von Kossa staining were performed as described previously.[154] Calcium content was determined by dissolving mineralized regions with 1 N acetic acid overnight. 25 µl of appropriately diluted sample was added to 300 µl of arsenazo III-containing Calcium Reagent (Diagnostic Services Ltd., Oxford, CT). The absorbance of the resulting samples was read at 650 nm and compared to a linear standard curve of $CaCl_2$ in 1 N acetic acid.

Scaffold Seeding and Analysis

Fibrous collagen disks (5 mm x 1.5 mm, Kensey Nash, Exton, PA) were incubated overnight in 10% FBS in phosphate buffered saline (PBS). 250,000 cells in 10 µl of growth media were seeded onto each side of the disk in a non-tissue culture treated 24 well plate, for a total of 500,000 cells/construct. Four hours later, scaffolds were immersed in 2 ml of growth media. After twenty-four hours, growth media was changed to 2 ml of differentiation media with or without 100 ng/ml aTc. Media was replaced every three days until terminal assay. FT-IR spectroscopy and DNA content were assessed as described previously.[157]

Intramuscular Implantation

Scaffolds seeded with engineered or unmodified myoblasts were cultured for 28 days *in vitro* and implanted into the hind limbs and 6 week old immunocompetent male

Balb/c mice (Jackson Labs, Bar Harbor, ME) in accordance with an IACUC-approved protocol. A longitudinal 1 cm incision was made in the skin overlying the gastrocnemius muscle, and the muscle was exposed. Scaffolds were inserted into the muscles of both legs through an atraumatic longitudinal split in the direction of the fibers. The muscle was closed over the implants (without suturing) and the skin closed with wound clips. Drinking water containing 5% sucrose with or without 1 mg/ml aTc was replaced every 3 days. 28 days after implantation mice were euthanized by CO_2 inhalation and lower legs were harvested, skinned, and fixed in 10% neutral buffered formalin.

Micro-Computed Tomography

Mineralization of 3-D scaffolds was quantified by high resolution X-ray micro-computed tomography (micro-CT) using a Scanco Medical VivaCT 40 imaging system (Bassersdorf, Switzerland). Specimens were scanned at 21 μm voxel resolution and evaluated at a threshold corresponding to a linear attenuation of 1.92 cm^{-1}, filter width of 1.2, and filter support of 2.0. The reconstructed and thresholded 3-D images were evaluated using direct distance transformation methods to calculate mineralized matrix volume within each construct.[135]

Histological Analysis

Formalin-fixed samples were paraffin embedded for von Kossa-nuclear fast red or hematoxylin-eosin staining, or decalcified with 5% formic acid prior to embedding for Masson's trichrome staining. 5 μm sections were deparaffinized and stained as indicated.

Data Analysis

Data are reported as mean ± standard error of the mean (SEM), and statistical comparisons using SYSTAT 8.0 were based on an analysis of variance (ANOVA) and Tukey's test for pairwise comparisons, with a p-value < 0.05 considered significant. Dose response curves were fitted to a 4-parameter sigmoid, and R-squared values calculated with SigmaPlot 2001.

Results

Tetracycline-inducible Runx2 expression system

Primary skeletal myoblasts from mature male mice were transduced simultaneously with pTJ66-tTA and pXF40-Runx2 retroviral supernatants (Fig. 6.1A) in the presence of anhydrotetracycline (aTc). aTc is a tetracycline derivative that has higher affinity for tTA and lower antibiotic activity than tetracycline.[168] Cells were passaged in growth media supplemented with 100 ng/ml aTc, 500 μg/ml zeocin, and 500 μg/ml G418 sulfate to select for cells which had integrated both retroviral vectors. After 2 weeks, selective antibiotics were removed from the media and cells were plated for experiments in growth media with 100 ng/ml aTc. Flow cytometry indicated that this cell population strongly expressed eGFP from the pTJ66-tTA vector (Fig. 6.1B), demonstrating successful retroviral transduction and integration, antibiotic selection, and transgene expression. Twenty-four hours after plating, growth media was replaced with differentiation media with the indicated concentration of aTc. Quantitative RT-PCR (qRT-PCR) and Western blotting at 7 days demonstrated high levels of Runx2 expression in the absence of aTc and a dose-dependent decrease in Runx2 expression with aTc

concentration (Fig. 6.1C-D). Although the profile of Runx2 mRNA expression is accurately represented in Figure 6.1C, the magnitude of change in Runx2 expression is possibly skewed by the detection of antisense Runx2 mRNA transcribed by the 5' LTR promoter of pXF40-Runx2. Therefore the degree of inducibility with this system is likely much greater than the 3-fold increase observed by qRT-PCR and is more accurately represented by protein levels displayed in Figure 6.1D. Importantly, no Runx2 protein was detected at high levels of aTc, suggesting that Runx2 expression can be adequately suppressed in the "off" condition. These results demonstrate a functioning aTc-inducible Runx2 expression system in primary skeletal myoblasts.

Osteogenic and myogenic gene expression

Runx2 is a known regulator of many osteoblast-specific genes[20] and repressor of myogenesis.[154] Therefore we assessed the effects of inducible Runx2 expression on osteoblastic and myogenic gene expression by qRT-PCR after 7 days in the indicated aTc concentration (Fig. 6.2). Expression of the osteoblastic markers osteocalcin, bone sialoprotein, osteopontin, and Osterix was dependent on aTc concentration and correlated strongly with Runx2 expression. These markers were repressed to levels equivalent to expression by unmodified myoblasts by 10 ng/ml aTc, demonstrating rigorous control of Runx2 expression and transactivation. Conversely, myogenin and troponin T, markers associated with myoblastic differentiation, were regulated in an opposite fashion by aTc, indicating Runx2-dependent suppression of myogenesis. Interestingly, these results suggest that the phenotype of these cells can be controlled by aTc concentration. In the presence of aTc, the cells maintain the predetermined myogenic differentiation program.

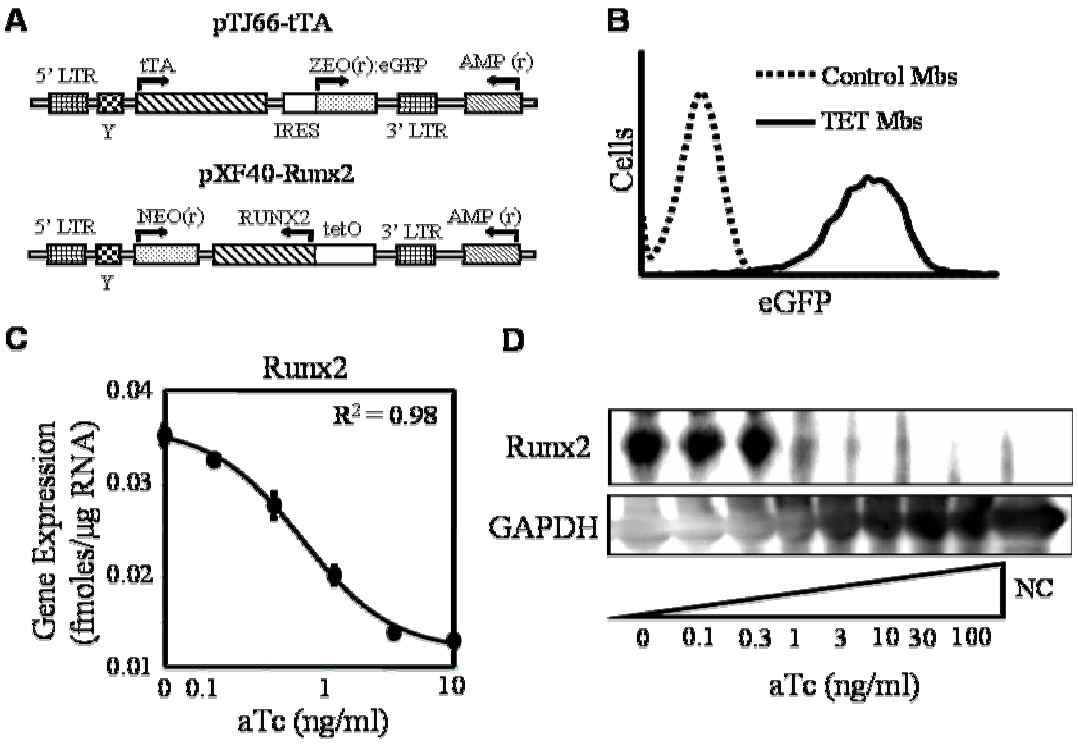

Figure 6.1. Tetracycline-inducible Runx2 expression system. (A) Retroviral vectors. The tetracycline-controlled transactivator (tTA) was constitutively expressed by pTJ66-tTA. Runx2 expression was controlled via the tet operon of pXF40-Runx2. (B) Detection of eGFP expression by flow cytometry confirmed retroviral transduction and antibiotic selection of primary skeletal myoblasts. (C) Runx2 mRNA (mean ± SEM, n=3) and (D) protein levels are dependent on aTc concentration after 7 days in differentiation media, demonstrating a functional aTc-inducible Runx2 expression system in primary skeletal myoblasts. The magnitude of Runx2 mRNA levels (C) is skewed by detection of Runx2 antisense mRNA transcribed by the 5' LTR promoter. However, Western blotting (D) confirmed undetectable levels of Runx2 protein at ≥10 ng/ml aTc, similar to unmodified myoblasts (NC).

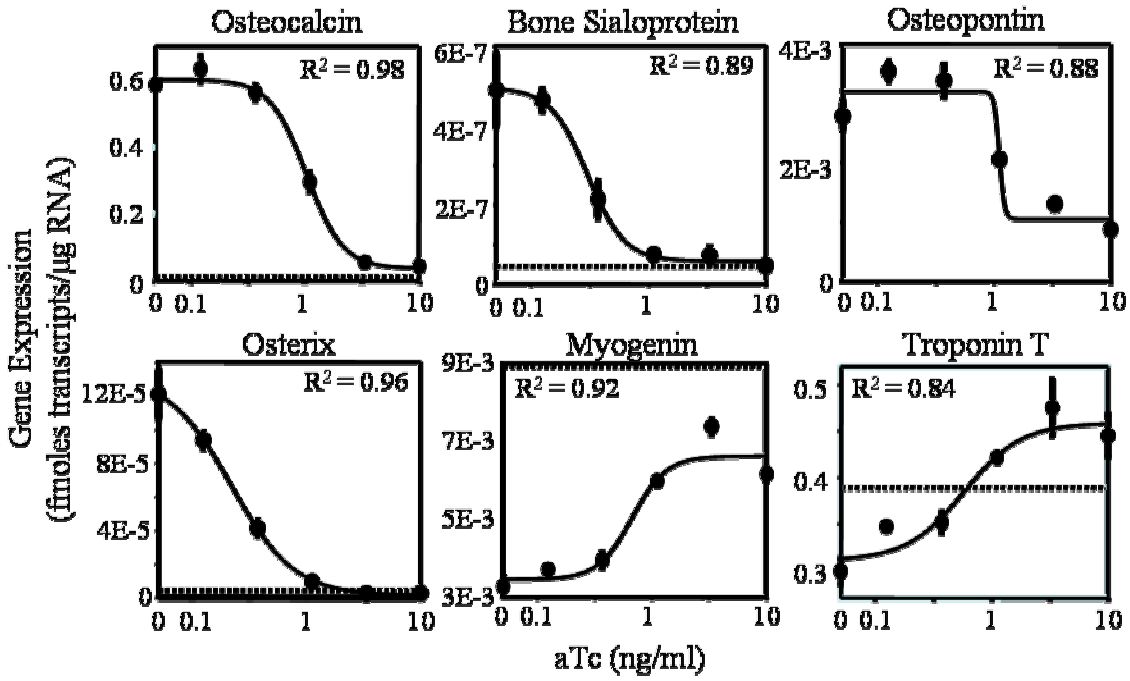

Figure 6.2. Inducible regulation of osteogenic and myogenic gene expression (mean ± SEM, n=3). Osteoblastic markers osteocalcin, bone sialoprotein, osteopontin, and Osterix were expressed at high levels in the absence of aTc and showed a dose-dependent decrease to background levels with aTc concentration. Conversely, myogenin and troponin T, markers of myogenic differentiation, increased with aTc concentration, indicating Runx2-dependent suppression of myogenesis. These results demonstrate cells maintaining a myogenic phenotype in the presence of ≥10 ng/ml aTc and an osteoblastic phenotype in the absence of aTc. Dotted line represents expression levels in unmodified primary skeletal myoblasts.

However, in the absence of aTc, Runx2 expression results in the upregulation of osteoblastic markers and suppression of myogenesis.

In vitro mineralization

The functional effects of inducible gene expression on osteoblastic differentiation were examined by alkaline phosphatase biochemical activity at 14 days and matrix mineralization at 28 days via calcium content analysis and von Kossa staining for phosphate deposits (Fig. 6.3). All of these assays followed a similar aTc-dependent pattern as Runx2 and osteoblastic gene expression, with high levels of mineralization in the absence of aTc (high Runx2 levels) and undetectable amounts of alkaline phosphatase activity, calcium and phosphate in as low as 1 ng/ml aTc (low Runx2 levels). Additionally, cultures with ≥10 ng/ml aTc consisted of large multinucleated myotubes demonstrating myogenic differentiation, whereas cultures without aTc contained mononucleated cells with cobblestone morphology, typical of the osteoblast phenotype. These results suggest that myoblasts engineered with an inducible Runx2 expression system transdifferentiate into an osteoblastic phenotype in the absence of aTc, similar to myoblasts engineered to constitutively express a Runx2 transgene.[154]

Temporal regulation of osteoblastic differentiation

One major advantage of inducible expression systems is the ability to exogenously manipulate transgene expression over time. To investigate the effects of temporal modulation of Runx2 expression, cells were cultured in differentiation media with or without 100 ng/ml aTc. After 8 days, aTc was either removed or added to the

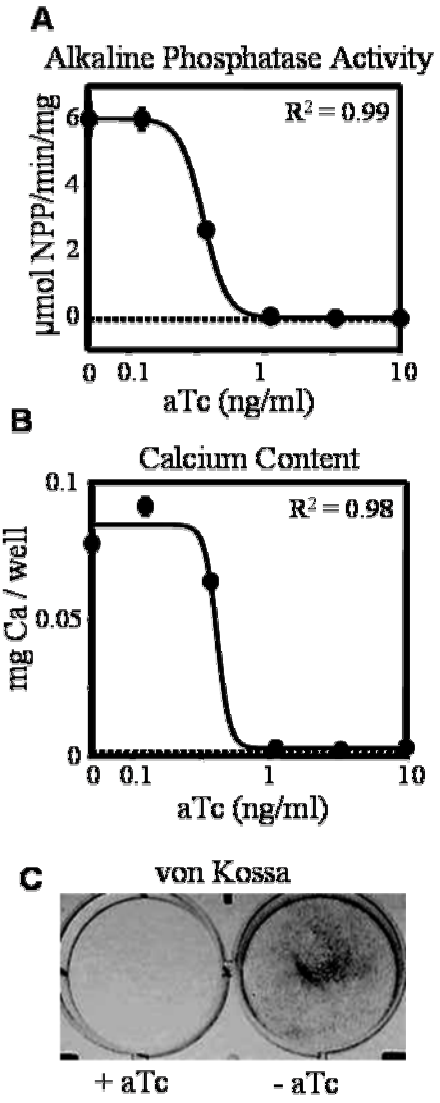

Figure 6.3. Inducible regulation of osteoblast differentiation. (A) Alkaline phosphatase biochemical activity and (B) calcium content decreased in a dose-dependent manner with aTc concentration (mean ± SEM, n=3), correlating with Runx2 and osteoblastic gene expression. Dotted line represents levels in unmodified primary skeletal myoblasts. (C) von Kossa staining showed significant phosphate deposits in cultures without aTc, whereas cultures with 100 ng/ml aTc showed no positive staining. These results demonstrate inducible regulation of mineralization in these cultures.

media for another 8 days. Samples were taken every 2 days to measure Runx2 protein levels (Fig. 6.4A) and osteocalcin gene expression (Fig. 6.4B). Both Runx2 and osteocalcin levels increased over 8 days in the absence of aTc, but rapidly returned to background levels after aTc was added back to cultures. There was a short lag time (~2 days) between reaching maximum levels of Runx2 protein and osteocalcin mRNA. Notably, myoblasts that were cultured in differentiation media with 100 ng/ml aTc for 8 days and allowed to undergo myogenic differentiation also upregulated Runx2 and osteocalcin upon induction with similar kinetics as cells that upregulated Runx2 directly after removal of growth media. This suggests that both undifferentiated myoblasts and cells in the later stages of terminal myogenic differentiation convert to an osteoblastic phenotype in response to forced Runx2 expression with a similar manner and magnitude. These results indicate that the cellular response to Runx2 activity is not affected by the differentiation state of primary skeletal myoblasts. This hypothesis was corroborated by assessing mineralization in cells cultured with or without 100 ng/ml aTc for 28 and 56 days (Fig. 6.4C). Cells without aTc incorporated significant amounts of calcium into their matrix, whereas cultures in the presence of aTc did not exhibit detectable levels of calcium incorporation. However, when aTc was added to cultures at 28 days, the rate of calcium incorporation was significantly decreased relative to cells without aTc. The increase in calcium levels despite aTc supplementation may be the result of nucleation of mineral deposits already present and/or continued mineralization during the degradation of Runx2-dependent osteoblastic protein and mRNA molecules. Additionally, myoblasts cultured in differentiation media with aTc for 28 days incorporated higher ($p<1E-5$) levels of calcium upon removal of aTc than mineralizing cultures at 28 days which

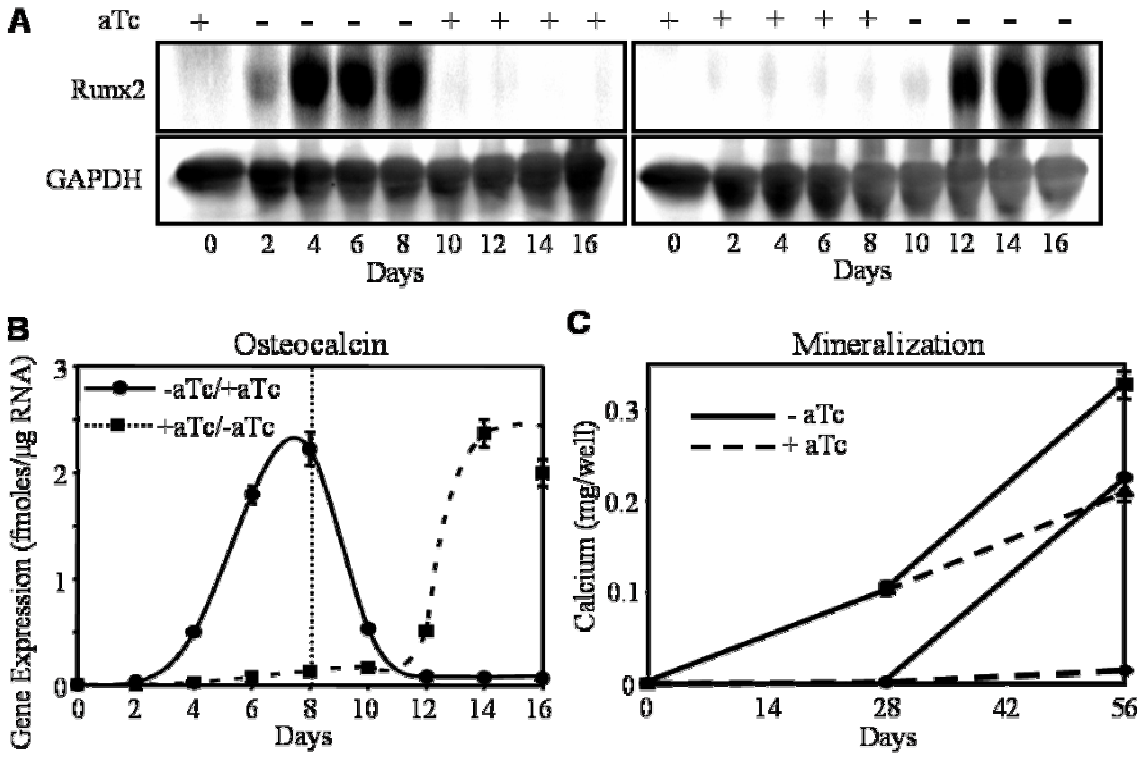

Figure 6.4. Temporal regulation of Runx2-stimulated osteoblastic differentiation. Cells were cultured with or without 100 ng/ml aTc for 8 days before aTc was removed or added back to the media. Cultures were harvested every 2 days to assess (A) Runx2 protein by Western blot or (B) osteocalcin mRNA by qRT-PCR (mean ± SEM, n=3, ANOVA p<9E-12). Both Runx2 and osteocalcin increased over 8 days without aTc and were subsequently suppressed to background levels after aTc was added back to the culture media. Additionally, myoblasts cultured in differentiation media with aTc for 8 days upregulated Runx2 and osteocalcin to similar levels as cultures in which aTc was removed at the same time as growth media. (C) Mineralization by cells cultured without aTc for 28 days was significantly decreased by adding aTc back to media as measured by calcium content at 56 days (mean ± SEM, n=3, ANOVA p<7E-12). 100 ng/ml aTc repressed mineralization in cells for 56 days, but calcium content was enhanced in the same cultures when aTc was removed at 28 days.

upregulated Runx2 before undergoing long-term myogenic differentiation. This result can be explained by the greater cell number at 28 days of culture relative to cultures that upregulated Runx2 beginning 1 day after seeding. Collectively, these results demonstrate a functioning inducible Runx2 expression system which regulates the conversion of primary skeletal myoblasts into an osteoblastic phenotype.

In vivo mineralization

Cells were seeded onto fibrous collagen scaffolds to evaluate this inducible Runx2 expression system in the context of a three-dimensional tissue-engineered environment. DNA content gradually decreased over 56 days of *in vitro* culture (Fig. 6.5A), potentially due to loss of nonadherent cells and cell death in the construct interior due to nutrient transport limitations associated with static culture.[139,157] This effect is enhanced in constructs without aTc at 56 days, likely due to the mineral deposits that occur predominantly at the construct periphery. Micro-computed tomography (micro-CT) was used to detect mineralized regions at 28 and 56 days (Fig. 6.5B). Consistent with the mineralization analyses of monolayer cultures, constructs cultured in 100 ng/ml aTc did not develop any mineralized regions. In contrast, constructs cultured without aTc developed punctate mineralized regions by 56 days. Fourier transform infrared (FT-IR) spectroscopy was used to determine the chemical composition of this mineral phase (Fig. 6.5C). Spectra of constructs cultured without aTc exhibited peaks representative of a carbonate-containing, biological hydroxyapatite similar to that of cranial bone.[130] Spectra of samples cultured with aTc contained only amide peaks, which are representative of an unmineralized extracellular matrix.

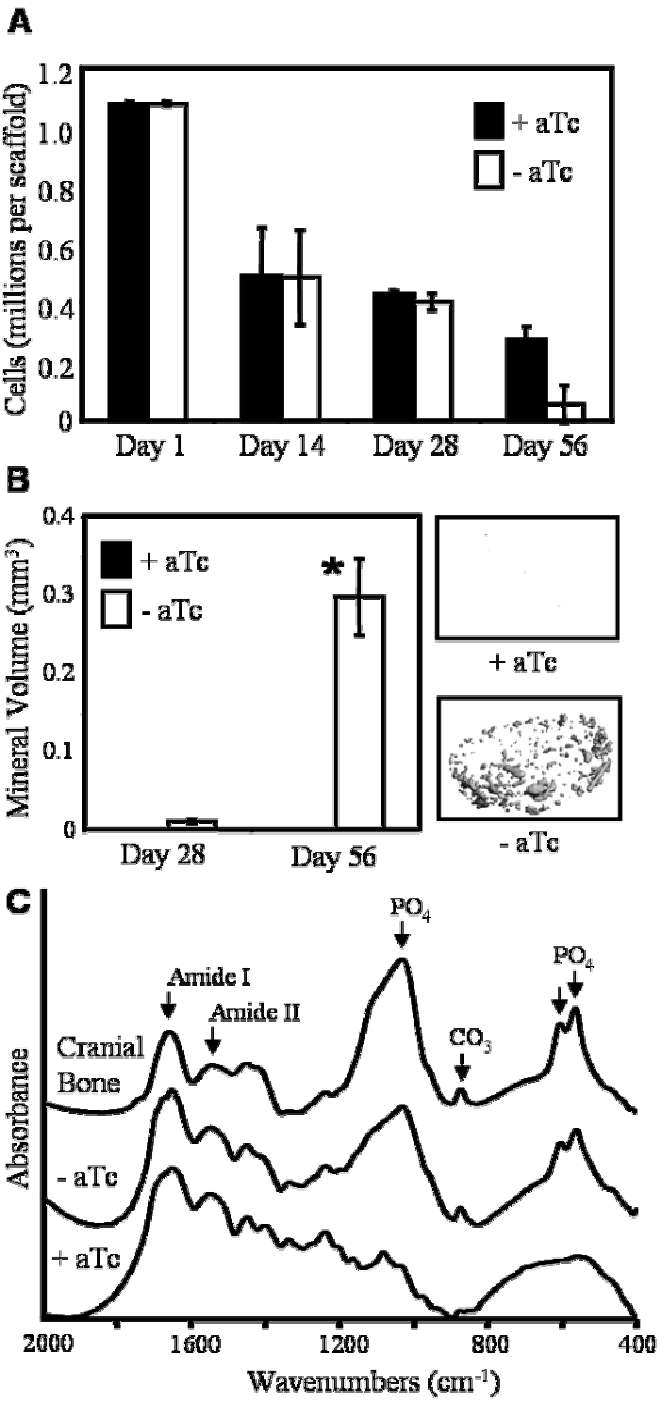

Figure 6.5. *In vitro* mineralization of collagen scaffolds seeded with Runx2-engineered myoblasts. Cell-seeded scaffolds were cultured for the indicated time *in vitro*. (A) DNA content decreased over time (mean ± SEM, n=3, ANOVA p<7E-12). (B) Mineralized regions were detectable by micro-CT at 56 days in samples without aTc (mean ± SEM, n=6, ANOVA p<3E-4, * vs. day 56 + aTc p<5E-3). Images are representative of 56 day constructs. (C) FT-IR spectroscopy confirmed that mineral deposits were a carbonate-containing biological hydroxyapatite, similar in chemical composition to cranial bone.

The ultimate application of a tetracycline-inducible Runx2 expression system is to control bone formation *in vivo*. Therefore we implanted constructs consisting of collagen scaffolds and Runx2-engineered myoblasts in the hind limb muscles of immunocompetent syngeneic mice for 28 days. Constructs were cultured for 28 days *in vitro* with or without 100 ng/ml aTc prior to implantation to allow for maturation of the cell-scaffold composite.[77] Drinking water was supplemented with 5% sucrose and 1 mg/ml aTc where indicated. Explants were analyzed by micro-CT and histochemical staining for mineralization and cellular morphology and distribution. Micro-CT showed distinct mineralization of constructs explanted from mice fed with sucrose only (Fig. 6.6A). These mineralized regions attenuated x-rays similarly to native trabecular bone in the femur and tibia. Explants from mice which were fed aTc displayed no mineralization above background, similar to control constructs seeded with untransduced myoblasts. von Kossa staining for phosphate deposits showed mineralized regions dispersed throughout the implant without aTc, whereas no positive staining was present in constructs with aTc (Fig. 6.6B). These results show that *in vivo* mineralization by these engineered cells can be exogenously regulated through aTc supplementation of the drinking water. Hematoxylin and eosin staining showed significantly higher cellularity in constructs without aTc (Fig. 6.6C), despite equivalent cell numbers at implantation (Fig. 6.5A). Also, a considerable amount of collagen scaffold (pink regions) was still present in samples with aTc after 28 days of implantation. This finding suggests both a higher degree of scaffold/matrix remodeling as well as cell proliferation and/or recruitment in constructs containing Runx2-expressing cells. Masson's trichrome staining of collagen (blue) displayed large amounts of acellular residual scaffold in implants with aTc (Fig.

6.6D). However, in addition to acellular scaffold material, implants without aTc contained significant collagen staining aligned and interwoven in highly cellularized regions, indicating matrix remodeling and/or deposition in a manner resembling early intramembranous bone formation. Histological staining of implants seeded with unmodified skeletal myoblasts and engineered cells in the presence of aTc were similar for all analyses, suggesting no adverse responses to retrovirally transduced cells.

Discussion

The exogenous regulation of Runx2-stimulated osteogenesis is significant for developing safe and controlled methods for gene therapy-based approaches to orthopedic regenerative medicine. This system also represents a useful tool for studying the regulation of osteoblastic differentiation, including the modulation of kinetics and magnitude of gene expression and cellular activity. We have demonstrated dose-dependent control of osteoblastic gene expression and mineralization with aTc concentration as well as suppression of myogenic gene expression in primary skeletal myoblasts. Following induction, osteoblastic markers were suppressible to background levels by addition of aTc to the media, demonstrating effective repression of Runx2-mediated effects in the "off" condition. The rate of mineralization could also be reduced by adding aTc to the media after 4 weeks of induction, demonstrating the potential to avoid bone overproduction in which bone production extends beyond the defect site.[88,89] Furthermore, cells precultured in differentiation conditions responded to the removal of aTc in the same fashion as cells in growth media, indicating comparable effects of Runx2 overexpression on myoblasts at distinct stages of differentiation. Finally, mineralization

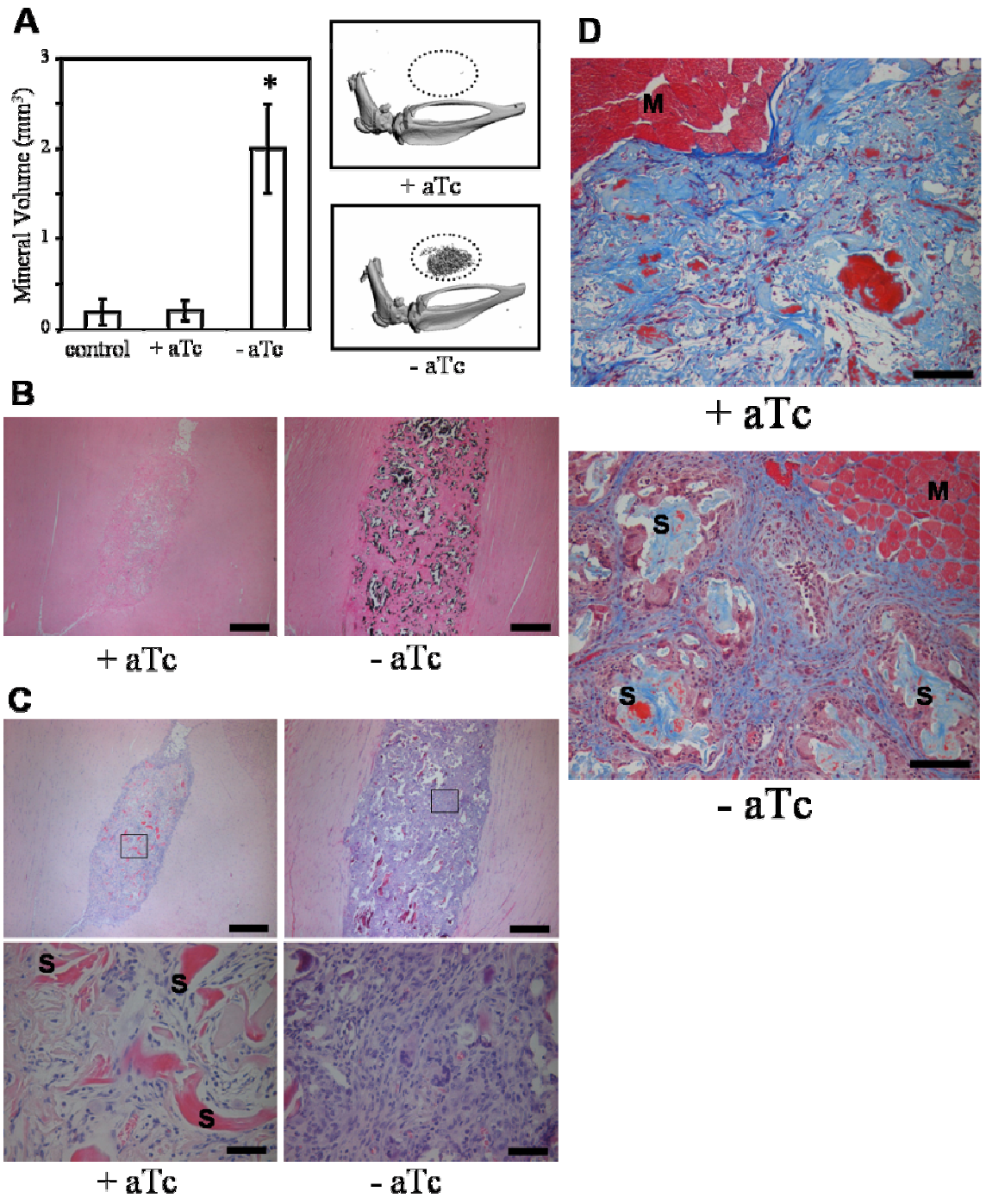

Figure 6.6. Regulation of *in vivo* mineralization with inducible Runx2 expression. Cell-seeded fibrous collagen scaffolds were cultured with or without 100 ng/ml aTc for 28 days *in vitro* and implanted in the hind limb muscles of immunocompetent syngeneic mice for 28 days. Mice received drinking water with or without 1 mg/ml aTc. (A) Micro-CT showed significant mineralization of cell-scaffold implants in mice that did not

receive aTc (mean ± SEM, n=6, ANOVA p<5E-3, * vs. + aTc p<9E-3). Mice receiving aTc produced background levels of attenuating material, similar to implants seeded with unmodified myoblasts (control). (B) von Kossa staining showed significant phosphate deposits in the absence of aTc. Scale bars indicate 100 μm. (C) Hematoxylin and eosin staining showed greater cellularity and less residual scaffold material (S, pink) in the absence of aTc. Scale bars indicate 100 μm (low magnification) and 10 μm (inset). (D) Masson's trichrome staining of collagen (blue) displayed large amounts of acellular residual scaffold in implants with aTc. In addition to acellular scaffold material (S), implants without aTc contained significant collagen staining aligned and interwoven in highly cellularized regions, indicating matrix remodeling and/or deposition in a manner resembling intramembranous bone formation. Endogenous muscle tissue (M) is stained red. Scale bars indicate 50 μm. Histological staining of implants seeded with unmodified skeletal myoblasts and engineered cells in the presence of aTc were similar for all analyses.

by engineered myoblasts could be regulated with aTc on collagen scaffolds *in vitro* and in an ectopic implant site *in vivo*. Greater cell numbers were consistently present on implants without aTc, despite equal cell numbers at implantation. This result is potentially due to differences in proliferation of implanted cells, infiltration of native cells, and/or cell survival. These differences are expected due to the varied autocrine and paracrine signaling of myoblastic (with aTc) and osteoblastic (without aTc) cell types, as well as differences in the structure of the local microenvironment of these samples, including extracellular matrix and mineralization. Collectively, these results show efficient and precise control of Runx2 expression and its downstream effects.

Inducible expression systems are notoriously troublesome in establishing successful routines for controlling transgene expression.[74] Typical complications associated with these systems include low levels of induction in the "on" state, high levels of expression in the "off" state, insufficient sensitivity to inducer levels, promoter interference of vectors expressing multiple transgenes, gene silencing, and inadequate

methods for transferring multiple components of the system into target cells. The results presented here demonstrate a system with undetectable transgene levels in the off state, high levels of expression in the on state for prolonged culture periods, and tight dose-dependent control of transgene levels over two orders of magnitude of inducer concentration. The success of this system may be attributed to the organization of the retroviral vectors, the antibiotic selection strategy for engineered cells, the cell type used, and/or the potency of Runx2 transcriptional activity.

Although tetracycline and its derivatives are known to affect cell activity, the amounts of aTc used in this study are orders of magnitude below toxic concentrations.[168] Furthermore, primary skeletal myoblasts retrovirally engineered to constitutively express a Runx2 transgene[154] showed equivalent levels of osteoblastic differentiation and *in vitro* and *in vivo* mineralization with or without aTc (unpublished results). These results indicate that the effect of aTc on overall cell activity is specific to the regulation of Runx2 expression from the retroviral vector. Interestingly, low levels of aTc (1 ng/ml) were necessary to suppress bone sialoprotein and Osterix expression, alkaline phosphatase activity, and mineralization. However, 10 ng/ml aTc was necessary for complete suppression of osteocalcin expression, a direct target gene of Runx2. This suggests that different threshold levels of Runx2 expression may be necessary to activate the many levels of the osteoblastic differentiation cascade. In fact, Runx2 has been proposed as a scaffold for assembling transcriptional machinery in addition to its own transactivation capabilities.[133] Furthermore, forced expression of Runx2 is commonly used to study mechanistic aspects of osteoblastic differentiation. However, currently used techniques do not mimic the physiological expression patterns of this tightly

regulated transcription factor with respect to magnitude or duration. Therefore this inducible expression system represents a promising tool for elucidating the effects of physiological and abnormal expression levels on the multifunctional roles of Runx2 in osteoblast differentiation.

Significant levels of *in vivo* mineralization and collagen remodeling were detected by ectopically implanted cells in the absence of aTc. These results establish inducible Runx2 expression in primary skeletal myoblasts as a promising strategy for cell-based orthopedic regeneration. However, we did not observe the development of osteocytes, cartilage, or marrow cavities as has been demonstrated by ectopically implanted Runx2-engineered cell lines in immunodeficient mice.[78] This discrepancy may be due to the primary cells and immunocompetent mice used in the present study, and longer implantation times may be necessary for the development of more complex tissues.

We utilized the "tet-off" system to regulate Runx2-stimulated osteogenesis because it is the most characterized and successful of the available inducible expression systems. However, the clinical application of the "tet-off" system would require patients to receive tetracycline for an indefinite period of time following bone healing to suppress transgene expression and bone overproduction. Therefore the "tet-on" system may be more clinically relevant for this application, considering the patient would only receive tetracycline during bone healing. In fact, recent modifications of the "tet-on" system have shown improved induction levels and lower basal activity in the "off" state.[93,94]

This system utilized two retroviral vectors to deliver the necessary components of an aTc-inducible Runx2 expression system.[156] The tetracycline-inducible expression system has also been incorporated into a single autoregulatory retroviral cassette,[169]

which may circumvent clinical limitations associated with transducing cells with two independent retroviral supernatants. Self-inactivating deletions within retroviral long terminal repeats can also be used to enhance expression from inducible promoters,[65] which may be limited in certain applications due to promoter interference.[98] Furthermore, tetracycline-regulated expression from adeno-associated virus (AAV) vectors[71] may avoid safety concerns associated with insertional mutagenesis and retroviral integrations.[170] In fact, allografts coated with AAV particles encoding osteogenic factors have recently been shown to increase bone healing.[73] Despite the numerous advances in gene transfer and inducible expression systems[74], it is clear that considerable research is necessary to optimize the effectiveness and clinical utility of these approaches. Additionally, the optimal gene or combinations of genes to deliver is still unclear and may be application-specific. In addition to BMPs and the Runx2 transcription factor, promising results have been achieved with strategies focusing on VEGF and RANK-L,[72] constitutively active BMP receptors,[73] LIM-mineralization protein,[81] and synergistic approaches incorporating multiple transgenes[70,78] and transgenes supplemented with glucocorticoids[83] or immunosuppressive agents.[84,85] Efficacy of these approaches may also be dependent on cell type[24] and *in vitro* preculture of cell-scaffold composites.[77] Nevertheless, inducible expression systems show significant promise in developing safe and controlled gene therapy strategies for bone tissue engineering.

This work establishes a controlled and effective alternative to genetic engineering with secreted growth factors for gene therapy-based orthopedic regeneration. Additionally, this system represents a method for regulating the magnitude and temporal

expression of the osteoblastic phenotype. Finally, this approach will be useful for elucidating biochemical properties of Runx2 activity and the stability of transgene-induced cellular phenotypes.

CHAPTER 7

FUTURE CONSIDERATIONS

This work has established Runx2-engineered primary skeletal myoblasts as a promising cell source for bone tissue engineering. However, there are several areas of research to be pursued before this strategy is validated as a clinical approach for orthopedic regeneration. Primarily, these cells should be implanted into an orthotopic defect and assessed for the ability to stimulate bone repair and restore function. In particular, our collaborators have recently established rodent cranial[67] and long bone segmental[171] defect models. Furthermore, the scaffold choice will be critical to interpreting the results of these experiments, as several recent studies have demonstrated substantial healing of bone defects with scaffolds alone[67], or scaffolds supplemented directly with osteogenic proteins[172] or gene delivery vehicles.[64,72,73] Therefore it is critical to identify the defect criteria that justify the added complexity, cost, and safety concerns of implanting genetically engineered osteogenic cells to achieve bone healing.

It is also important to identify the appropriate *in vitro* culture conditions to achieve optimal bone healing *in vivo*. We have demonstrated that *in vitro* preculture of tissue engineered constructs can have a significant impact on *in vivo* mineralization.[77,173] However, it is unclear how *in vitro* maturation of the constructs affects the ability of native cells to infiltrate and remodel these engineered tissues, including the development of complex structures such as blood vessels and marrow cavities. Additionally, incorporating methods to improve the mineral and cellular distribution throughout these constructs, such as perfusion culture[139], may significantly enhance the activity of these genetically engineered cells.

Many gene delivery vehicles have been utilized for orthopedic gene delivery, including plasmid DNA[64], adenovirus[55,69], adeno-associated virus[72,73], and retrovirus[65,82]. However, the optimal vehicle for orthopedic regeneration remains unclear. We hypothesized that sustained retroviral expression of an osteogenic factor would be necessary to achieve significant levels of osteoblast differentiation and mineralization. However, recent work has suggested that short-term expression, similar to that of adenoviral and adeno-associated viral vectors, is sufficient for bone production.[97] Furthermore, retroviral vectors have been associated with adverse side effects due to insertional mutagenesis[174], although these reports may be specific to the conditions of the particular study[175]. Further work is necessary to elucidate the optimal gene delivery method, including examining the efficiency of bone healing, biocompatibility, and safety of various systems specifically in the environment of bone regeneration.

We used the "tet-off" inducible expression system as a model for exogenously regulating osteoblastic differentiation and mineralization. However, several other inducible expression systems have been developed or been improved during the course of this work[95]. In particular, a system that activates expression in the presence of inducing agent would be more practical, as this approach would involve administration of the inducing agent only for the duration of bone healing. In fact, the "tet-on" system has been recently modified for enhanced regulation of expression levels[93,94] and is currently involved in clinical trials[95]. Incorporating Runx2-based gene therapy into this system, or a similar strategy, would advance the clinical relevance of this approach.

Present strategies in tissue engineering have focused on seeding a scaffold of uniform architecture with a single cell source to produce a homogeneous construct.

However, the native tissue to be repaired is typically heterogeneous with respect to cell type, composition, and function. These tissues are often composed of transition zones which consist of gradients from one tissue type to another, such as bone-cartilage, bone-ligament, bone-periosteum, and muscle-tendon interfaces. The successful integration and performance of engineered tissues is dependent on the development of new methods to replicate these transition zones *in vitro*. Few attempts have been made to replicate the multi-functional nature of these tissues. Typical approaches to this problem have involved seeding two independent scaffolds with different cell types and then fusing the two scaffolds together, or seeding opposite ends of a scaffold with different cell types[176,177]. These methods do not accurately reproduce the transitional nature of these tissues and are therefore biologically and functionally inferior to the native tissue. The successful engineering of these tissues will simulate their developmental nature: the influence of cell behavior by the chemotactic and haptotactic gradients of signaling molecules. Current work by our group is using inducible regulation of Runx2-stimulated transdifferentiation of skeletal myoblasts into a mineralizing osteoblastic phenotype to simulate this developmental system *in vitro*. We are applying a diffusion gradient of tetracycline across a hydrogel seeded with these genetically engineered cells to generate a continuous construct with muscle-like tissue at one end and bone-like tissue at the opposite end. This work will establish a novel method for engineering complex and heterogeneous tissues *in vitro* that more accurately replicate native tissue structure and function.

REFERENCES

1. Yaszemski,M.J., Payne,R.G., Hayes,W.C., Langer,R. & Mikos,A.G. Evolution of bone transplantation: molecular, cellular and tissue strategies to engineer human bone. *Biomaterials* 17, 175-185 (1996).

2. Marks,S.C. & Hermey,D.C. Priniciples of Bone Biology. Bilezikian,J., Raisz,L. & Rodan,G. (eds.), pp. 3-14 (The Academic Press, San Diego,1996).

3. Aubin,J.E. & Liu,F. Principles of Bone Biology. Bilezikian,J., Raisz,L. & Rodan,G. (eds.), pp. 51-68 (The Academic Press, San Diego,1996).

4. Vaccaro,A.R. The role of the osteoconductive scaffold in synthetic bone graft. *Orthopedics* 25, s571-s578 (2002).

5. Stein,G.S., Lian,J.B. & Owen,T.A. Relationship of cell growth to the regulation of tissue-specific gene expression during osteoblast differentiation. *FASEB J* 4, 3111-3123 (1990).

6. Urist,M.R. Bone: formation by autoinduction. *Science* 150, 893-899 (1965).

7. Schmitt,J.M., Hwang,K., Winn,S.R. & Hollinger,J.O. Bone morphogenetic proteins: an update on basic biology and clinical relevance. *J. Orthop. Res.* 17, 269-278 (1999).

8. Yoon,S.T. & Boden,S.D. Osteoinductive molecules in orthopaedics: basic science and preclinical studies. *Clin. Orthop.* 395, 33-43 (2002).

9. Nishimura,R., Hata,K., Harris,S.E., Ikeda,F. & Yoneda,T. Core-binding factor alpha 1 (Cbfa1) induces osteoblastic differentiation of C2C12 cells without interactions with Smad1 and Smad5. *Bone* 31, 303-312 (2002).

10. Derynck,R. & Zhang,Y.E. Smad-dependent and Smad-independent pathways in TGF-beta family signalling. *Nature* 425, 577-584 (2003).

11. Lee,K.S., Kim,H.J., Li,Q.L., Chi,X.Z., Ueta,C., Komori,T. *et al.* Runx2 is a common target of transforming growth factor beta1 and bone morphogenetic protein 2, and cooperation between Runx2 and Smad5 induces osteoblast-specific gene expression in the pluripotent mesenchymal precursor cell line C2C12. *Mol. Cell Biol.* 20, 8783-8792 (2000).

12. Katagiri,T., Yamaguchi,A., Ikeda,T., Yoshiki,S., Wozney,J.M., Rosen,V. *et al.* The non-osteogenic mouse pluripotent cell line, C3H10T1/2, is induced to differentiate into osteoblastic cells by recombinant human bone morphogenetic protein-2. *Biochem. Biophys. Res. Commun.* 172, 295-299 (1990).

13. Katagiri,T., Yamaguchi,A., Komaki,M., Abe,E., Takahashi,N., Ikeda,T. *et al.* Bone morphogenetic protein-2 converts the differentiation pathway of C2C12 myoblasts into the osteoblast lineage. *J. Cell Biol.* 127, 1755-1766 (1994).

14. Lee,M.H., Javed,A., Kim,H.J., Shin,H.I., Gutierrez,S., Choi,J.Y. *et al.* Transient upregulation of CBFA1 in response to bone morphogenetic protein-2 and transforming growth factor beta1 in C2C12 myogenic cells coincides with suppression of the myogenic phenotype but is not sufficient for osteoblast differentiation. *J. Cell Biochem.* 73, 114-125 (1999).

15. Katagiri,T., Akiyama,S., Namiki,M., Komaki,M., Yamaguchi,A., Rosen,V. *et al.* Bone morphogenetic protein-2 inhibits terminal differentiation of myogenic cells by suppressing the transcriptional activity of MyoD and myogenin. *Exp. Cell Res.* 230, 342-351 (1997).

16. Chalaux,E., Lopez-Rovira,T., Rosa,J.L., Bartrons,R. & Ventura,F. JunB is involved in the inhibition of myogenic differentiation by bone morphogenetic protein-2. *J. Biol. Chem.* 273, 537-543 (1998).

17. Weintraub,H. The MyoD family and myogenesis: redundancy, networks, and thresholds. *Cell* 75, 1241-1244 (1993).

18. Ogata,T., Wozney,J.M., Benezra,R. & Noda,M. Bone morphogenetic protein 2 transiently enhances expression of a gene, Id (inhibitor of differentiation), encoding a helix-loop-helix molecule in osteoblast-like cells. *Proc. Natl. Acad. Sci. U. S. A* 90, 9219-9222 (1993).

19. Hollnagel,A., Oehlmann,V., Heymer,J., Ruther,U. & Nordheim,A. Id genes are direct targets of bone morphogenetic protein induction in embryonic stem cells. *J. Biol. Chem.* 274, 19838-19845 (1999).

20. Ducy,P., Zhang,R., Geoffroy,V., Ridall,A.L. & Karsenty,G. Osf2/Cbfa1: a transcriptional activator of osteoblast differentiation. *Cell* 89, 747-754 (1997).

21. Komori,T., Yagi,H., Nomura,S., Yamaguchi,A., Sasaki,K., Deguchi,K. *et al.* Targeted disruption of Cbfa1 results in a complete lack of bone formation owing to maturational arrest of osteoblasts. *Cell* 89, 755-764 (1997).

22. Mundlos,S., Otto,F., Mundlos,C., Mulliken,J.B., Aylsworth,A.S., Albright,S. *et al.* Mutations involving the transcription factor CBFA1 cause cleidocranial dysplasia. *Cell* 89, 773-779 (1997).

23. Zhang,Y.W., Yasui,N., Ito,K., Huang,G., Fujii,M., Hanai,J. *et al.* A RUNX2/PEBP2alpha A/CBFA1 mutation displaying impaired transactivation and Smad interaction in cleidocranial dysplasia. *Proc. Natl. Acad. Sci. U. S. A* 97, 10549-10554 (2000).

24. Byers,B.A., Pavlath,G.K., Murphy,T.J., Karsenty,G. & Garcia,A.J. Cell-type-dependent up-regulation of in vitro mineralization after overexpression of the osteoblast-specific transcription factor Runx2/Cbfal. *J. Bone Miner. Res.* 17, 1931-1944 (2002).

25. Groppe,J., Greenwald,J., Wiater,E., Rodriguez-Leon,J., Economides,A.N., Kwiatkowski,W. *et al.* Structural basis of BMP signalling inhibition by the cystine knot protein Noggin. *Nature* 420, 636-642 (2002).

26. Gazzerro,E., Du,Z., Devlin,R.D., Rydziel,S., Priest,L., Economides,A.N. *et al.* Noggin arrests stromal cell differentiation in vitro(small star, filled). *Bone* 32, 111-119 (2003).

27. Zhu,H., Kavsak,P., Abdollah,S., Wrana,J.L. & Thomsen,G.H. A SMAD ubiquitin ligase targets the BMP pathway and affects embryonic pattern formation. *Nature* 400, 687-693 (1999).

28. Ying,S.X., Hussain,Z.J. & Zhang,Y.E. Smurf1 Facilitates Myogenic Differentiation and Antagonizes the Bone Morphogenetic Protein-2-induced Osteoblast Conversion by Targeting Smad5 for Degradation. *J. Biol. Chem.* 278, 39029-39036 (2003).

29. McLarren,K.W., Lo,R., Grbavec,D., Thirunavukkarasu,K., Karsenty,G. & Stifani,S. The mammalian basic helix loop helix protein HES-1 binds to and modulates the transactivating function of the runt-related factor Cbfa1. *J. Biol. Chem.* 275, 530-538 (2000).

30. Dodig,M., Tadic,T., Kronenberg,M.S., Dacic,S., Liu,Y.H., Maxson,R. *et al.* Ectopic Msx2 overexpression inhibits and Msx2 antisense stimulates calvarial osteoblast differentiation. *Dev. Biol.* 209, 298-307 (1999).

31. Shirakabe,K., Terasawa,K., Miyama,K., Shibuya,H. & Nishida,E. Regulation of the activity of the transcription factor Runx2 by two homeobox proteins, Msx2 and Dlx5. *Genes Cells* 6, 851-856 (2001).

32. Ryoo,H.M., Hoffmann,H.M., Beumer,T., Frenkel,B., Towler,D.A., Stein,G.S. *et al.* Stage-specific expression of Dlx-5 during osteoblast differentiation: involvement in regulation of osteocalcin gene expression. *Mol. Endocrinol.* 11, 1681-1694 (1997).

33. Lee,M.H., Kim,Y.J., Kim,H.J., Park,H.D., Kang,A.R., Kyung,H.M. *et al.* BMP-2-induced Runx2 Expression Is Mediated by Dlx5, and TGF-{beta}1 Opposes the BMP-2-induced Osteoblast Differentiation by Suppression of Dlx5 Expression. *J. Biol. Chem.* 278, 34387-34394 (2003).

34. Javed,A., Guo,B., Hiebert,S., Choi,J.Y., Green,J., Zhao,S.C. *et al.* Groucho/TLE/R-esp proteins associate with the nuclear matrix and repress RUNX

(CBF(alpha)/AML/PEBP2(alpha)) dependent activation of tissue-specific gene transcription. *J. Cell Sci.* 113, 2221-2231 (2000).

35. Perry,C.R. Bone repair techniques, bone graft, and bone graft substitutes. *Clin. Orthop.* 360, 71-86 (1999).

36. Finkemeier,C.G. Bone-grafting and bone-graft substitutes. *J. Bone Joint Surg. Am.* 84-A, 454-464 (2002).

37. Bucholz,R.W. Nonallograft osteoconductive bone graft substitutes. *Clin. Orthop.* 395, 44-52 (2002).

38. Bruder,S.P. & Fox,B.S. Tissue engineering of bone. Cell based strategies. *Clin. Orthop.* 367 Suppl, S68-S83 (1999).

39. Doll,B., Sfeir,C., Winn,S., Huard,J. & Hollinger,J. Critical aspects of tissue-engineered therapy for bone regeneration. *Crit Rev. Eukaryot. Gene Expr.* 11, 173-198 (2001).

40. Martin,I., Padera,R.F., Vunjak-Novakovic,G. & Freed,L.E. In vitro differentiation of chick embryo bone marrow stromal cells into cartilaginous and bone-like tissues. *J. Orthop. Res.* 16, 181-189 (1998).

41. Bruder,S.P., Kraus,K.H., Goldberg,V.M. & Kadiyala,S. The effect of implants loaded with autologous mesenchymal stem cells on the healing of canine segmental bone defects. *J. Bone Joint Surg. Am.* 80, 985-996 (1998).

42. Bruder,S.P., Kurth,A.A., Shea,M., Hayes,W.C., Jaiswal,N. & Kadiyala,S. Bone regeneration by implantation of purified, culture-expanded human mesenchymal stem cells. *J. Orthop. Res.* 16, 155-162 (1998).

43. Breitbart,A.S., Grande,D.A., Mason,J.M., Barcia,M., James,T. & Grant,R.T. Gene-enhanced tissue engineering: applications for bone healing using cultured periosteal cells transduced retrovirally with the BMP-7 gene. *Ann. Plast. Surg.* 42, 488-495 (1999).

44. Petite,H., Viateau,V., Bensaid,W., Meunier,A., de Pollak,C., Bourguignon,M. *et al.* Tissue-engineered bone regeneration. *Nat. Biotechnol.* 18, 959-963 (2000).

45. Quarto,R., Mastrogiacomo,M., Cancedda,R., Kutepov,S.M., Mukhachev,V., Lavroukov,A. *et al.* Repair of large bone defects with the use of autologous bone marrow stromal cells. *N. Engl. J. Med.* 344, 385-386 (2001).

46. Horwitz,E.M., Gordon,P.L., Koo,W.K., Marx,J.C., Neel,M.D., McNall,R.Y. *et al.* Isolated allogeneic bone marrow-derived mesenchymal cells engraft and stimulate growth in children with osteogenesis imperfecta: Implications for cell therapy of bone. *Proc. Natl. Acad. Sci. U. S. A* 99, 8932-8937 (2002).

47. Bruder,S.P., Jaiswal,N. & Haynesworth,S.E. Growth kinetics, self-renewal, and the osteogenic potential of purified human mesenchymal stem cells during extensive subcultivation and following cryopreservation. *J. Cell Biochem.* 64, 278-294 (1997).

48. Shi,S., Gronthos,S., Chen,S., Reddi,A., Counter,C.M., Robey,P.G. *et al.* Bone formation by human postnatal bone marrow stromal stem cells is enhanced by telomerase expression. *Nat. Biotechnol.* 20, 587-591 (2002).

49. Simonsen,J.L., Rosada,C., Serakinci,N., Justesen,J., Stenderup,K., Rattan,S.I. *et al.* Telomerase expression extends the proliferative life-span and maintains the osteogenic potential of human bone marrow stromal cells. *Nat. Biotechnol.* 20, 592-596 (2002).

50. Mueller,S.M. & Glowacki,J. Age-related decline in the osteogenic potential of human bone marrow cells cultured in three-dimensional collagen sponges. *J. Cell Biochem.* 82, 583-590 (2001).

51. Turgeman,G., Pittman,D.D., Muller,R., Kurkalli,B.G., Zhou,S., Pelled,G. *et al.* Engineered human mesenchymal stem cells: a novel platform for skeletal cell mediated gene therapy. *J. Gene Med.* 3, 240-251 (2001).

52. Cheng,S.L., Lou,J., Wright,N.M., Lai,C.F., Avioli,L.V. & Riew,K.D. In vitro and in vivo induction of bone formation using a recombinant adenoviral vector carrying the human BMP-2 gene. *Calcif. Tissue Int.* 68, 87-94 (2001).

53. Abe,N., Lee,Y.P., Sato,M., Zhang,X., Wu,J., Mitani,K. *et al.* Enhancement of bone repair with a helper-dependent adenoviral transfer of bone morphogenetic protein-2. *Biochem. Biophys. Res. Commun.* 297, 523-527 (2002).

54. Sugiyama,O., Orimo,H., Suzuki,S., Yamashita,K., Ito,H. & Shimada,T. Bone formation following transplantation of genetically modified primary bone marrow stromal cells. *J. Orthop. Res.* 21, 630-637 (2003).

55. Krebsbach,P.H., Gu,K., Franceschi,R.T. & Rutherford,R.B. Gene therapy-directed osteogenesis: BMP-7-transduced human fibroblasts form bone in vivo. *Hum. Gene Ther.* 11, 1201-1210 (2000).

56. Hirata,K., Tsukazaki,T., Kadowaki,A., Furukawa,K., Shibata,Y., Moriishi,T. *et al.* Transplantation of skin fibroblasts expressing BMP-2 promotes bone repair more effectively than those expressing Runx2. *Bone* 32, 502-512 (2003).

57. Lee,J.Y., Musgrave,D., Pelinkovic,D., Fukushima,K., Cummins,J., Usas,A. *et al.* Effect of bone morphogenetic protein-2-expressing muscle-derived cells on healing of critical-sized bone defects in mice. *J. Bone Joint Surg. Am.* 83-A, 1032-1039 (2001).

58. Bosch,P., Musgrave,D.S., Lee,J.Y., Cummins,J., Shuler,T., Ghivizzani,T.C. *et al.* Osteoprogenitor cells within skeletal muscle. *J. Orthop. Res.* 18, 933-944 (2000).

59. Young,B.H., Peng,H. & Huard,J. Muscle-based gene therapy and tissue engineering to improve bone healing. *Clin. Orthop.* 403 Suppl, S243-S251 (2002).

60. Chen,Y., Luk,K.D., Cheung,K.M., Xu,R., Lin,M.C., Lu,W.W. *et al.* Gene therapy for new bone formation using adeno-associated viral bone morphogenetic protein-2 vectors. *Gene Ther.* 10, 1345-1353 (2003).

61. Jankowski,R.J., Deasy,B.M. & Huard,J. Muscle-derived stem cells. *Gene Ther.* 9, 642-647 (2002).

62. Springer,M.L. & Blau,H.M. High-efficiency retroviral infection of primary myoblasts. *Somat. Cell Mol. Genet.* 23, 203-209 (1997).

63. Baltzer,A.W. & Lieberman,J.R. Regional gene therapy to enhance bone repair. *Gene Ther.* 11, 344-350 (2004).

64. Huang,Y.C., Kaigler,D., Rice,K.G., Krebsbach,P.H. & Mooney,D.J. Combined angiogenic and osteogenic factor delivery enhances bone marrow stromal cell-driven bone regeneration. *J Bone Miner. Res.* 20, 848-857 (2005).

65. Peng,H., Usas,A., Gearhart,B., Young,B., Olshanski,A. & Huard,J. Development of a self-inactivating tet-on retroviral vector expressing bone morphogenetic protein 4 to achieve regulated bone formation. *Mol. Ther.* 9, 885-894 (2004).

66. Wright,V., Peng,H., Usas,A., Young,B., Gearhart,B., Cummins,J. *et al.* BMP4-expressing muscle-derived stem cells differentiate into osteogenic lineage and improve bone healing in immunocompetent mice. *Mol. Ther.* 6, 169-178 (2002).

67. Byers,B.A., Guldberg,R.E., Hutmacher,D.W. & Garcia,A.J. Effects of Runx2 genetic engineering and in vitro maturation of tissue-engineered constructs on the repair of critical size bone defects. *J Biomed. Mater. Res. A* 76, 646-655 (2006).

68. Sugiyama,O., An,D.S., Kung,S.P., Feeley,B.T., Gamradt,S., Liu,N.Q. *et al.* Lentivirus-mediated gene transfer induces long-term transgene expression of BMP-2 in vitro and new bone formation in vivo. *Mol. Ther.* 11, 390-398 (2005).

69. Musgrave,D.S., Bosch,P., Ghivizzani,S., Robbins,P.D., Evans,C.H. & Huard,J. Adenovirus-mediated direct gene therapy with bone morphogenetic protein-2 produces bone. *Bone* 24, 541-547 (1999).

70. Zhao,M., Zhao,Z., Koh,J.T., Jin,T. & Franceschi,R.T. Combinatorial gene therapy for bone regeneration: cooperative interactions between adenovirus vectors expressing bone morphogenetic proteins 2, 4, and 7. *J Cell Biochem.* 95, 1-16 (2005).

71. Gafni,Y., Pelled,G., Zilberman,Y., Turgeman,G., Apparailly,F., Yotvat,H. *et al.* Gene therapy platform for bone regeneration using an exogenously regulated, AAV-2-based gene expression system. *Mol. Ther.* 9, 587-595 (2004).

72. Ito,H., Koefoed,M., Tiyapatanaputi,P., Gromov,K., Goater,J.J., Carmouche,J. *et al.* Remodeling of cortical bone allografts mediated by adherent rAAV-RANKL and VEGF gene therapy. *Nat. Med.* 11, 291-297 (2005).

73. Koefoed,M., Ito,H., Gromov,K., Reynolds,D.G., Awad,H.A., Rubery,P.T. *et al.* Biological effects of rAAV-caAlk2 coating on structural allograft healing. *Mol. Ther.* 12, 212-218 (2005).

74. Goverdhana,S., Puntel,M., Xiong,W., Zirger,J.M., Barcia,C., Curtin,J.F. *et al.* Regulatable gene expression systems for gene therapy applications: progress and future challenges. *Mol. Ther.* 12, 189-211 (2005).

75. Tsuda,H., Wada,T., Ito,Y., Uchida,H., Dehari,H., Nakamura,K. *et al.* Efficient BMP2 gene transfer and bone formation of mesenchymal stem cells by a fiber-mutant adenoviral vector. *Mol. Ther.* 7, 354-365 (2003).

76. Gazit,D., Turgeman,G., Kelley,P., Wang,E., Jalenak,M., Zilberman,Y. *et al.* Engineered pluripotent mesenchymal cells integrate and differentiate in regenerating bone: a novel cell-mediated gene therapy. *J. Gene Med.* 1, 121-133 (1999).

77. Byers,B.A., Guldberg,R.E. & Garcia,A.J. Synergy between genetic and tissue engineering: Runx2 overexpression and in vitro construct development enhance in vivo mineralization. *Tissue Eng* 10, 1757-1766 (2004).

78. Yang,S., Wei,D., Wang,D., Phimphilai,M., Krebsbach,P.H. & Franceschi,R.T. In vitro and in vivo synergistic interactions between the Runx2/Cbfa1 transcription factor and bone morphogenetic protein-2 in stimulating osteoblast differentiation. *J. Bone Miner. Res.* 18, 705-715 (2003).

79. Zheng,H., Guo,Z., Ma,Q., Jia,H. & Dang,G. Cbfa1/osf2 transduced bone marrow stromal cells facilitate bone formation in vitro and in vivo. *Calcif. Tissue Int.* 74, 194-203 (2004).

80. Peng,H., Wright,V., Usas,A., Gearhart,B., Shen,H.C., Cummins,J. *et al.* Synergistic enhancement of bone formation and healing by stem cell-expressed VEGF and bone morphogenetic protein-4. *J Clin. Invest* 110, 751-759 (2002).

81. Pola,E., Gao,W., Zhou,Y., Pola,R., Lattanzi,W., Sfeir,C. *et al.* Efficient bone formation by gene transfer of human LIM mineralization protein-3. *Gene Ther.* 11, 683-693 (2004).

82. Byers,B.A. & Garcia,A.J. Exogenous Runx2 expression enhances in vitro osteoblastic differentiation and mineralization in primary bone marrow stromal cells. *Tissue Eng* 10, 1623-1632 (2004).

83. Phillips,J.E., Gersbach,C.A., Wojtowicz,A.M. & Garcia,A.J. Glucocorticoid-induced osteogenesis is negatively regulated by Runx2/Cbfa1 serine phosphorylation. *J Cell Sci.* 119, 581-591 (2006).

84. Li,J.Z., Li,H., Hankins,G.R., Dunford,B. & Helm,G.A. Local immunomodulation with CD4 and CD8 antibodies, but not cyclosporine A, improves osteogenesis induced by ADhBMP9 gene therapy. *Gene Ther.* 12, 1235-1241 (2005).

85. Kaihara,S., Bessho,K., Okubo,Y., Sonobe,J., Kawai,M. & Iizuka,T. Simple and effective osteoinductive gene therapy by local injection of a bone morphogenetic protein-2-expressing recombinant adenoviral vector and FK506 mixture in rats. *Gene Ther.* 11, 439-447 (2004).

86. Ide,H., Yoshida,T., Matsumoto,N., Aoki,K., Osada,Y., Sugimura,T. *et al.* Growth regulation of human prostate cancer cells by bone morphogenetic protein-2. *Cancer Res.* 57, 5022-5027 (1997).

87. Pouliot,F., Blais,A. & Labrie,C. Overexpression of a dominant negative type II bone morphogenetic protein receptor inhibits the growth of human breast cancer cells. *Cancer Res.* 63, 277-281 (2003).

88. Moutsatsos,I.K., Turgeman,G., Zhou,S., Kurkalli,B.G., Pelled,G., Tzur,L. *et al.* Exogenously regulated stem cell-mediated gene therapy for bone regeneration. *Mol. Ther.* 3, 449-461 (2001).

89. Peng,H., Usas,A., Hannallah,D., Olshanski,A., Cooper,G.M. & Huard,J. Noggin improves bone healing elicited by muscle stem cells expressing inducible BMP4. *Mol. Ther.* 12, 239-246 (2005).

90. Gossen,M. & Bujard,H. Tight control of gene expression in mammalian cells by tetracycline-responsive promoters. *Proc. Natl. Acad. Sci. U. S. A* 89, 5547-5551 (1992).

91. Gossen,M., Freundlieb,S., Bender,G., Muller,G., Hillen,W. & Bujard,H. Transcriptional activation by tetracyclines in mammalian cells. *Science* 268, 1766-1769 (1995).

92. Mizuguchi,H. & Hayakawa,T. The tet-off system is more effective than the tet-on system for regulating transgene expression in a single adenovirus vector. *J Gene Med.* 4, 240-247 (2002).

93. Urlinger,S., Baron,U., Thellmann,M., Hasan,M.T., Bujard,H. & Hillen,W. Exploring the sequence space for tetracycline-dependent transcriptional

activators: novel mutations yield expanded range and sensitivity. *Proc. Natl. Acad. Sci. U. S. A* 97, 7963-7968 (2000).

94. Salucci,V., Scarito,A., Aurisicchio,L., Lamartina,S., Nicolaus,G., Giampaoli,S. *et al.* Tight control of gene expression by a helper-dependent adenovirus vector carrying the rtTA2(s)-M2 tetracycline transactivator and repressor system. *Gene Ther.* 9, 1415-1421 (2002).

95. Weber,W. & Fussenegger,M. Pharmacologic transgene control systems for gene therapy. *J Gene Med.* (2006).

96. Hasharoni,A., Zilberman,Y., Turgeman,G., Helm,G.A., Liebergall,M. & Gazit,D. Murine spinal fusion induced by engineered mesenchymal stem cells that conditionally express bone morphogenetic protein-2. *J Neurosurg. Spine* 3, 47-52 (2005).

97. Noel,D., Gazit,D., Bouquet,C., Apparailly,F., Bony,C., Plence,P. *et al.* Short-term BMP-2 expression is sufficient for in vivo osteochondral differentiation of mesenchymal stem cells. *Stem Cells* 22, 74-85 (2004).

98. Emerman,M. & Temin,H.M. Genes with promoters in retrovirus vectors can be independently suppressed by an epigenetic mechanism. *Cell* 39, 449-467 (1984).

99. Prince,M., Banerjee,C., Javed,A., Green,J., Lian,J.B., Stein,G.S. *et al.* Expression and regulation of Runx2/Cbfa1 and osteoblast phenotypic markers during the growth and differentiation of human osteoblasts. *J. Cell Biochem.* 80, 424-440 (2001).

100. Rando,T.A. & Blau,H.M. Primary mouse myoblast purification, characterization, and transplantation for cell-mediated gene therapy. *J. Cell Biol.* 125, 1275-1287 (1994).

101. Banerjee,C., Javed,A., Choi,J.Y., Green,J., Rosen,V., Van Wijnen,A.J. *et al.* Differential regulation of the two principal Runx2/Cbfa1 n-terminal isoforms in response to bone morphogenetic protein-2 during development of the osteoblast phenotype. *Endocrinology* 142, 4026-4039 (2001).

102. Harada,H., Tagashira,S., Fujiwara,M., Ogawa,S., Katsumata,T., Yamaguchi,A. *et al.* Cbfa1 isoforms exert functional differences in osteoblast differentiation. *J. Biol. Chem.* 274, 6972-6978 (1999).

103. Liu,F., Malaval,L. & Aubin,J.E. The mature osteoblast phenotype is characterized by extensive plasticity. *Exp. Cell Res.* 232, 97-105 (1997).

104. Seibel,M.J. Molecular markers of bone turnover: biochemical, technical and analytical aspects. *Osteoporos. Int.* 11 Suppl 6, S18-S29 (2000).

105. Nakashima,K., Zhou,X., Kunkel,G., Zhang,Z., Deng,J.M., Behringer,R.R. *et al.* The novel zinc finger-containing transcription factor osterix is required for osteoblast differentiation and bone formation. *Cell* 108, 17-29 (2002).

106. Tadic,T., Dodig,M., Erceg,I., Marijanovic,I., Mina,M., Kalajzic,Z. *et al.* Overexpression of Dlx5 in chicken calvarial cells accelerates osteoblastic differentiation. *J. Bone Miner. Res.* 17, 1008-1014 (2002).

107. Atkinson,B.L., Fantle,K.S., Benedict,J.J., Huffer,W.E. & Gutierrez-Hartmann,A. Combination of osteoinductive bone proteins differentiates mesenchymal C3H/10T1/2 cells specifically to the cartilage lineage. *J. Cell Biochem.* 65, 325-339 (1997).

108. Chen,D., Ji,X., Harris,M.A., Feng,J.Q., Karsenty,G., Celeste,A.J. *et al.* Differential roles for bone morphogenetic protein (BMP) receptor type IB and IA in differentiation and specification of mesenchymal precursor cells to osteoblast and adipocyte lineages. *J. Cell Biol.* 142, 295-305 (1998).

109. Stricker,S., Fundele,R., Vortkamp,A. & Mundlos,S. Role of Runx genes in chondrocyte differentiation. *Dev. Biol.* 245, 95-108 (2002).

110. Sauer,G.R. & Wuthier,R.E. Fourier transform infrared characterization of mineral phases formed during induction of mineralization by collagenase-released matrix vesicles in vitro. *J. Biol. Chem.* 263, 13718-13724 (1988).

111. Wagers,A.J. & Weissman,I.L. Plasticity of adult stem cells. *Cell* 116, 639-648 (2004).

112. Xiao,G., Gopalakrishnan,R., Jiang,D., Reith,E., Benson,M.D. & Franceschi,R.T. Bone morphogenetic proteins, extracellular matrix, and mitogen-activated protein kinase signaling pathways are required for osteoblast-specific gene expression and differentiation in MC3T3-E1 cells. *J. Bone Miner. Res.* 17, 101-110 (2002).

113. Lemonnier,J., Ghayor,C., Guicheux,J. & Caverzasio,J. Protein kinase C-independent activation of protein kinase D is involved in BMP-2-induced activation of stress mitogen-activated protein kinases JNK and p38 and osteoblastic cell differentiation. *J Biol. Chem.* 279, 259-264 (2004).

114. Hay,E., Lemonnier,J., Fromigue,O. & Marie,P.J. Bone morphogenetic protein-2 promotes osteoblast apoptosis through a Smad-independent, protein kinase C-dependent signaling pathway. *J. Biol. Chem.* 276, 29028-29036 (2001).

115. Xiao,G., Jiang,D., Thomas,P., Benson,M.D., Guan,K., Karsenty,G. *et al.* MAPK pathways activate and phosphorylate the osteoblast-specific transcription factor, Cbfa1. *J Biol. Chem.* 275, 4453-4459 (2000).

116. Gallea,S., Lallemand,F., Atfi,A., Rawadi,G., Ramez,V., Spinella-Jaegle,S. *et al.* Activation of mitogen-activated protein kinase cascades is involved in regulation

of bone morphogenetic protein-2-induced osteoblast differentiation in pluripotent C2C12 cells. *Bone* 28, 491-498 (2001).

117. Hassel,S., Schmitt,S., Hartung,A., Roth,M., Nohe,A., Petersen,N. *et al.* Initiation of Smad-dependent and Smad-independent signaling via distinct BMP-receptor complexes. *J. Bone Joint Surg. Am.* 85-A Suppl 3, 44-51 (2003).

118. Suzawa,M., Tamura,Y., Fukumoto,S., Miyazono,K., Fujita,T., Kato,S. *et al.* Stimulation of Smad1 transcriptional activity by Ras-extracellular signal-regulated kinase pathway: a possible mechanism for collagen-dependent osteoblastic differentiation. *J Bone Miner. Res.* 17, 240-248 (2002).

119. Guicheux,J., Lemonnier,J., Ghayor,C., Suzuki,A., Palmer,G. & Caverzasio,J. Activation of p38 mitogen-activated protein kinase and c-Jun-NH2-terminal kinase by BMP-2 and their implication in the stimulation of osteoblastic cell differentiation. *J Bone Miner. Res.* 18, 2060-2068 (2003).

120. Lee,K.S., Hong,S.H. & Bae,S.C. Both the Smad and p38 MAPK pathways play a crucial role in Runx2 expression following induction by transforming growth factor-beta and bone morphogenetic protein. *Oncogene* 21, 7156-7163 (2002).

121. Drissi,H., Luc,Q., Shakoori,R., Chuva De Sousa,L.S., Choi,J.Y., Terry,A. *et al.* Transcriptional autoregulation of the bone related CBFA1/RUNX2 gene. *J. Cell Physiol* 184, 341-350 (2000).

122. Sudhakar,S., Li,Y., Katz,M.S. & Elango,N. Translational regulation is a control point in RUNX2/Cbfa1 gene expression. *Biochem. Biophys. Res. Commun.* 289, 616-622 (2001).

123. Xiao,G., Jiang,D., Gopalakrishnan,R. & Franceschi,R.T. Fibroblast growth factor 2 induction of the osteocalcin gene requires MAPK activity and phosphorylation of the osteoblast transcription factor, Cbfa1/Runx2. *J. Biol. Chem.* 277, 36181-36187 (2002).

124. Ziros,P.G., Gil,A.P., Georgakopoulos,T., Habeos,I., Kletsas,D., Basdra,E.K. *et al.* The bone-specific transcriptional regulator Cbfa1 is a target of mechanical signals in osteoblastic cells. *J. Biol. Chem.* 277, 23934-23941 (2002).

125. Selvamurugan,N., Pulumati,M.R., Tyson,D.R. & Partridge,N.C. Parathyroid hormone regulation of the rat collagenase-3 promoter by protein kinase A-dependent transactivation of core binding factor alpha1. *J. Biol. Chem.* 275, 5037-5042 (2000).

126. Franceschi,R.T. & Xiao,G. Regulation of the osteoblast-specific transcription factor, Runx2: Responsiveness to multiple signal transduction pathways. *J. Cell Biochem.* 88, 446-454 (2003).

127. Gilbert,L., He,X., Farmer,P., Rubin,J., Drissi,H., Van Wijnen,A.J. *et al.* Expression of the osteoblast differentiation factor RUNX2 (Cbfa1/AML3/Pebp2alpha A) is inhibited by tumor necrosis factor-alpha. *J. Biol. Chem.* 277, 2695-2701 (2002).

128. Lee,M.H., Kwon,T.G., Park,H.S., Wozney,J.M. & Ryoo,H.M. BMP-2-induced Osterix expression is mediated by Dlx5 but is independent of Runx2. *Biochem. Biophys. Res. Commun.* 309, 689-694 (2003).

129. Chung,C.H., Golub,E.E., Forbes,E., Tokuoka,T. & Shapiro,I.M. Mechanism of action of beta-glycerophosphate on bone cell mineralization. *Calcif. Tissue Int.* 51, 305-311 (1992).

130. Bonewald,L.F., Harris,S.E., Rosser,J., Dallas,M.R., Dallas,S.L., Camacho,N.P. *et al.* von Kossa staining alone is not sufficient to confirm that mineralization in vitro represents bone formation. *Calcif. Tissue Int.* 72, 537-547 (2003).

131. Kundu,M., Javed,A., Jeon,J.P., Horner,A., Shum,L., Eckhaus,M. *et al.* Cbfbeta interacts with Runx2 and has a critical role in bone development. *Nat. Genet.* 32, 639-644 (2002).

132. D'Alonzo,R.C., Selvamurugan,N., Karsenty,G. & Partridge,N.C. Physical interaction of the activator protein-1 factors c-Fos and c-Jun with Cbfa1 for collagenase-3 promoter activation. *J. Biol. Chem.* 277, 816-822 (2002).

133. Franceschi,R.T. Functional cooperativity between osteoblast transcription factors: evidence for the importance of subnuclear macromolecular complexes? *Calcif. Tissue Int.* 72, 638-642 (2003).

134. Xiao,Z.S., Thomas,R., Hinson,T.K. & Quarles,L.D. Genomic structure and isoform expression of the mouse, rat and human Cbfa1/Osf2 transcription factor. *Gene* 214, 187-197 (1998).

135. Hildebrand,T., Laib,A., Muller,R., Dequeker,J. & Ruegsegger,P. Direct three-dimensional morphometric analysis of human cancellous bone: microstructural data from spine, femur, iliac crest, and calcaneus. *J. Bone Miner. Res.* 14, 1167-1174 (1999).

136. Holst,D., Luquet,S., Kristiansen,K. & Grimaldi,P.A. Roles of peroxisome proliferator-activated receptors delta and gamma in myoblast transdifferentiation. *Exp. Cell Res.* 288, 168-176 (2003).

137. Glowacki,J., Mizuno,S. & Greenberger,J.S. Perfusion enhances functions of bone marrow stromal cells in three-dimensional culture. *Cell Transplant.* 7, 319-326 (1998).

138. Bancroft,G.N., Sikavitsas,V.I., van den,D.J., Sheffield,T.L., Ambrose,C.G., Jansen,J.A. *et al.* Fluid flow increases mineralized matrix deposition in 3D

perfusion culture of marrow stromal osteoblasts in a dose-dependent manner. *Proc. Natl. Acad. Sci. U. S. A* 99, 12600-12605 (2002).

139. Cartmell,S.H., Porter,B.D., Garcia,A.J. & Guldberg,R.E. Effects of Medium Perfusion Rate on Cell-Seeded Three-Dimensional Bone Constructs in Vitro. *Tissue Engineering* 9, 1197-1203 (2003).

140. Marra,K.G., Szem,J.W., Kumta,P.N., DiMilla,P.A. & Weiss,L.E. In vitro analysis of biodegradable polymer blend/hydroxyapatite composites for bone tissue engineering. *J. Biomed. Mater. Res.* 47, 324-335 (1999).

141. Gomes,M.E., Sikavitsas,V.I., Behravesh,E., Reis,R.L. & Mikos,A.G. Effect of flow perfusion on the osteogenic differentiation of bone marrow stromal cells cultured on starch-based three-dimensional scaffolds. *J. Biomed. Mater. Res.* 67A, 87-95 (2003).

142. Ishaug,S.L., Yaszemski,M.J., Bizios,R. & Mikos,A.G. Osteoblast function on synthetic biodegradable polymers. *J. Biomed. Mater. Res.* 28, 1445-1453 (1994).

143. Hutmacher,D.W., Schantz,T., Zein,I., Ng,K.W., Teoh,S.H. & Tan,K.C. Mechanical properties and cell cultural response of polycaprolactone scaffolds designed and fabricated via fused deposition modeling. *J. Biomed. Mater. Res.* 55, 203-216 (2001).

144. Chevallay,B. & Herbage,D. Collagen-based biomaterials as 3D scaffold for cell cultures: applications for tissue engineering and gene therapy. *Med. Biol. Eng Comput.* 38, 211-218 (2000).

145. Lee,C.H., Singla,A. & Lee,Y. Biomedical applications of collagen. *Int. J. Pharm.* 221, 1-22 (2001).

146. Green,J., Schotland,S., Stauber,D.J., Kleeman,C.R. & Clemens,T.L. Cell-matrix interaction in bone: type I collagen modulates signal transduction in osteoblast-like cells. *Am. J. Physiol* 268, C1090-C1103 (1995).

147. Lynch,M.P., Stein,J.L., Stein,G.S. & Lian,J.B. The influence of type I collagen on the development and maintenance of the osteoblast phenotype in primary and passaged rat calvarial osteoblasts: modification of expression of genes supporting cell growth, adhesion, and extracellular matrix mineralization. *Exp. Cell Res.* 216, 35-45 (1995).

148. Reyes,C.D. & Garcia,A.J. alpha2beta1 Integrin-Specific Collagen Mimetic Surfaces that Support Osteoblastic Differentiation. *J. Biomed. Mater. Res.* (in press)., (2004).

149. Rutherford,R.B., Moalli,M., Franceschi,R.T., Wang,D., Gu,K. & Krebsbach,P.H. Bone morphogenetic protein-transduced human fibroblasts convert to osteoblasts and form bone in vivo. *Tissue Eng* 8, 441-452 (2002).

150. Lieberman,J.R., Daluiski,A., Stevenson,S., Wu,L., McAllister,P., Lee,Y.P. *et al.* The effect of regional gene therapy with bone morphogenetic protein-2-producing bone-marrow cells on the repair of segmental femoral defects in rats. *J. Bone Joint Surg. Am.* 81, 905-917 (1999).

151. Viggeswarapu,M., Boden,S.D., Liu,Y., Hair,G.A., Louis-Ugbo,J., Murakami,H. *et al.* Adenoviral delivery of LIM mineralization protein-1 induces new-bone formation in vitro and in vivo. *J. Bone Joint Surg. Am.* 83-A, 364-376 (2001).

152. Franceschi,R.T., Yang,S., Rutherford,R.B., Krebsbach,P.H., Zhao,M. & Wang,D. Gene therapy approaches for bone regeneration. *Cells Tissues. Organs* 176, 95-108 (2004).

153. Feeley,B.T., Gamradt,S.C., Hsu,W.K., Liu,N., Krenek,L., Robbins,P. *et al.* Influence of BMPs on the formation of osteoblastic lesions in metastatic prostate cancer. *J Bone Miner. Res.* 20, 2189-2199 (2005).

154. Gersbach,C.A., Byers,B.A., Pavlath,G.K. & Garcia,A.J. Runx2/Cbfa1 stimulates transdifferentiation of primary skeletal myoblasts into a mineralizing osteoblastic phenotype. *Exp. Cell Res.* 300, 406-417 (2004).

155. Zhao,Z., Zhao,M., Xiao,G. & Franceschi,R.T. Gene transfer of the Runx2 transcription factor enhances osteogenic activity of bone marrow stromal cells in vitro and in vivo. *Mol. Ther.* 12, 247-253 (2005).

156. Murphy,T.J., Pavlath,G.K., Wang,X., Boss,V., Abbott,K.L., Robida,A.M. *et al.* Retroviral vectors applied to gene regulation studies. *Methods Enzymol.* 345, 539-551 (2002).

157. Gersbach,C.A., Byers,B.A., Pavlath,G.K., Guldberg,R.E. & Garcia,A.J. Runx2/Cbfa1-genetically engineered skeletal myoblasts mineralize collagen scaffolds in vitro. *Biotechnol. Bioeng.* 88, 369-378 (2004).

158. Pratap,J., Galindo,M., Zaidi,S.K., Vradii,D., Bhat,B.M., Robinson,J.A. *et al.* Cell growth regulatory role of Runx2 during proliferative expansion of preosteoblasts. *Cancer Res.* 63, 5357-5362 (2003).

159. Chen,S., Guttridge,D.C., Tang,E., Shi,S., Guan,K. & Wang,C.Y. Suppression of tumor necrosis factor-mediated apoptosis by nuclear factor kappaB-independent bone morphogenetic protein/Smad signaling. *J Biol. Chem.* 276, 39259-39263 (2001).

160. Kale,S., Biermann,S., Edwards,C., Tarnowski,C., Morris,M. & Long,M.W. Three-dimensional cellular development is essential for ex vivo formation of human bone. *Nat. Biotechnol.* 18, 954-958 (2000).

161. Huang,W., Carlsen,B., Wulur,I., Rudkin,G., Ishida,K., Wu,B. *et al.* BMP-2 exerts differential effects on differentiation of rabbit bone marrow stromal cells grown in

two-dimensional and three-dimensional systems and is required for in vitro bone formation in a PLGA scaffold. *Exp. Cell Res.* 299, 325-334 (2004).

162. Hosseinkhani,H., Azzam,T., Kobayashi,H., Hiraoka,Y., Shimokawa,H., Domb,A.J. *et al.* Combination of 3D tissue engineered scaffold and non-viral gene carrier enhance in vitro DNA expression of mesenchymal stem cells. *Biomaterials* 27, 4269-4278 (2006).

163. Choi,K.Y., Kim,H.J., Lee,M.H., Kwon,T.G., Nah,H.D., Furuichi,T. *et al.* Runx2 regulates FGF2-induced Bmp2 expression during cranial bone development. *Dev. Dyn.* 233, 115-121 (2005).

164. Phimphilai,M., Zhao,Z., Boules,H., Roca,H. & Franceschi,R.T. BMP signaling is required for RUNX2-dependent induction of the osteoblast phenotype. *J Bone Miner. Res.* 21, 637-646 (2006).

165. Helvering,L.M., Sharp,R.L., Ou,X. & Geiser,A.G. Regulation of the promoters for the human bone morphogenetic protein 2 and 4 genes. *Gene* 256, 123-138 (2000).

166. Jane,J.A., Jr., Dunford,B.A., Kron,A., Pittman,D.D., Sasaki,T., Li,J.Z. *et al.* Ectopic osteogenesis using adenoviral bone morphogenetic protein (BMP)-4 and BMP-6 gene transfer. *Mol. Ther.* 6, 464-470 (2002).

167. Dunn,C.A., Jin,Q., Taba,M., Jr., Franceschi,R.T., Bruce,R.R. & Giannobile,W.V. BMP gene delivery for alveolar bone engineering at dental implant defects. *Mol. Ther.* 11, 294-299 (2005).

168. Gossen,M. & Bujard,H. Anhydrotetracycline, a novel effector for tetracycline controlled gene expression systems in eukaryotic cells. *Nucleic Acids Res.* 21, 4411-4412 (1993).

169. Hofmann,A., Nolan,G.P. & Blau,H.M. Rapid retroviral delivery of tetracycline-inducible genes in a single autoregulatory cassette. *Proc. Natl. Acad. Sci. U. S. A* 93, 5185-5190 (1996).

170. Baum,C., von Kalle,C., Staal,F.J., Li,Z., Fehse,B., Schmidt,M. *et al.* Chance or necessity? Insertional mutagenesis in gene therapy and its consequences. *Mol. Ther.* 9, 5-13 (2004).

171. Guldberg,R.E., Oest,M., Lin,A.S., Ito,H., Chao,X., Gromov,K. *et al.* Functional integration of tissue-engineered bone constructs. *J Musculoskelet. Neuronal. Interact.* 4, 399-400 (2004).

172. Lutolf,M.P., Weber,F.E., Schmoekel,H.G., Schense,J.C., Kohler,T., Muller,R. *et al.* Repair of bone defects using synthetic mimetics of collagenous extracellular matrices. *Nat. Biotechnol.* 21, 513-518 (2003).

173. Gersbach,C.A., Guldberg,R.E. & Garcia,A.J. In Vitro and In Vivo Osteoblastic Differentiation of BMP-2- and Runx2-Engineered Skeletal Myoblasts. *Submitted* (2006).

174. Hacein-Bey-Abina,S., von Kalle,C., Schmidt,M., McCormack,M.P., Wulffraat,N., Leboulch,P. *et al.* LMO2-associated clonal T cell proliferation in two patients after gene therapy for SCID-X1. *Science* 302, 415-419 (2003).

175. Dave,U.P., Jenkins,N.A. & Copeland,N.G. Gene therapy insertional mutagenesis insights. *Science* 303, 333 (2004).

176. Tuli,R., Nandi,S., Li,W.J., Tuli,S., Huang,X., Manner,P.A. *et al.* Human mesenchymal progenitor cell-based tissue engineering of a single-unit osteochondral construct. *Tissue Eng* 10, 1169-1179 (2004).

177. Hung,C.T., Lima,E.G., Mauck,R.L., Taki,E., LeRoux,M.A., Lu,H.H. *et al.* Anatomically shaped osteochondral constructs for articular cartilage repair. *J Biomech* 36, 1853-64 (2003).